Deutsches Zentrum
für Luft- und Raumfahrt e.V.
in der Helmholtz-Gemeinschaft

EnMAP Ground Segment

Mission Quarterly Report #12

01.04.2025 to 30.06.2025

Restriction: public

Doc. ID	EN-GS-RPT-1112
Issue	1.0
Date	07.10.2025

Configuration Controlled: Yes

German Remote Sensing Data Center (DFD)
Remote Sensing Technology Institute (IMF)
German Space Operations Center (GSOC)
Helmholtz Centre for Geosciences (GFZ)
German Space Agency at DLR

TABLE OF SIGNATURES

Prepared

Emiliano Carmona Flores

Digitally signed by Emiliano Carmona Flores
DN: PostalCode=51147, O=Deutsches Zentrum fuer Luft- und Raumfahrt e. V. (DLR), STREET=Linder Höhe, S=Nordrhein-Westfalen, C=DE, CN=Emiliano Carmona Flores, E=emiliano.carmona@dlr.de
Reason: I am the author of this document
Location:
Date: 2025.10.17 16:00:07+02'00'
Foxit PDF Reader Version: 2025.2.0

Date — Emiliano Carmona, (DLR MF-PBA, EnMAP OMM)

Sabine Chabrillat

Digital unterschrieben von Sabine Chabrillat
Datum: 2025.10.17 16:09:54 +02'00'

Date — Sabine Chabrillat, (GFZ, EnMAP SciLead)

Reviewed

i. A. D. Schulze

Digital signiert von Daniel Schulze
Datum: 2025.10.20 07:54:28+02'00'

Date — Daniel Schulze, (DLR RB-MIB, dep. EnMAP OMM)

Sabine Engelbrecht

Digital signiert von Sabine Engelbrecht
DN: PostalCode=51147, O=Deutsches Zentrum fuer Luft- und Raumfahrt e. V. (DLR), STREET=Linder Höhe, S=Nordrhein-Westfalen, C=DE, CN=Sabine Engelbrecht, E=sabine.engelbrecht@dlr.de
Grund: Ich habe dieses Dokument geprüft
Ort:
Datum: 2025.10.20 09:14:46+02'00'
Foxit PDF Editor Version: 14.0.0

Date — Sabine Engelbrecht, (DLR DFD-INF, EOC PAD)

Sabine Engelbrecht

Digital signiert von Sabine Engelbrecht
DN: PostalCode=51147, O=Deutsches Zentrum fuer Luft- und Raumfahrt e. V. (DLR), STREET=Linder Höhe, S=Nordrhein-Westfalen, C=DE, CN=Sabine Engelbrecht, E=sabine.engelbrecht@dlr.de
Grund: Ich habe dieses Dokument geprüft, in Vertretung für R. Größel
Ort:
Datum: 2025.10.20 09:16:03+02'00'
Foxit PDF Editor Version: 14.0.0

Date — Robert Größel, (DLR RB-CTA, GSOC PAD)

Karl Segl

Digital unterschrieben von Karl Segl
Datum: 2025.10.17 16:25:43 +02'00'

Date — Karl Segl, (GFZ, dep. EnMAP SciLead)

Approved & Released

i. A. Laura La Porta

2025.10.27
10:41:24+01'00'
14.0.0

Date — Laura La Porta, (DLR AR-AO, EnMAP MM)

DISTRIBUTION LIST

The document is publicly available via www.enmap.org.

CHANGE RECORD

Version	Date	Chapter	Comment
1.0	07.10.2025	All	First issue of Mission Quarterly Report #12 corresponding to 01.04.2025 to 30.06.2025.

Custodian of this document is Carmona, Emiliano.

CONTENTS

LIST OF FIGURES

LIST OF TABLES

1 Introduction

1.1 Purpose

This mission quarterly report (MQR) states information on the EnMAP mission status with regard to the registered user community, announcements-of-opportunities and observations as well as the status of the user interfaces, satellite (platform and payload), ground stations (S-band and X-band), processor (Archive, Level 1B, Level 1C, Level 2A (land and water)), calibration (spectral, radiometric, geometric), data quality control and validation of EnMAP.

Please visit www.enmap.org for further information on EnMAP.

1.2 Scope

This 12th Mission Quarterly Report (MQR) applies to the operations of EnMAP in the reporting period of Routine Phase (RP) from **01.04.2025 to 30.06.2025 (Q2 2025)**.

2 References

Reference Identifier	**Document Identifier and Title**
[1]	L. Guanter et al. (2015) The EnMAP Spaceborne Imaging Spectroscopy Mission for Earth Observation. Remote Sensing, Issue 7, pp. 8830-8857.
[2]	EN-GS-UM-6020 Portals User Manual, Version 1.4
[3]	EN-PCV-ICD-2009-2 Product Specification, Version 1.9
[4]	EN-PCV-TN-4006 Level 1B ATBD, Version 1.10
[5]	EN-PCV-TN-5006 Level 1C ATBD, Version 1.7
[6]	EN-PCV-TN-6007 Level 2A (land) ATBD, Version 2.4
[7]	EN-PCV-TN-6008 Level 2A (water) ATBD, Version 3.1
[8]	Chabrillat, S. et al. (2022) EnMAP Science Plan. EnMAP Technical Report, DOI: 10.48440/enmap.2022.001
[9]	Storch, T.; Honold, H.-P.; Chabrillat, et al. The EnMAP imaging spectroscopy mission towards operations. Remote Sens. Environ. 2023, 294, 113632. DOI: 10.1016/j.rse.2023.113632

Table 2-1 References

3 Terms, Definitions and Abbreviations

Terms, definitions and abbreviations for EnMAP are collected in a database which is publicly accessible via Internet on www.enmap.org.

An Earth observation of swath length n × 30 km (and swath width 30 km) is separated into n tiles of size 30 km × 30 km.

4 Mission

4.1 Mission Objectives

The primary goal of EnMAP (Environmental Mapping and Analysis Program) is to measure, derive and analyze quantitative diagnostic parameters describing key processes on the Earth's surface [1].

During the mission operations, with the successful launch on 1st of April 2022 and an expected operational mission lifetime of at least 5 years, EnMAP will provide valuable information for various application fields comprising soil and geology, agriculture, forestry, urban areas, aquatic systems, ecosystem transitions.

4.2 Mission Description

The major elements of the EnMAP mission are the EnMAP Space Segment, built by OHB System AG and owned by the German Space Agency at DLR, the EnMAP Ground Segment built and operated by DLR institutes DFD, MF, RB, and the EnMAP User and Science Segment represented by GFZ. The project management of the EnMAP mission is responsibility of the German Space Agency at DLR.

The EnMAP Space Segment is composed of

- the platform providing power and thermal stability, orbit and attitude control, memory, S-band uplink/downlink for TM/TC data transmission/reception, X-band downlink for payload data transmission, and
- the payload realized as a pushbroom imaging dual-spectrometer covering the wavelength range between 420 nm and 2450 nm with a nominal spectral resolution ≤ 10 nm and allows in combination with a high radiometric resolution and stability to measure subtle reflectance changes.

The EnMAP satellite is operated on a sun-synchronous repeat orbit to observe any location on the globe with comparable illumination conditions. This allows a maximum reflected solar input radiance at the sensor with an acceptable risk for cloud coverage.

The EnMAP Ground Segment is the interface between Space Segment and User and Science Segment. It comprises functionalities to

- perform planning of imaging, communication and orbit maneuver operations, provision of orbit and attitude data, command and control of the satellite, ground station networks (in particular: Weilheim, Germany, for S-band and Neustrelitz, Germany, for X-Band), receive satellite data, perform long-term archiving and delivery of products, and
- perform processing chain (for systematic and radiometric correction, orthorectification, atmospheric compensation), instrument calibration operations, and the data quality control of the products.

The EnMAP mission interfaces to the international science and user community through the EnMAP Portal www.enmap.org with official information related to EnMAP by DLR and GFZ-Potsdam (as the document in hand) and links for ordering observations and products.

The EnMAP Science Segment is represented by the EnMAP Science Advisory Group chaired by the mission principal investigator at the GFZ-Potsdam. The Science Segment addresses aspects such as

- supporting and performing validation activities to improve sensor performance and product quality
- developing scientific and application research to fully exploit the scientific potential of EnMAP [8] including provision of software tools for EnMAP data processing and analyses (EnMAP-Box) and provision of teaching and education materials (HYPERedu)

- Organizing workshops, summer schools and in general information, training and networking activities for the user community

The EnMAP User Segment is the community of German and international users ordering acquisitions and accessing products of EnMAP.

4.3 Mission Status Summary

The mission successfully finished the commissioning phase (CP) on 01.11.2022 [9] and entered its routine phase (RP) on 02.11.2022. In the reporting period, from 01.04.2025 to 30.06.2025, there have been no major issues affecting the instrument or the satellite, although some minor issues have caused the loss of observation time.

During the period 01.04.2025 to 30.06.2025 (91 days in total), data acquisition was suspended for a cumulative total of 6 days. Three different issues resulted in HSI SAFE_ERRORs, but only the event on 06.06.2025 caused the loss of several days of observation time. The other 2 events resulted in the loss of some hours of observation time. In all cases the data quality is analyzed after resuming operations and no effect was found on the newly acquired data. During normal operations, the mission is regularly reaching and surpassing the initially planned maximum acquisition capacity of 5000 km / day.

In this period, 2056 Earth observations of 30 km swath width and up to 990 km swath length were successfully performed which resulted in 20631 archived Earth observation tiles of 30 km × 30 km and 19 calibration acquisitions. In addition, 22381 products were delivered from catalog orders. In total, 17596 Earth observations were performed until 30.06.2025 by the EnMAP team and the 4006 registered users with at least one active user role. This results in 154001 archived Earth observation images (194134 products including the different versions of the re-processed products) and 286055 Earth products delivered from observations requests (158249) and catalogue orders (127806) since the start of the mission. More details are presented in sections 5 and 6.

No major limitations are applicable at 30.06.2025. For minor limitations affecting data processing, check section 7.4. Other effects observed in the data by our Quality Control team are reported in section 7.6 while they are investigated in more detail.

Activities within the EnMAP Mission and in particular the Ground Segment have been reported in different conferences and workshops. More details are available in Section 9.

The following changes were implemented in the reporting period:

- Processing of all archived L0 data into L2A ARD for the EOC Geoservice and EO-Lab was finished at the start of Q2 2025. All products available on the EnMAP archive shall be available through EOC Geoservice and EO-Lab.

- Introduction of expiration dates in the Instrument Planning Portal for the Announcements of Oportunities and the proposals. For more details check Section 7.1.

The EnMAP processor version did not change during the reporting period and it is still V01.05.02. The list of changes introduced in this and previous processor updates is available at:

https://www.enmap.org/data/doc/EnMAP_processor_changelog.pdf

In August 2024 it was announced the availability of EnMAP products through the EOC Geoservice (https://geoservice.dlr.de/) and the EO-Lab platform (https://eo-lab.org/). These possibilities allow the direct download of EnMAP L2A products generated by the EnMAP Ground Segment with a standard set of parameters. Since these L2A products are already processed, users can directly download these products without waiting times, allowing a fast way to get large amounts of EnMAP products from the mission archive. Notice that both EOC Geoservice and EO-Lab are not part of the standard services offered by the EnMAP mission but are accessible with the GS/IPS EnMAP account. More information on the number of products downloaded through Geoservice can be found in section 6.2.1.

The following changes are expected to be performed in the next quarters:

- Start re-processing of L0 products to L2A ARD products with V01.05.02 for the EOC Geoservice and EO-Lab. Products in these services will benefit from being processed with the currently latest version of the processor.

- Implementation of new linearity calibration (and updated calibration) to improve the VNIR-SWIR matching between spectrometers, specially at low radiances.

5 Users and Announcements-of-Opportunities

5.1 Users

	Country/Continent (No of Countries) *(of reporting period)* *(since beginning of routine phase)*	Reporting Period 01.04.2025 to 30.06.2025	Since beginning of routine phase until 30.06.2025 (end of reporting period)
Total European Users	Europe *(25)(36)*	178	2504
European	• Germany	74	1049
	• Italy	18	223
	• France	16	219
	• United Kingdom	8	153
	• Spain	12	136
	• Netherlands	8	111
	• Poland	3	102
	• Finland	1	52
	• Belgium	5	47
	• Greece	1	42
	• Switzerland	1	40
	• Norway	1	38
	• Portugal	0	38
	• Sweden	2	37
	• Austria	0	36
	• Czechia	5	32
	• Others (10)(20)	18	149
Non European	North America *(6)(15)*	65	711
	South America *(7)(10)*	49	297
	Asia *(23)(37)*	190	1566
	Africa *(16)(34)*	37	258
	Oceania *(3)*	20	213
	Total *(80)(134)*	**539**	**5549**

Table 5-1 Number of registered users per continent (number of user countries during reporting period)

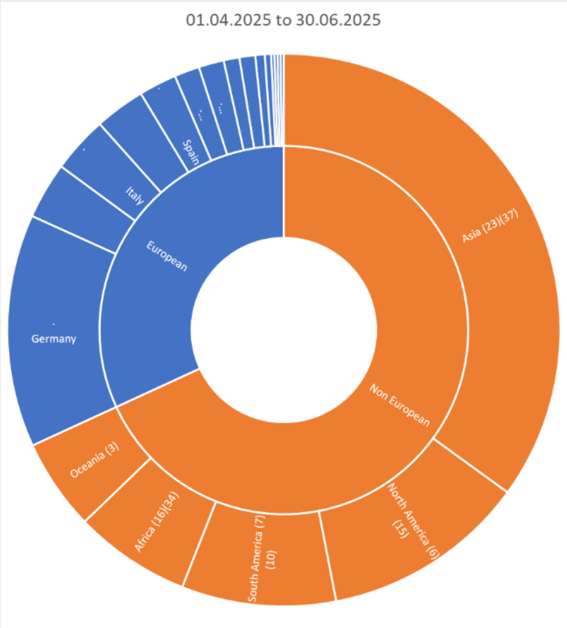

Reporting Period 01.04.2025 to 30.06.2025 with a total of 539 Users of 80 different countries.

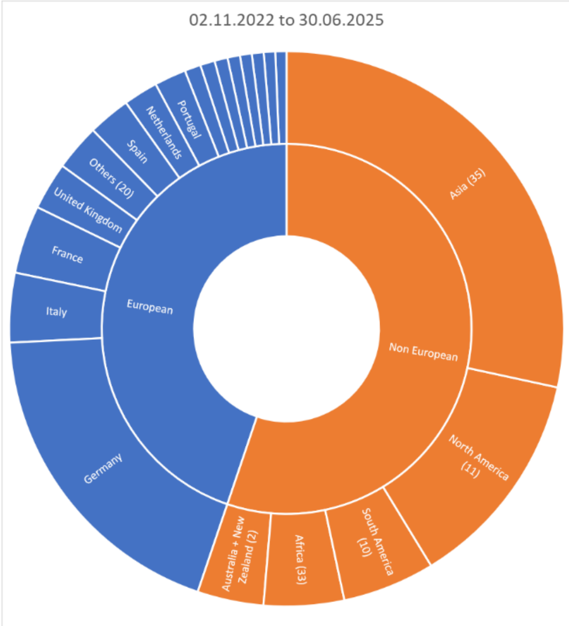

Since beginning of operational phase until 30.06.2025 (end of reporting period) with total of 5549 Users of 134 different countries.

Figure 5-1 Number of registered users per country

User per Category		New within reporting period 01.04.2025 to 30.06.2025	Since beginning of routine phase start until 30.06.2025 (end of reporting period)
Registered users	Total	539	5549
	with active role assignment*	445	4006
Cat-1 Science	Total	360	3262
	AO Process 00001*	352	3157
	AO Process 00002*	35	636
	AO Process 00003*	36	221
Cat-2 Commercial	Total	19	30
Cat-1 Distributor**	Total	297	3041

Table 5-2 Number of registered users and number of released user roles per category (Cat-1 Science, Cat-2 Commercial and Cat-1 Distributor)

*Registered users with at least one active user role

**Catalogue User, ordering EnMAP data from archive

Notice that registered users belong to different categories, therefore the sum of Cat-1 Science and Cat-1 Distributors or other categories does not correspond to the total registered users.

5.2 Announcements-of-Opportunities

Announcement -of-Opportunity	New within reporting period 01.04.2025 to 30.06.2025		Since beginning of routine Phase until 30.06.2025 (end of reporting period)	
	Proposals	Total tiles granted	Proposals	Total tiles granted
A00001	101	4577	762	32626
A00002	0	0	126	10395
A00003	0	0	4	127
Total	101	4577	892	43148

Table 5-3 Number of released science proposals per Announcement-of-Opportunity (AOs#) and total number of granted tiles per AO#.

Icon	Topic	New within reporting period 01.04.2025 to 30.06.2025		Since beginning of routine Phase until 30.06.2025 (end of reporting period)	
		Proposal	Total tiles granted	Proposal	Total tiles granted
	VEGETATION	41	2056	341	18806
	GEO/SOIL	37	1282	284	8384
	WATER	10	550	105	4673
	SNOW/ICE	1	21	21	1181
	URBAN	0	0	13	476
	ATMOSPHERE	4	234	50	2998
	HAZARD/RISK	3	53	21	692
	METHODS	3	66	19	713
	CAL/VAL	2	315	38	5225
	Total	**101**	**4577**	**892**	**43148**

Table 5-4 Number of accepted science proposals and total number of granted tiles per topic

6 Archived and Delivered Observations

The following table shows the number of archived Earth Observation and Calibration products and their sizes within the specified time frames.

Acquisition Type	Archived	Reporting Period 01.04.2025 to 30.06.2025		Since beginning of Commissioning Phase until 30.06.2025 (end of reporting period)	
		Number Tiles / Observations	Size (in GB)	Number Tiles / Observations	Size (in GB)
Earth Observation (EO)	Total	20631 / 2056	10052.82	194134 / 17596	94595.28
	Average / Day	226.71 / 22.59	110.47	163.55 / 14.82	79.69
Calibration (CAL)	Total	26	108.56	439	1833.14
	Average / Day	0.28	1.19	0.36	1.54

Table 6-1 Number and size of archived and not archived products (more than one version of the same image can be archived)

The following table shows the number of delivered products and their sizes within the specified time frames. Product deliveries result either directly from acquisition orders (“Acquisition”) or catalog orders (“Archive”).

Acquisition Type	Order Type		Reporting Period 01.04.2025 to 30.06.2025		Since beginning of Commissioning Phase until 30.06.2025 (end of reporting period)	
			Number Tiles / Observations	Size (in GB)	Number Tiles / Observations	Size (in GB)
Earth Observation (EO)	Acquisition	Total	22381 / 2071	9890.14	158249 / 14503	70126.03
		Average / Day	245.94 / 22.75	108.68	133.31 / 12.21	59.07
	Archive	Total	13650	5267.69	127806	48162.44
		Average / Day	150.0	57.88	107.67	40.57
Calibration (CAL)	Acquisition	Total	26	108.26	270	1150.32
		Average / Day	0.28	1.18	0.22	0.96
	Archive	Total	10	48.90	77	394.93
		Average / Day	0.10	0.53	0.06	0.33

Table 6-2 Number and size of delivered products

6.1 Archived Acquisitions

The following figures show the heatmaps for the whole world and for Europe within the specified time frames. The heatmaps represent the frequencies of products at a geographic location, where the number of products increases from blue over red to yellow.

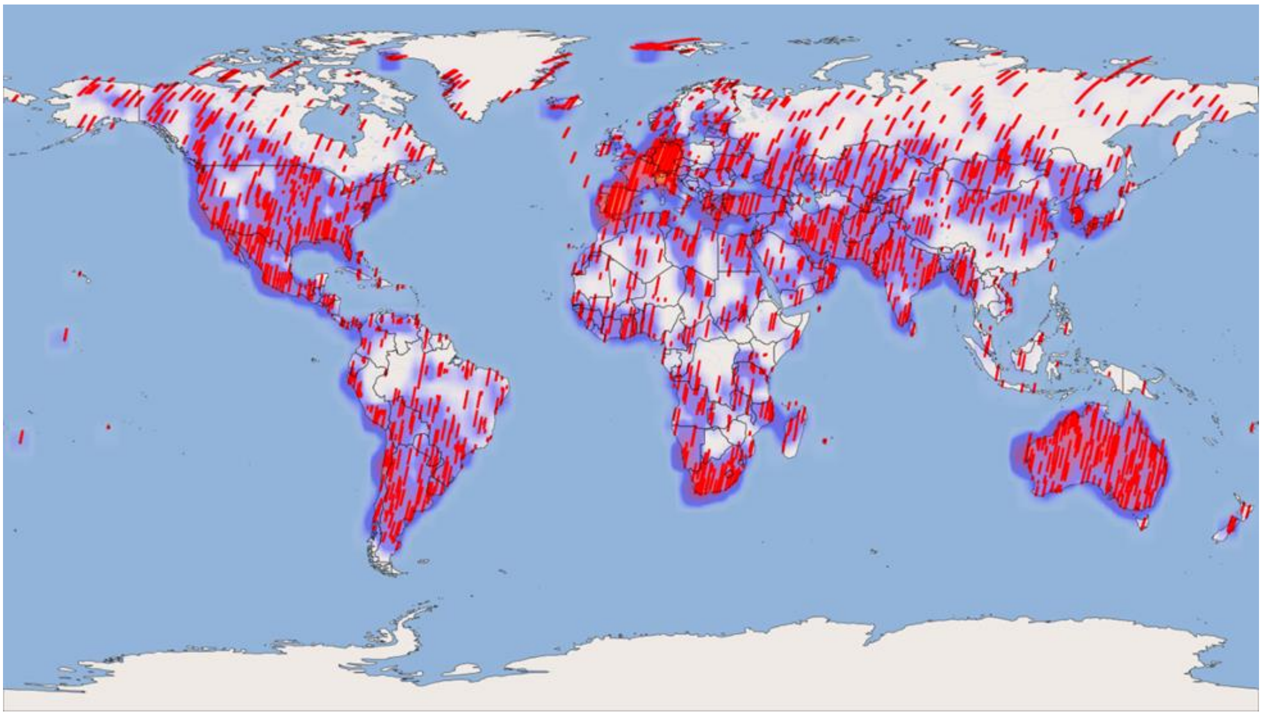

reporting period 01.04.2025 to 30.06.2025

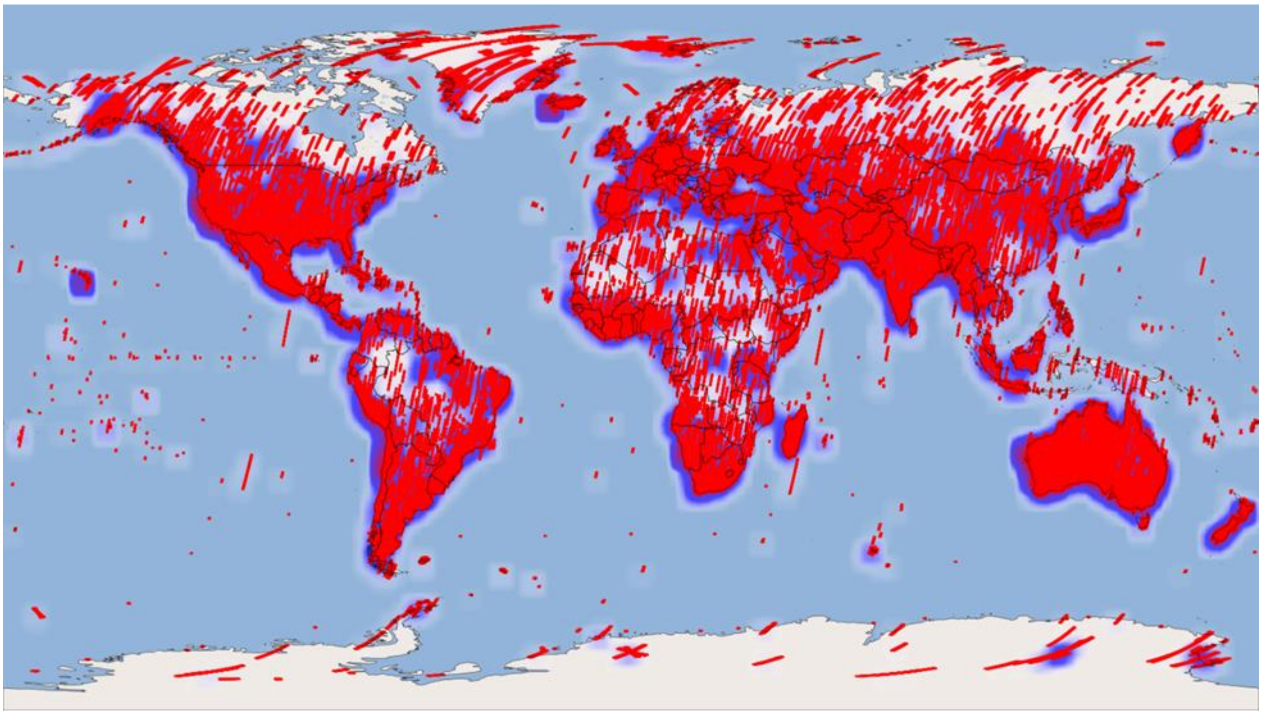

reporting period 2022-04-01 to 30.06.2025 includes commissioning phase acquisitions and different versions of the same tiles)

Figure 6-1 Geographic location of all Earth observation tiles archived, World

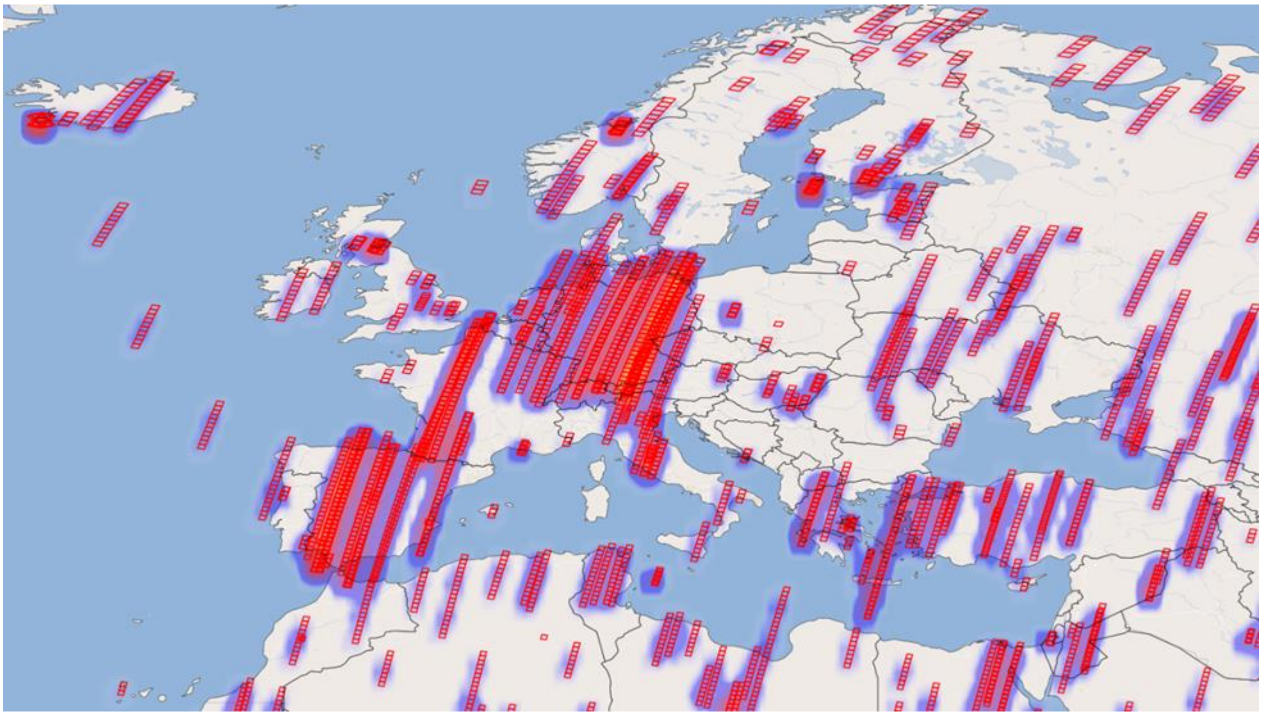

reporting period 01.04.2025 to 30.06.2025 Europe

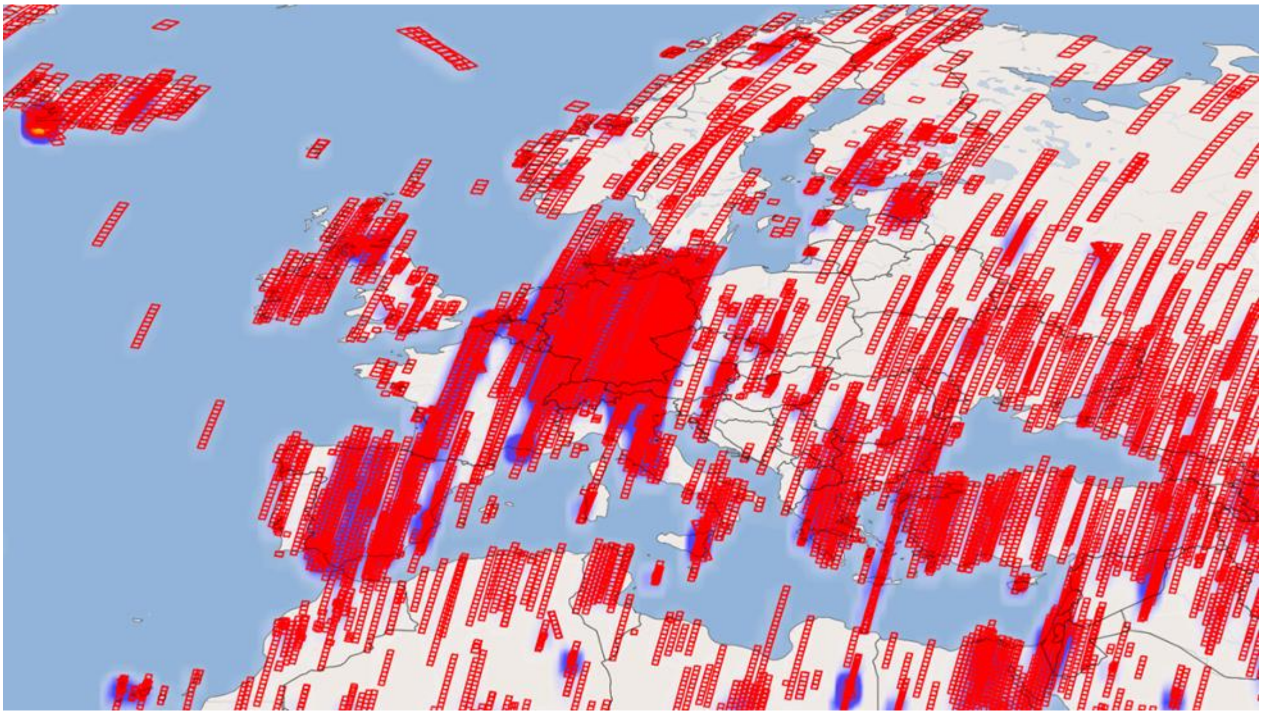

reporting period 2022-04-01 to 30.06.2025 Europe (includes commissioning phase acquisitions)

Figure 6-2 Geographic location of all Earth observation tiles archived, Europe

The following figures show the distribution of cloud coverage for the archived products.

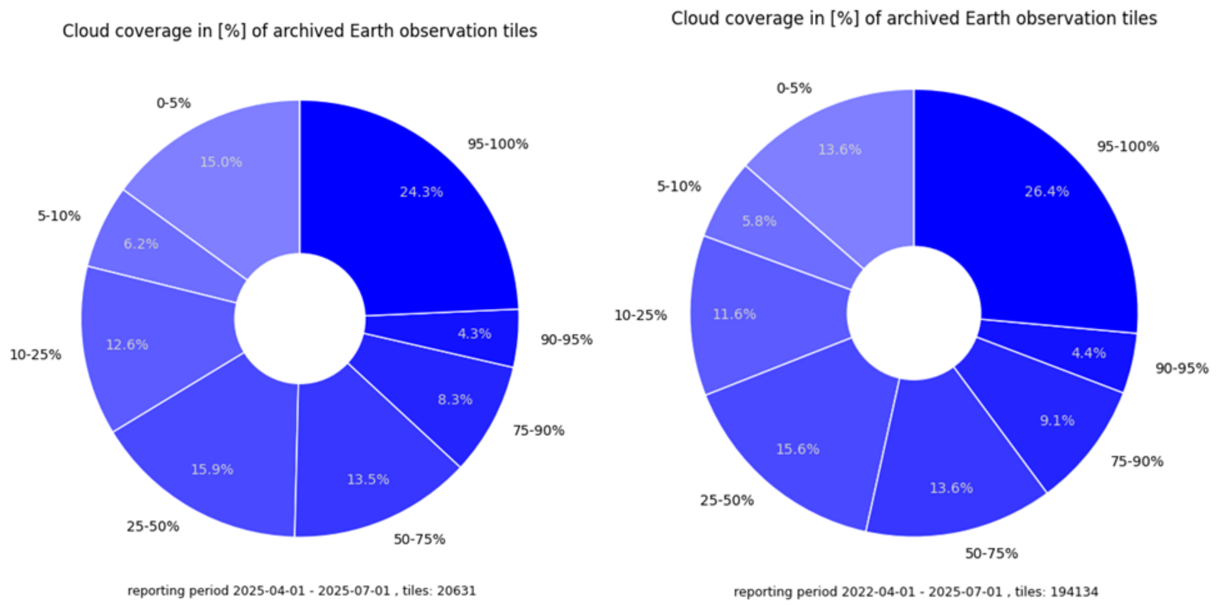

Figure 6-3 Cloud coverage in [%] of archived Earth observation tiles

The following figures show the distribution of observation angles for the archived products.

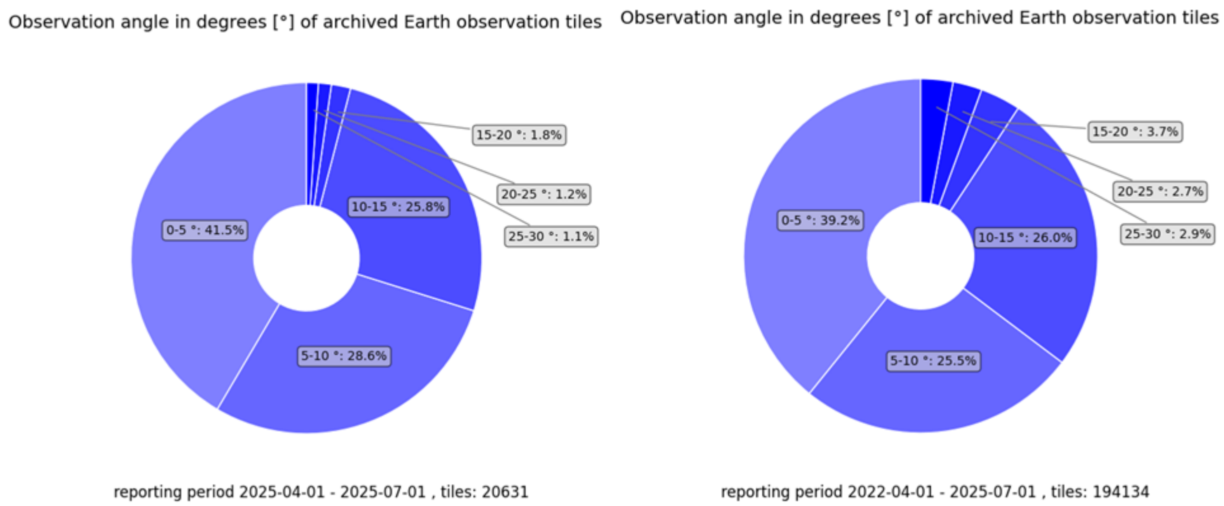

Figure 6-4 Observation angle of archived Earth observation tiles

6.2 Delivered Observations

The following figures show the distribution of processing level of the delivered products from acquisition orders.

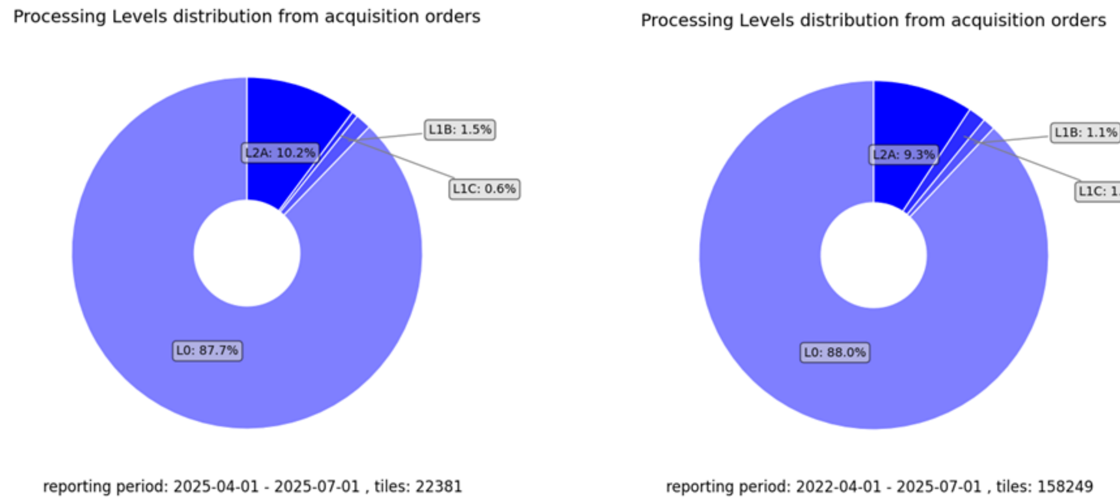

Figure 6-5 Levels of delivered Earth observation tiles from acquisition orders

The following figures show the distribution of processing level and correction type (for L2A) of the delivered products from catalog orders.

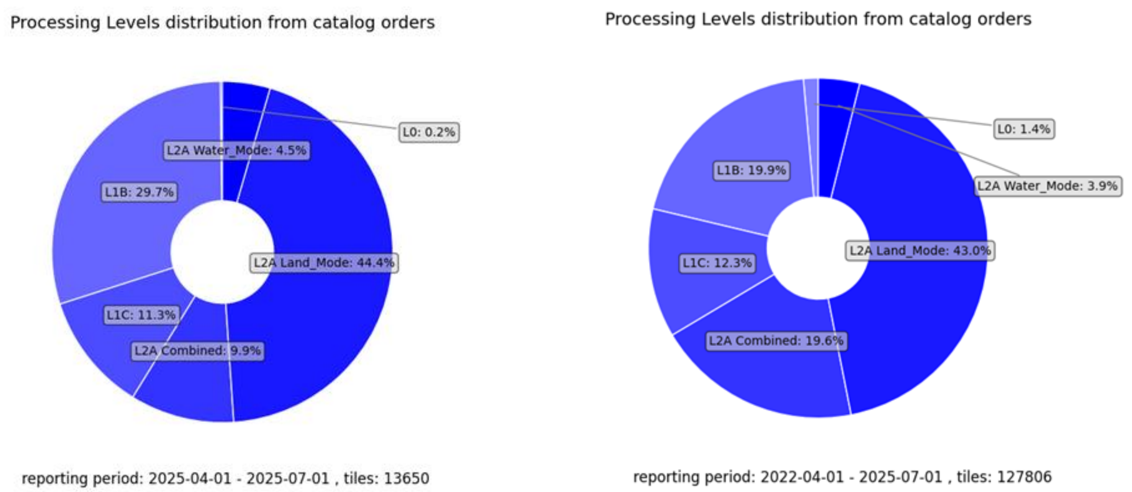

Figure 6-6 Levels of delivered Earth observation tiles from catalog orders

6.2.1 Delivered L2A products from the Download service (EOC Geoservice)

In order to reduce the workload of the system, the Ground Segment produces L2A products already processed with standard parameters that are available for direct download using the EOC Geoservice and the EOLab platform.

All recorded data is processed to L2A ARD format using EnMAP’s Ground Segment processors and default parameters, saving computational and waiting time. The default processing parameters of the L2A ARD are the following:

Product_Format = GeoTIFF+Metadata
Map Projection = UTM_Zone_of_Scene_Center
Image Resampling = Bilinear_Interpolation
Correction Type = Land_Mode
Cirrus Haze Removal = No
Band Interpolation = No
Terrain Correction = Automatic
Season = Automatic
Ozone column = Automatic

Table 6-3 Processing parameters used for the L2A ARD products in Geoservice / EOLab

In addition, take into account that:

- the versions of the L2A ARD products may differ depending on their generation time. The processor changelog (https://www.enmap.org/data/doc/EnMAP_processor_changelog.pdf) provides an overview of the software changes
- No L2A-water products are available as L2A ARD products in Geoservice. For the moment water processing is only available using the on-demand processing options in EOWeb.
- The L2A ARD archive is now complete. All the EnMAP products available in the Mission archive are available also as L2A ARD products at Geoservice / EOLab.

The total number of downloads using the EOC Geoservice is **871301** for this reporting period (01.04.2025 to 30.06.2025). Number of monthly downloads for this quarter are given in Table 6-4 and the graph with their evolution since the start of the service is shown in Figure 6-7.

Product	Month	# Downloads
ENMAP-L2A	2025-04	40689
ENMAP-L2A	2025-05	484787
ENMAP-L2A	2025-06	345825
Total in period		871301

Table 6-4 Absolut amount of downloads in Geoservice

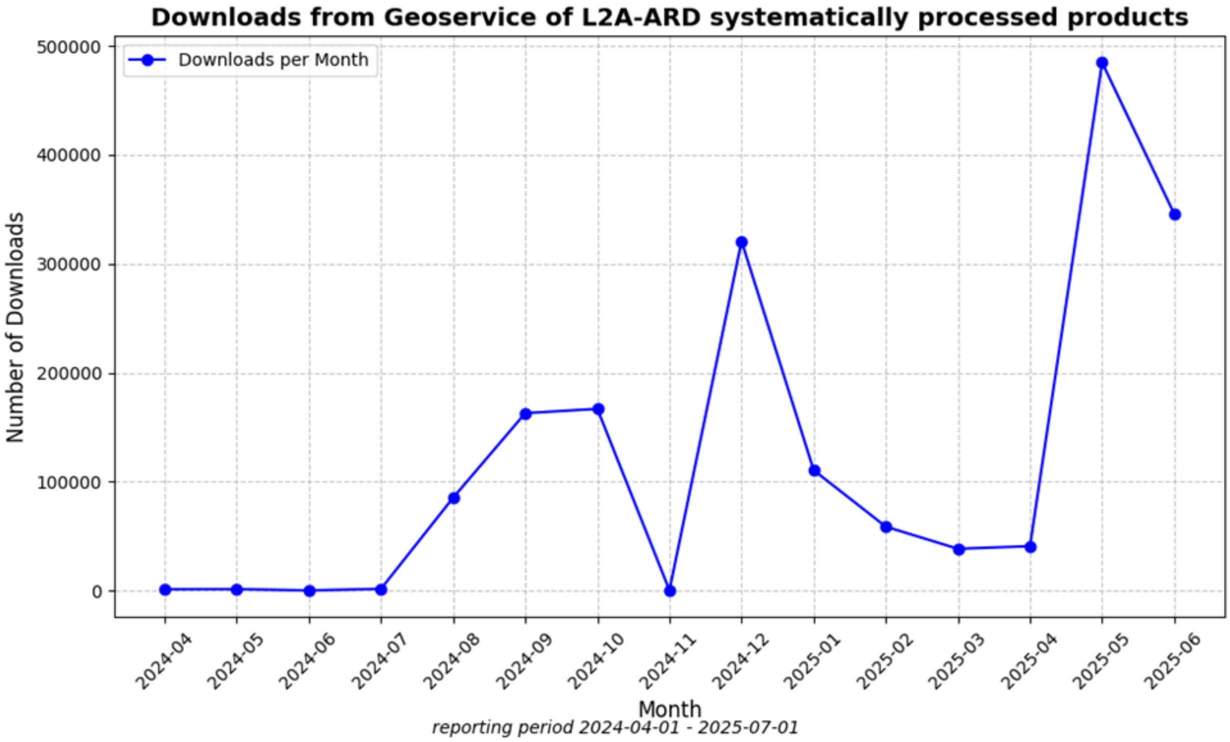

Figure 6-7 Downloads in Geoservice per month

7 Detailed Status

7.1 User Interfaces

Further improvements to the user interfaces are continuously on-going and will be reported in this section.

The Instrument Planning Portal has been updated to reflect changes in **proposal and announcement of opportunity (AO)** expiration dates. The update was implemented on June 3, 2025.

Since then, the following changes are in place:

- The maximum duration of a proposal is now 1 year
- Proposals that extend beyond 1 year require a new proposal submission
- New proposals shall be submitted to **AO#1**.
- The **AO#2** and **AO#3** are now set to expire on 30 June 2025.
- All granted proposals of AO#1 with valid contingent (=quota) will be prolongated until **Oct 2025**, even if the expiration date is before.
- The maximum possible end date of all future proposals and observations is the end of regular operations phase of the current mission lifetime (currently fixed for **30 April 2027**).

During the reporting period the Ground Segment of EnMAP continues to update the information on future high priority observations of the EnMAP mission (*Foreground Mission*). The tool displaying this information is available at the EnMAP web site under: https://www.enmap.org/data_tools/foreground_mission/

With this tool the users can get informed weeks in advance about future priority observations with EnMAP. Initially, a set of long flight-lines (990km) over Germany and other European countries have been identified together with the user community and will be regularly scheduled. Since July 2024, the Foreground mission has expanded to include additional European regions. The foreground mission returned during Q2 2025 to the usual focus in Germany and Europe, but it is expected that it shifts to southern Europe and the southern hemisphere during winter time.

7.2 Satellite

During the reporting period the mission has experienced 3 HSI SAFE_ERROR events that have resulted in the loss of observation time. The events took place on 09.05.2025, 06.06.2025 and 26.06.2025. In the first and third events, regular operations were resumed a few hours after detecting the event. The second event required a more detailed analysis and operations were resumed on 12.06.2025. As reported in all the previous events of this type, no consequences on the image or data quality are observed as a result of this events. For more details on data quality see sections 7.6 and 8.

The sporadic cancellation of acquisitions when the satellite is coming from the eclipse phase (known as “3-minute events”), has not been observed during the reporting period. It is expected that this known issue re-appears in the coming months given its connection with the Sun illumination during the different seasons of the year.

More details about different satellite aspects are reported in the following subsections.

7.2.1 Orbit

The reference orbit is a Sun-synchronous polar orbit with a mean local time of descending node of 11:00 hrs and a repeat cycle of 398 revolutions in 27 days at an altitude of 643 km.

The satellite orbit is controlled with respect to an Earth-fixed reference track over the entire orbit, analogous to a rim, with a control box of +/- 6 km in radial direction and +/- 22 km in normal direction.

During 2025 Q2, a total of 1780 ACS Precise Modes were executed onBoard, compared to 1357 during the previous quarter. Due to the implementation of Back-to-Back Image Acquisitions, the number of ACS

Precise Modes does not represent the number of performed activities. By executing two or three Images as one sequence, the total number of ACS Precise Modes decreases whereas the number of Image Acquisitions remains stable or increases. Over the whole mission, a total of 19535 ACS Precise Modes have been successfully executed.

During 2025 Q2, one in-plane and no out-of-plane maneuvers were executed. Two collision avoidance maneuvers were required, one for a close encounter with Fengyun-1C debris (NORAD-ID 30600) and one for a close encounter with an unknown object (000270416). The resulting performance error off all maneuvers was estimated by FDS to be between -3.2 % and -0.7 %. No actuations of the Ball Latch Valve or other OCS configuration changes were performed during 2025 Q2.

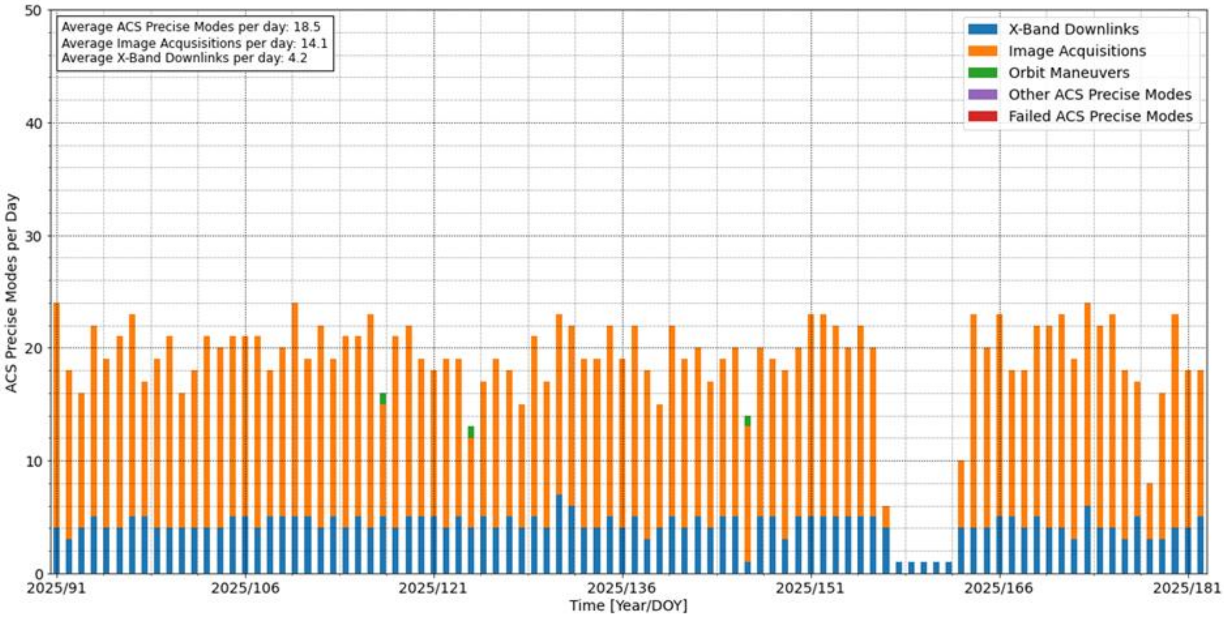

Figure 7-1 Number of ACS Precise Modes per day during Q2 2025

7.2.2 Life Limited Items

The life cycle of the life limited items is evaluated depending on their use. The life-limited items include the following optical and mechanical components:

Life-Limited Item	01.04.2025 to 30.06.2025	until 30.06.2025	Estimated minimum total lifetime / health of the system
Fuel(*)	+0,1 kg	8,4 kg	16.8 years
Battery and Solar Cells(**)	nominal	nominal	Nominal
Shutter Usage	+2,38%	20,56%	15,8 years (@ daily use)
FAD movements	+2,00%	29%	15,1 years (@ bimonthly use)
Diffuser exposure time based on sole measurement time(***)	+3,33%	48,33%	8,4 years (@ bimonthly use to reach 100% originally planned used)
Diffuser exposure time based on real cyclogram duration(***)	+3,99%	57,88%	6,8 years (@ bimonthly use to reach 100% originally planned used)
On-Board Calibration Equipment Usage	On-board calibration equipment:		
- OBCA SPC lamp 1	+1,20%	15,46%	19,4 years (@ biweekly use)
- OBCA RAD lamp 1/LED 1	+3,13%	31,83%	8,3 years (@ weekly use)
- FPA LEDs 1	+0,56%	7,30%	44,5 years (@ monthly use)

Table 7-1 Status of life-limited items

(*) During periods with higher temperature and pressure fluctuations due to e.g., an Instrument shutdown and startup, the calculation of the propellant mass via the Pressure-Volume-Temperature method contains a relatively large margin of errors.

(**) The Power Subsystem is working nominally and as expected. Voltage stays above any critical level.

(***) A 100% Sun diffuser exposure time corresponds to a total planned exposure of 2 hours after 5 years when performing monthly Solar calibrations. The contribution of the diffuser to the total radiometric uncertainty after reaching the reference 100% value is estimated to be **0.6%** according to the instrument manufacturer. This value is significantly below the 5% total radiometric uncertainty requirement, which indicates that the diffuser will not be a relevant contributor to the total radiometric uncertainty of the instrument even if the diffuser were to be used significantly above the originally allocated 2 hours of exposure time (reference 100% value). Nevertheless, the use of the diffuser is continuously monitored and accounted for in the Life-Limited Item list and thanks to the instrument stability the Sun calibration frequency is adjusted to reduce the number of necessary Solar calibrations.

The consumed resources (except fuel) are calculated based on the processed L0 product metadata, i.e. only successfully processed calibrations can be considered.

7.2.3 Redundancies

To date, the SWIR wavelength range is covered by SWIR-A (SWIR-B can be activated using a one-time switch mechanism).

All satellite subsystems are using nominal configurations.

7.3 Ground Stations

7.3.1 S-Band

S-Band Ground Stations	01.04.2025 to 30.06.2025		
	Total Passes	Non-Routine Passes (e.g. Anomaly Handling/SW Updates)	Failed Passes
All stations (Weilheim-Germany, Neustrelitz-Germany, Inuvik-Canada, O’Higgins-Antarctica, Svalbard-Norway)	565 (157 WHM, 248 NSG, 160 INU)	8	0

Table 7-2 S-Band Ground Station Passes

7.3.2 X-Band

X-Band Ground Stations	01.04.2025 to 30.06.2025	
	Executed Passes	Successful Passes
All stations (Neustrelitz-Germany, Inuvik-Canada)	381 (279 NZ, 102 INU)	381 (279 NZ, 102 INU)

Table 7-3 X-Band Ground Station Passes

Inuvik (Canada) station was integrated in Q4 2023 into the regular operations of the EnMAP Ground Segment for X-Band and S-Band downlinks. After integration, more data and more flexibility in S-band and X-band data reception is achieved, especially concerning image acquisitions over Europe.

7.4 Processors

Reference [3] provides the product specification and [4], [5], [6], [7] the algorithm theoretical basis for Level 1B, Level 1C and Level 2A (land / water).

During Q2 2025, the change log documenting the history of EnMAP processor updates continues to show the updates performed in the processing software. The document can be downloaded from the EnMAP website:

https://www.enmap.org/data/doc/EnMAP_processor_changelog.pdf

In the reporting period (01.04.2025 to 30.06.2025) there have been no updates in the EnMAP processing chain. The latest version of the EnMAP processing software continues to be version **V01.05.02**.

The following limitations are applicable as of 30.06.2025:

- The SWIR-A compressor cooler produces a micro-vibration pattern of horizontal stripes on SWIR bands with strong spectral gradients. All spectral and radiometric requirements are within the specification of the mission, but a correction has been investigated and tested extensively. Because the implementation of a solution to correct this effect always creates side effects on the image data, it has been decided within the EnMAP mission that no correction will be implemented on the processor for this effect. Instead, the correction will be provided within a future version of the EnMAP Box software, for the interested users to check the effect on their data and decide if they apply the correction or not on their analysis.

The following changes are expected to be performed in the future quarters:

- Update of the linearity calibration to improve the matching between VNIR and SWIR spectrometers, specially at low radiance level.

7.5 Calibrations

Table 7-4 summarizes the radiometric calibration observations acquired in this quarter and which will be described in the rest of this section. The calibration acquisitions were generally acquired according to the routine operations plan.

Category	01.04.2025 to 30.06.2025	
	Number of Archived Observations	Size (in GB)
Total	26	109.7
Deep Space	3	3.9
Rel. Radiometric	12	46.8
Abs. Radiometric	2	2.6
Linearity	3	51
Spectral Calibration	6	5.4

Table 7-4 Number and size of archived radiometric and spectral calibration observations

The continuous degradation of the VNIR sensor was monitored and quantified. The rate of degradation is constantly decreasing as illustrated in Figure 7-2 and by the end of March 2023 it has reached the point where it is practically negligible and has been kept that way during the reporting period. It shall be noted, though, that this average trend is different at different parts of the detector as illustrated for individual pixels in Figure 7-3. The effect on the radiometric calibration coefficients of a few selected bands is shown in Figure 7-4.

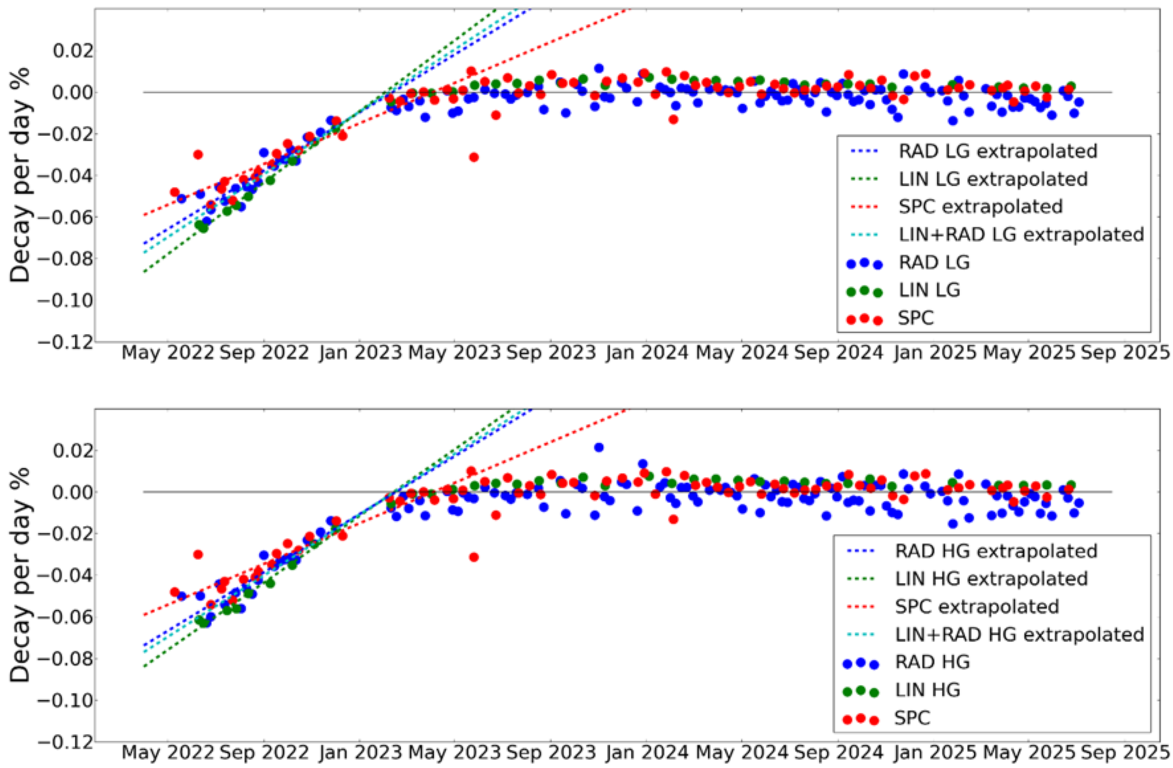

Figure 7-2 Decay per day from Lamp (RAD), Linearity (LIN) and Spectral (SPC) measurements for low gain (top) and high gain (bottom)

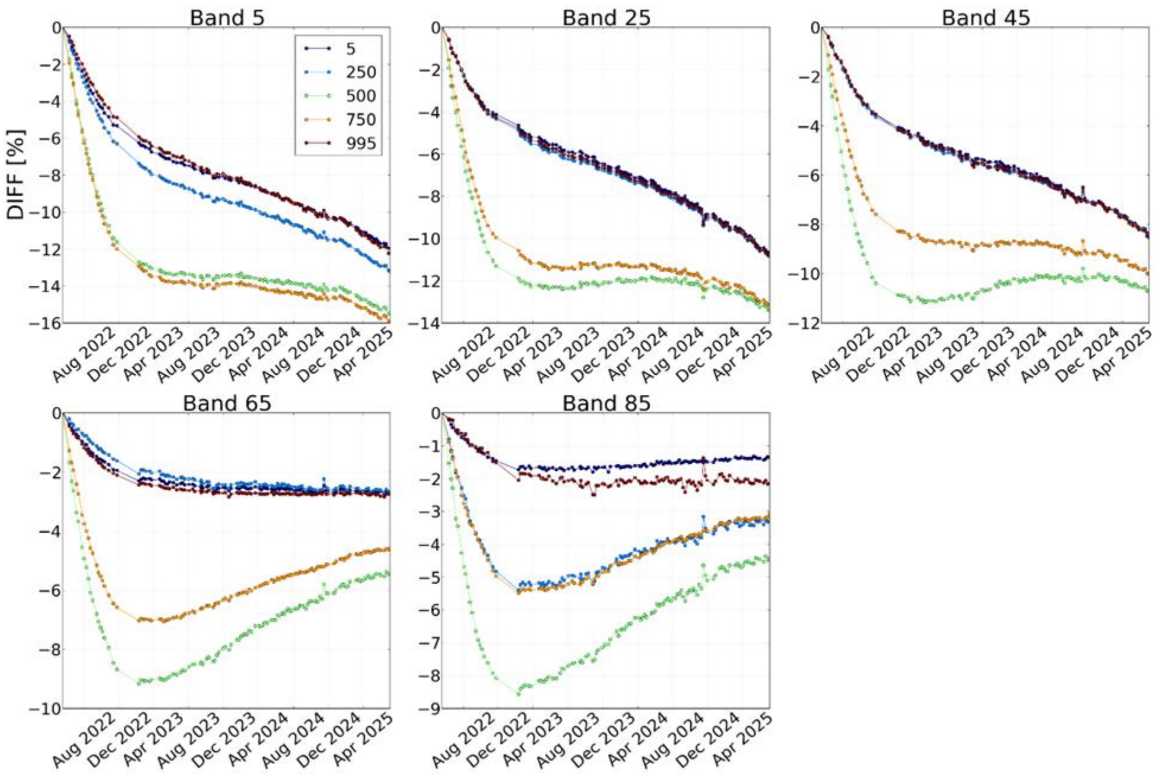

Figure 7-3 Change in percentage for individual pixels based on OBCA-Lamp measurements given for 5 bands and 5 cross track elements (coloured lines).

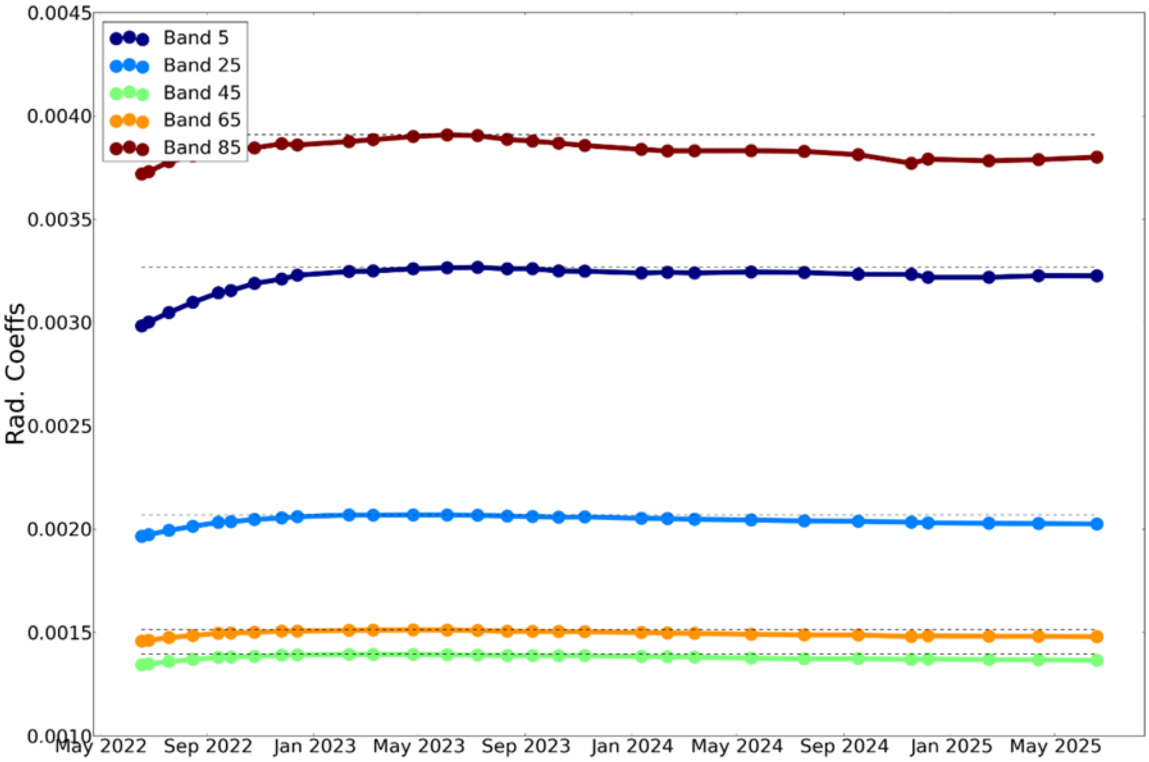

Figure 7-4 Average percentage change in the VNIR radiometric coefficients for five selected bands since launch

7.5.1 Dead Pixels

The following table shows the number and percentage of dead pixels. Figure 7-5 and Figure 7-6 show the position of the dead pixels in the focal plane of VNIR and SWIR sensors respectively. There have been no updates since 31.08.2022.

Defect Pixels	01.04.2025 to 30.06.2025	
	Number of Pixels	Percent
Total	1921	0.8
VNIR	137	0.2
SWIR	1784	1.2

Table 7-5 Number and percent of dead pixels

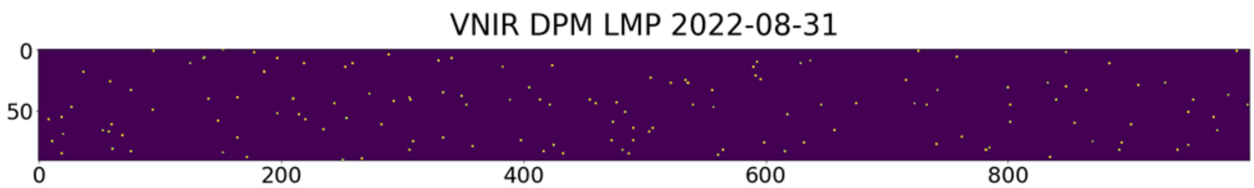

Figure 7-5 VNIR Dead Pixel Mask

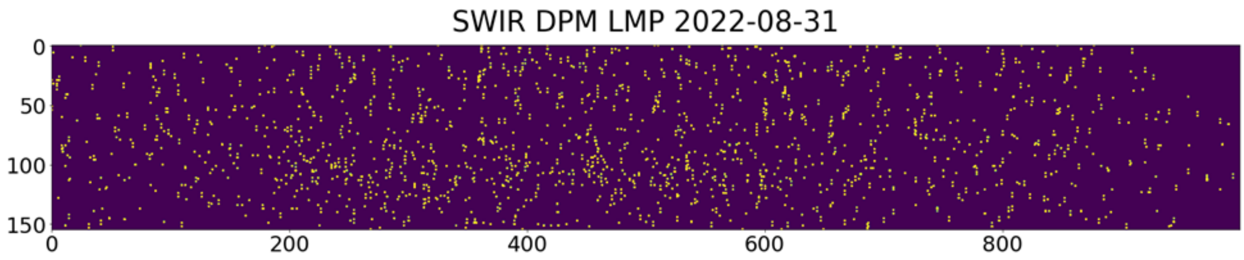

Figure 7-6 SWIR Dead Pixel Mask

There are no clusters of more than three spectrally or spatially adjacent dead pixels.

7.5.2 Spectral Calibration

Remark: In the following figures, OBCA is abbreviation for On-Board Calibration Assembly for spectral and radiometric calibrations.

Category	01.04.2025 to 30.06.2025	
	Number of Archived Observations	Size (in GB)
Total	6	5.4
Spectral Calibration	6	5.4

Table 7-6 Number and size of archived spectral calibration observations

The spectral properties – in particular center wavelength (CW) (see Figure 7-7 and Figure 7-8) and full width at half maximum (FWHM) (see Figure 7-9) for each band (spectral coordinate) and pixel (spatial coordinate) – have been characterized, considering all bands and pixels provided in Level 1B, Level 1C and Level 2A products.

The major conclusions of the monitoring of the spectral performance are summarized as follows:

- During the reporting period, 6 spectral calibration measurements were made which took place on: 04.04.2025, 11.04.2025, 25.04.2025, 09.05.2025, 24.05.2025 and 20.06.2025.
- The VNIR spectral range in this reporting period was found to be 418.5 – 993.4 nm over 91 bands (Figure 7-7). The average spectral sampling distance was 6.4 nm with a total range of 4.7 – 8.2 nm. This meets the requirement for overall wavelength coverage [HSI-POSS-0210], average spectral sampling distance [HSI-POSS-0310] and spectral sampling distance range [HSI-POSS-0320].
- The SWIR spectral range in this reporting period was found to be 902.2 – 2445.5 nm over 155 bands (Figure 7-7). The average spectral sampling distance was 10.0 nm with a total range of 7.5 – 12.0 nm. This meets the requirement for overall wavelength coverage [HSI-POSS-0210], average spectral sampling distance [HSI-POSS-0310] and spectral sampling distance range [HSI-POSS-0320].
- The spectral calibration measurements from this quarter show good temporal stability – measurements showed an absolute <0.16 nm change from the VNIR sensor and <0.35 nm change in SWIR (Figure 7-8) with respect to current spectral calibration table. All changes were below 0.5 nm between measurements for VNIR and below 0.5 nm SWIR. This meets the requirement for consecutive spectral stability [HSI-POSS-0510] and overall spectral stability [HSI-POSS-0520].
- FWHM for VNIR and SWIR (Figure 7-9) are shown below but are not recalculated inflight.
- A VNIR degradation pattern is not clearly visible between consecutive spectral reference measurements acquired in this period, but there are positive and negative changes across the detector and on average the signal appears to have increased by 0.04% across all pixels from 28.03.2025 to 20.06.2025. A slightly smaller change was reported in the previous quarter (0.16%). Although small, the monitoring of this behavior will continue in the next reporting period.

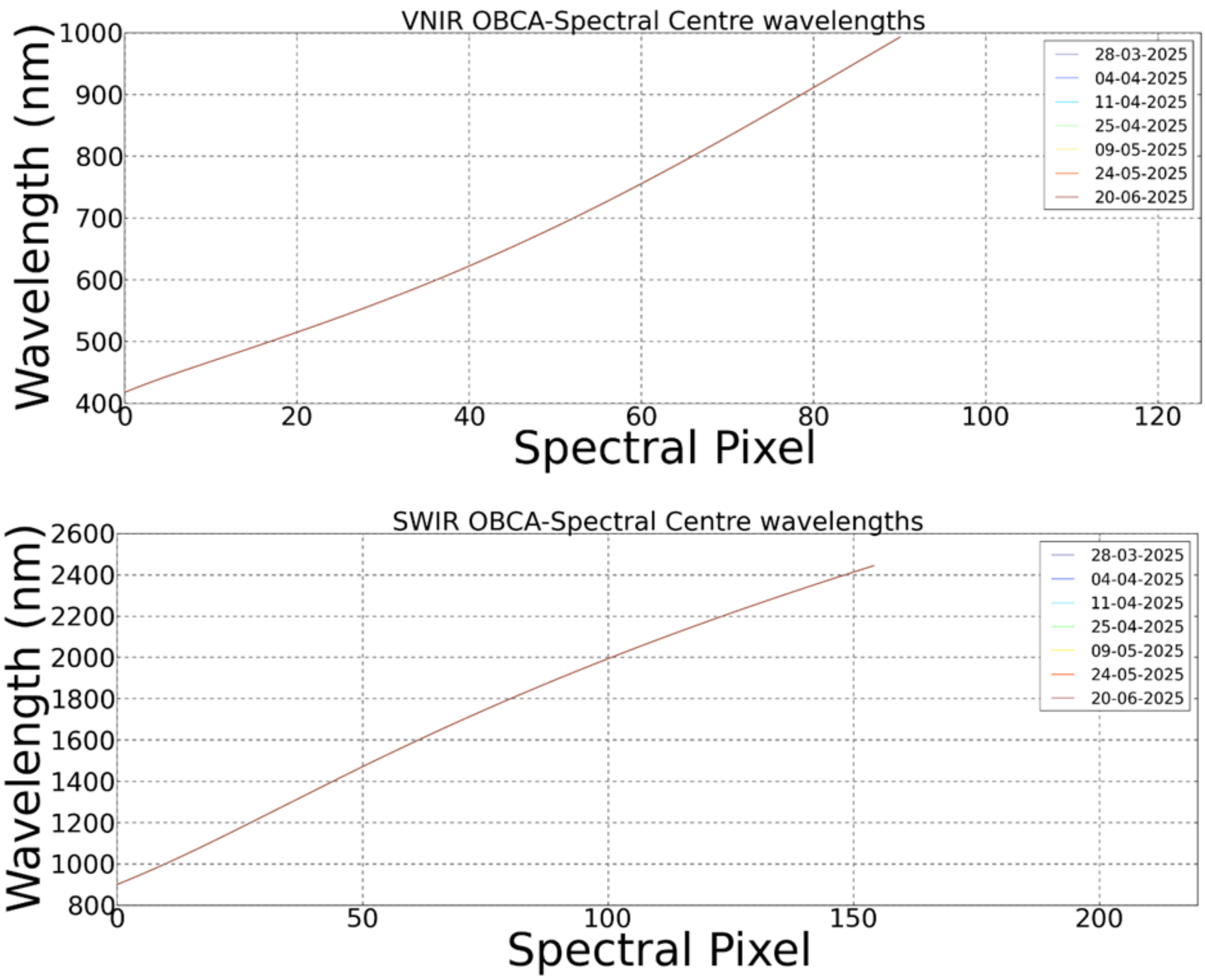

Figure 7-7 VNIR (top) and SWIR (bottom) center wavelength in nm

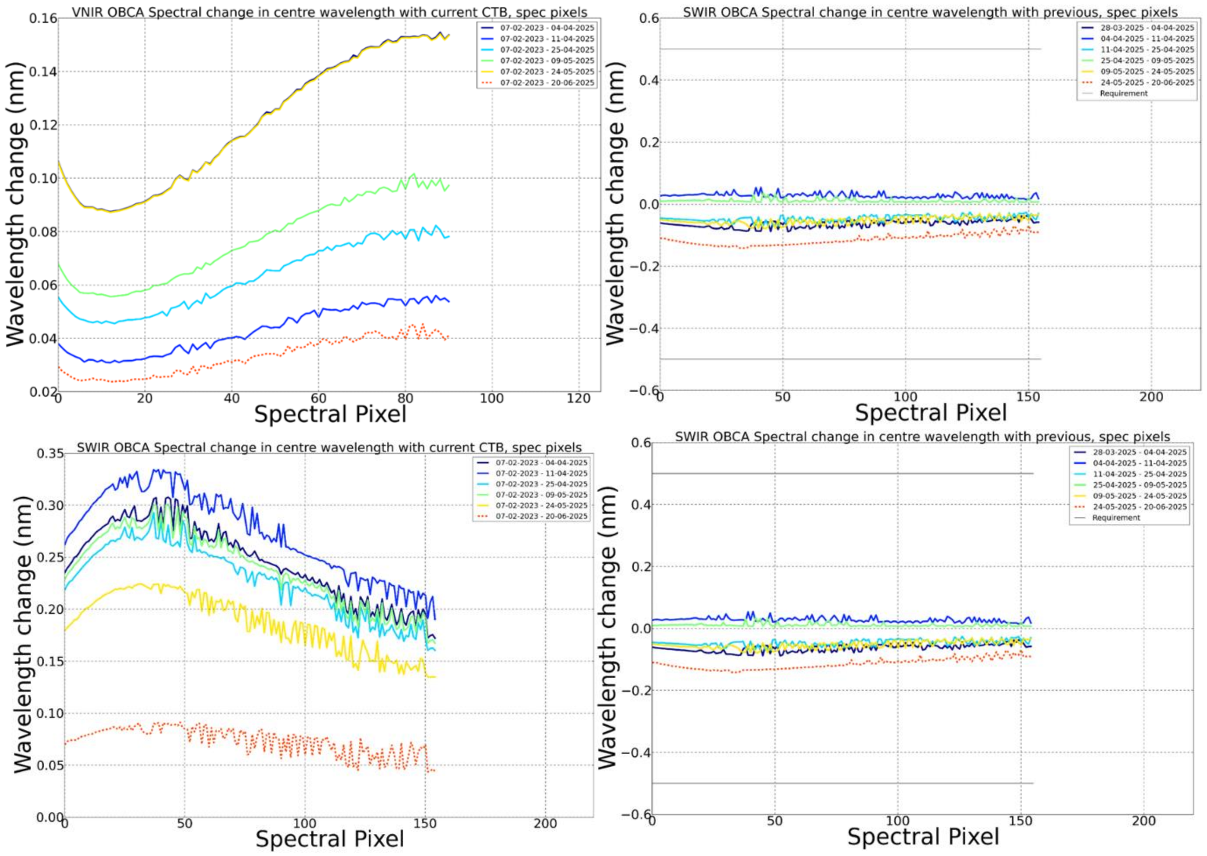

Figure 7-8 Change in center wavelength per spectral pixel for VNIR (top) and SWIR (bottom). Left panels show the changes with respect to current spectral calibration table in use and right panels with respect to the previous measurements.

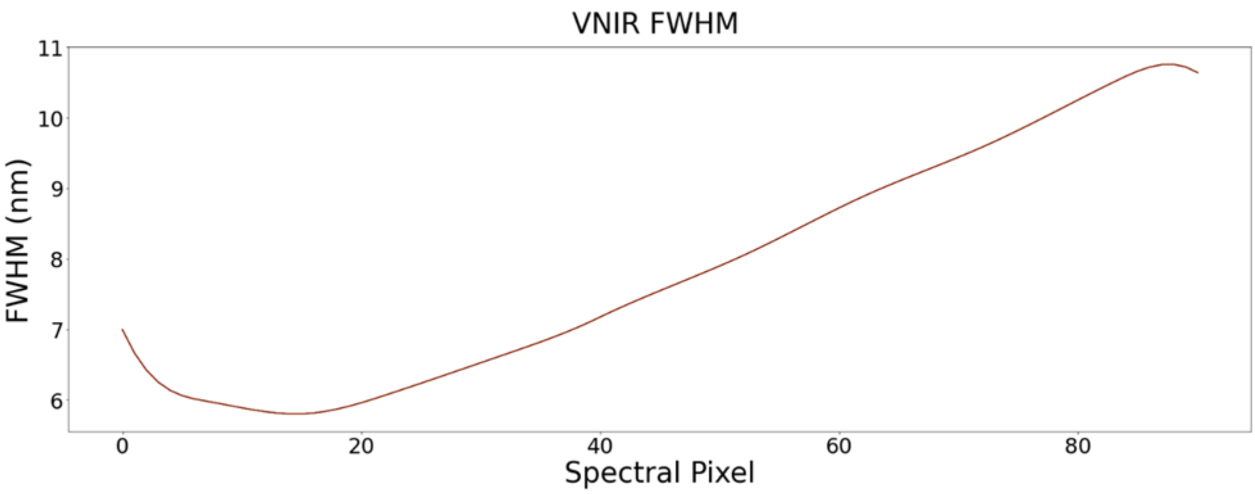

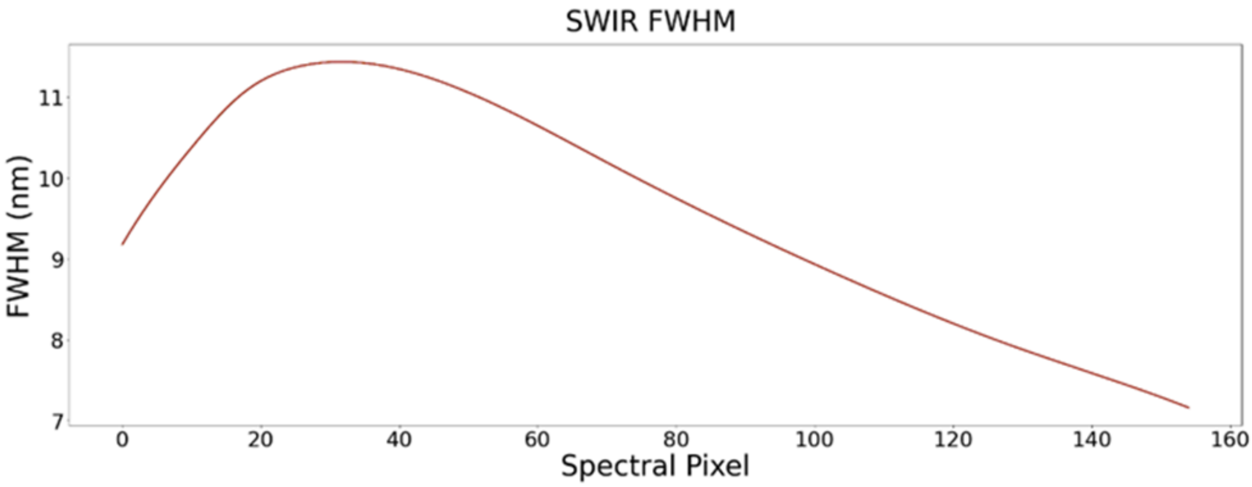

Figure 7-9 VNIR (top) and SWIR (bottom) FWHM in nm

CW and FWHM are available in the spectral calibration tables (see Table 7-7) and System Response Functions (SRF) per band are modelled by a Gaussian shape using those parameters.

Spectral calibration updates

No new calibration products were generated and delivered during the reporting period.

Product	Type	Date of Generation	Date of Validity Start	Date of Validity End	Delivered to

Table 7-7 Generated spectral calibration tables

7.5.3 Radiometric Calibration

Category	01.04.2025 to 30.06.2025	
	Number of Archived Observations	Size (in GB)
Total	20	104.3
Deep Space	3	3.9
Rel. Radiometric	12	46.8
Abs. Radiometric	2	2.6
Linearity	3	51

Table 7-8 Number and size of archived radiometric calibration observations

The radiometric properties – characterized in particular by the calibration coefficient for each band (spectral coordinate) and pixel (spatial coordinate) and radiance – during this reporting period are investigated, considering all bands and pixels and radiances provided in Level 1B, Level 1C and Level 2A products.

Radiometric calibration coefficients (see Figure 7-10, Figure 7-11 and Table 7-10) and VNIR RNU (response non-uniformity, see Figure 7-13) were affected by the degradation of the VNIR sensor during commissioning but have stabilized from Q1 2023. In-flight, the gain matching coefficients (see Figure 7-12), the SWIR calibration coefficients, and the SWIR RNU (response non-uniformity, see Figure 7-13) have been stable.

During the reporting period, 2 Absolute Radiometric Calibration measurement was obtained. These took place on: 12.04.2025 and 18.06.2025.

Albeit now relatively small in magnitude, changes in the VNIR sensor have led to the creation of new calibration and reference tables for the new absolute radiometric measurement.

Although the VNIR degradation has almost stopped, the overall effects are visible in the reference measurements of the sun. However geometric conditions (sun-earth distance, pointing angle) also play a role in the absolute magnitude so the degradation cannot be quantified with these reference measurements.

The major conclusions of the monitoring of the absolute performance is summarized as follows:

- Changes in the VNIR sensor have affected the absolute Radiometric calibration coefficients: the increasing signal in the VNIR sensor, although not homogeneous, has resulted in decreasing radiometric coefficients. In this reporting period, the calibration coefficients decreased by about -0.12% to offset the increase in absolute (Figure 7-10 and Figure 7-11). Regarding RNU, the degradation features are still visible in the focal plane (Figure 7-13). Lastly, the Gain Matching correction has been relatively stable during this reporting period (Figure 7-12).

- The SWIR sensor has shown good stability during this reporting period, with no significant changes in the gain matching, RNU or radiometric calibration coefficients (Figure 7-10 and Figure 7-11).

- Regarding the total change in calibration corrections as a result of the VNIR degradation, almost all pixels experienced a change of less than 2.5% between consecutive measurements as set in requirement [HSI-POSR-0410]. The only pixels which exceeded this value were already marked as dead during inflight assessment. No SWIR pixels experienced a change of more than 2.5% between consecutive absolute calibration measurements.

- New VNIR and SWIR calibration and reference tables were created for the absolute radiometric measurements from 12.04.2025 and 18.06.2025 (validity starting in Q3 2025), mainly due to the changes in the VNIR sensor. The VNIR radiometric calibration coefficients have decreased in this reporting period to offset the increasing VNIR signal. The changes are small, and within requirements, so the dynamic coefficients are not calculated and calibration coefficients are taken directly from the most recent calibration table as envisioned at the beginning of the mission.

- Since April 2024, Absolute Radiometric Calibration measurements are planned at intervals of two months, following the stable performance of both sensors, and to allow for the extension of the lifetime of the solar diffuser.

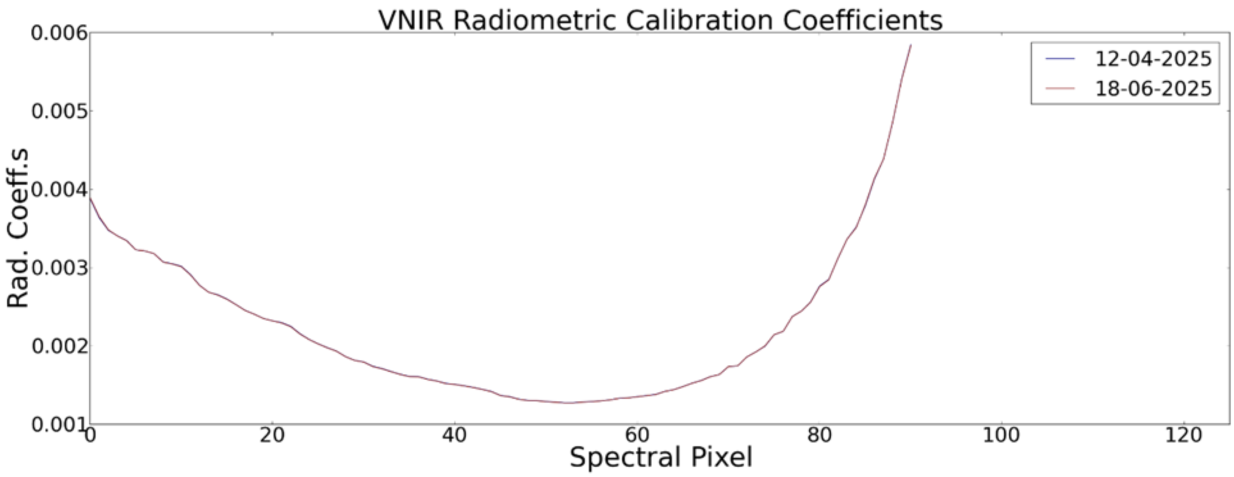

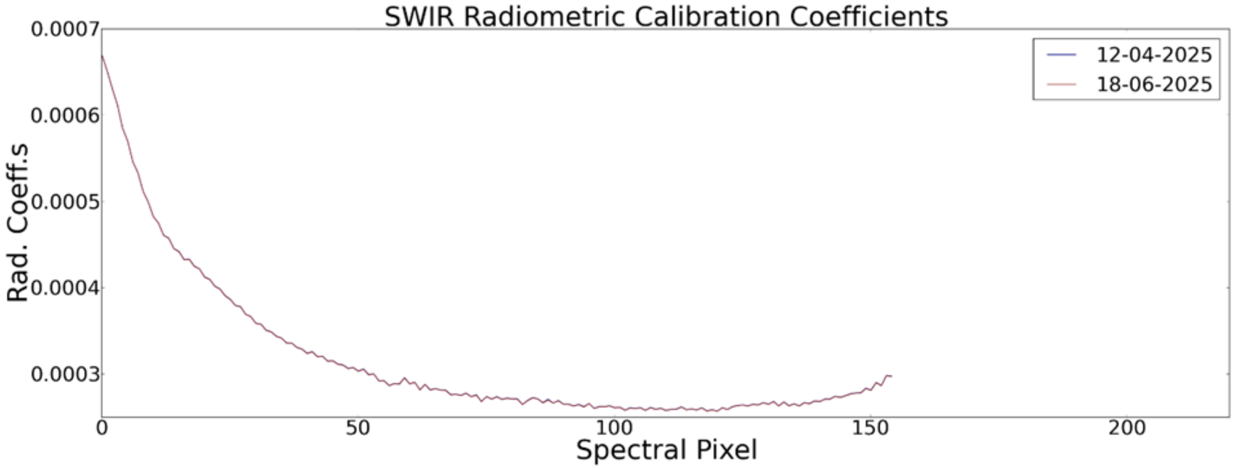

Figure 7-10 VNIR (top) and SWIR (bottom) calibration coefficient in mW/cm^2/sr/µm

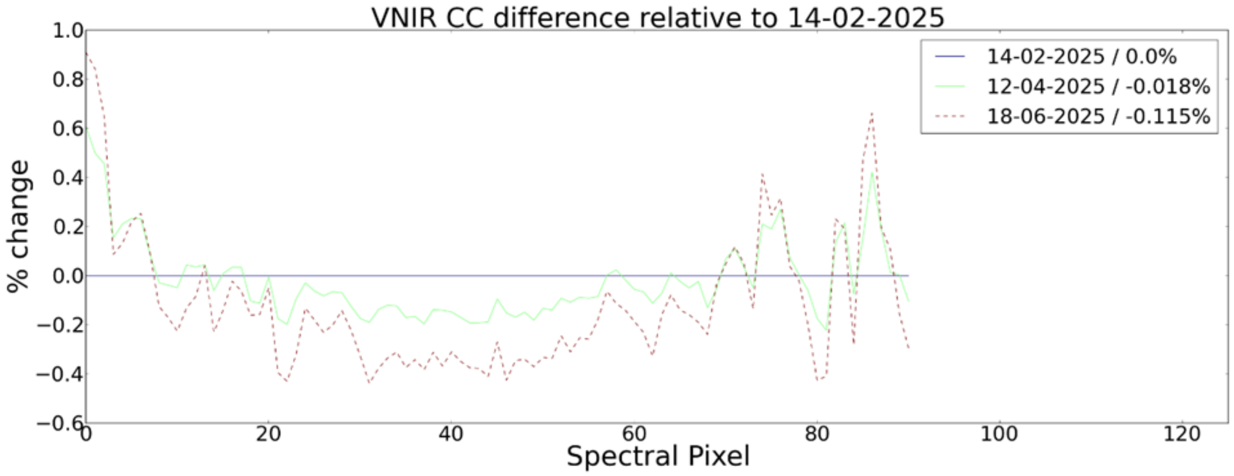

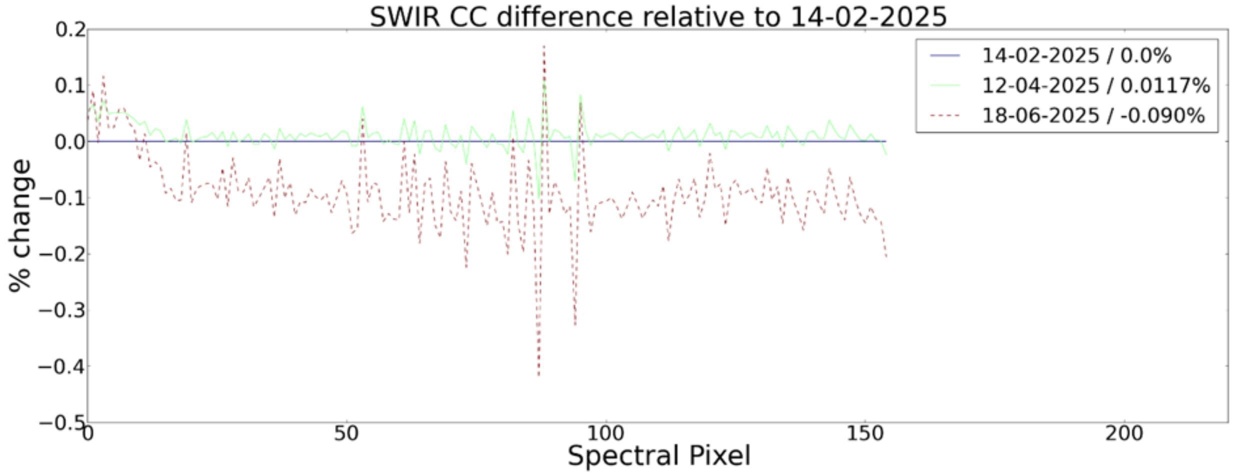

Figure 7-11 Percentage change in VNIR Calibration Coefficients (top) and SWIR Calibration Coefficients (bottom)

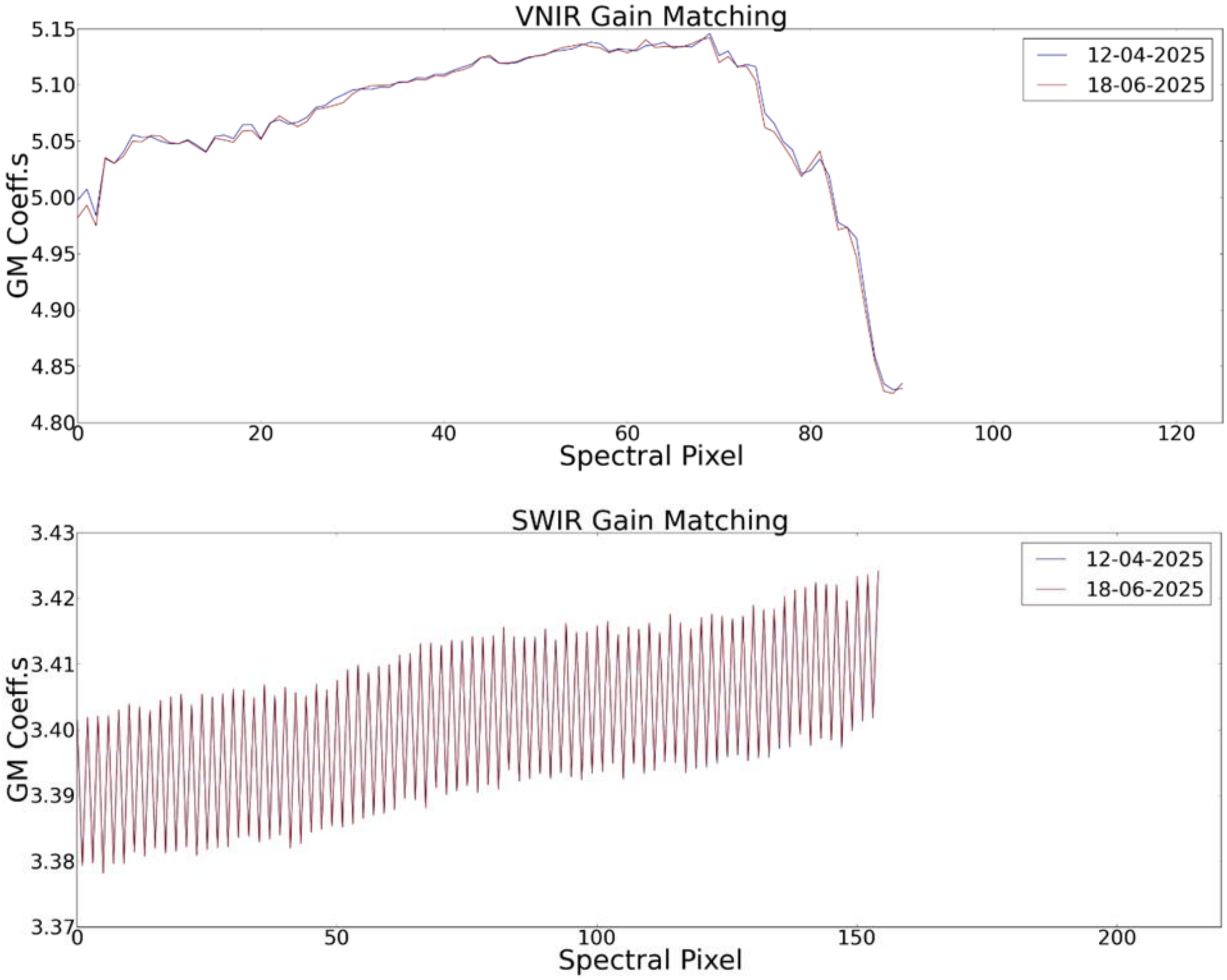

Figure 7-12 VNIR (top) and SWIR (bottom) gain matching calibration coefficients

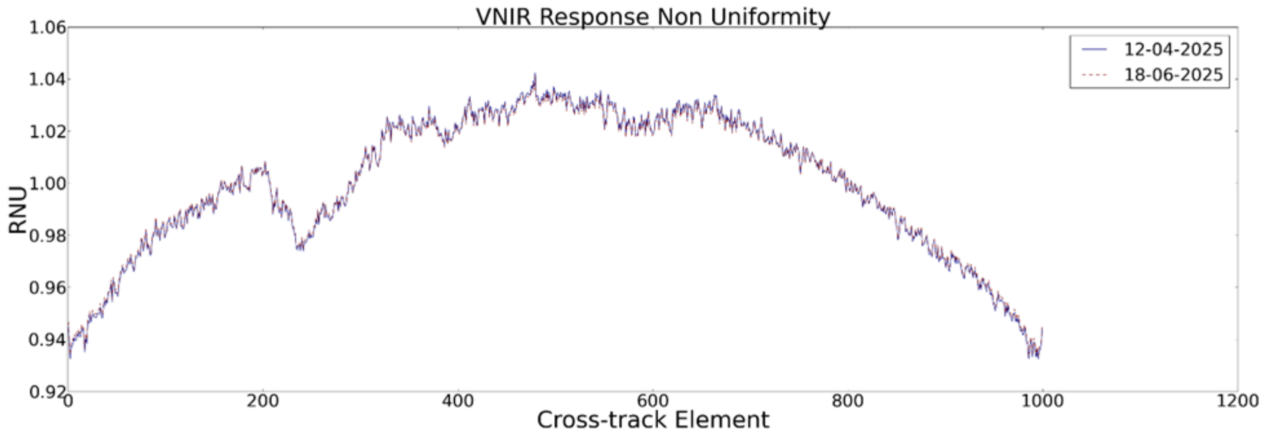

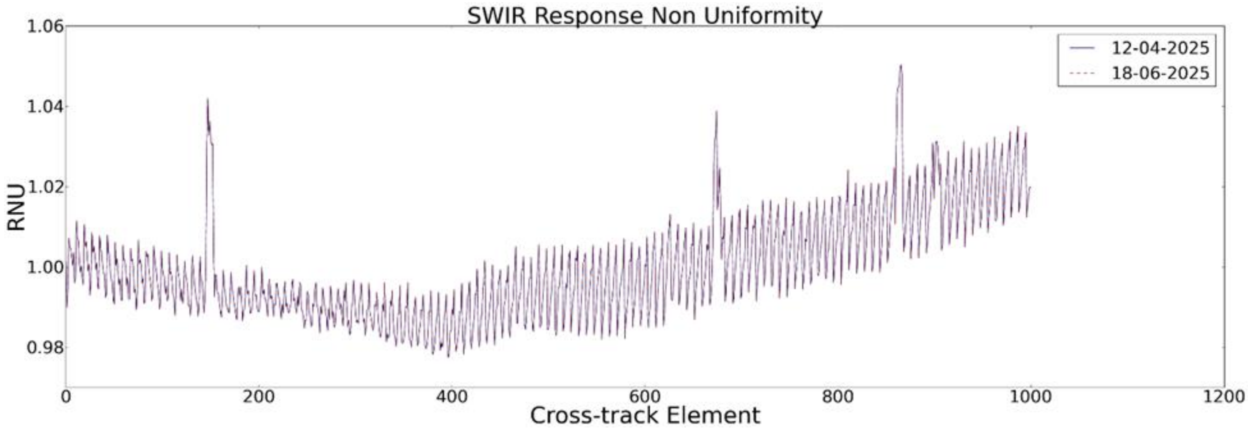

Figure 7-13 VNIR (top) and SWIR (bottom) response non-uniformity coefficients

Signal-to-Noise Ratio

The Signal-to-Noise Ratio (SNR) is derived from the Linearity reference measurements. This is not a perfect set-up for the assessment of the SNR as the linearity measurements only cover a single wavelength and light level at increasing integration times. However, it is well constrained, covering a wide range of radiances including the levels of the reference radiance spectrum that is used to evaluate the requirements (30% reflectance, 30° sun incidence angle, 21 km visibility, target 500 m above sea level). The lamp reference measurements are not used, as the reference spectrum is not well covered at the radiances of the lamp and extrapolation would be required to test the performance at the SNR requirements. Those requirements are: SNR greater than 500 at 495 nm in VNIR for the reference spectrum value given a 10 nm pixel; and SNR greater than 150 at 2200 nm in SWIR for the reference spectrum given a 10 nm pixel.

For the VNIR sensor, SNR is computed from the linearity calibration measurement. SNR values are shown as a contour map with the reference radiance spectrum as a blue line. Contour lines with SNR values of 150 and 500 are also shown in black. The plot in low gain mode includes the mission requirement which is evaluated at 495 nm for a radiance value of 36 mW/cm^2/μm/sr and is expected to be greater than 500: the calculated value here is **597**. The radiance value used here for the evaluation is the value at 495 nm of the reference radiance spectrum after bandwidth normalization to a 10 nm pixel (see Figure 7-15).

For the SWIR sensor, SNR is also computed from the linearity calibration measurement. SNR values for the high gain mode are shown as a contour map with the reference radiance spectrum as a blue line. Contour lines with SNR values of 150 and 500 are also shown in black. The plot in high gain mode includes the mission requirement which is evaluated at 2200 nm for a radiance value of 0.5 mW/cm^2/μm/sr and is expected to be greater than 150: the calculated value here is **200**. The radiance value used here for the evaluation is the value at 2200 nm of the reference radiance spectrum after bandwidth normalization to a 10 nm pixel (see Figure 7-16).

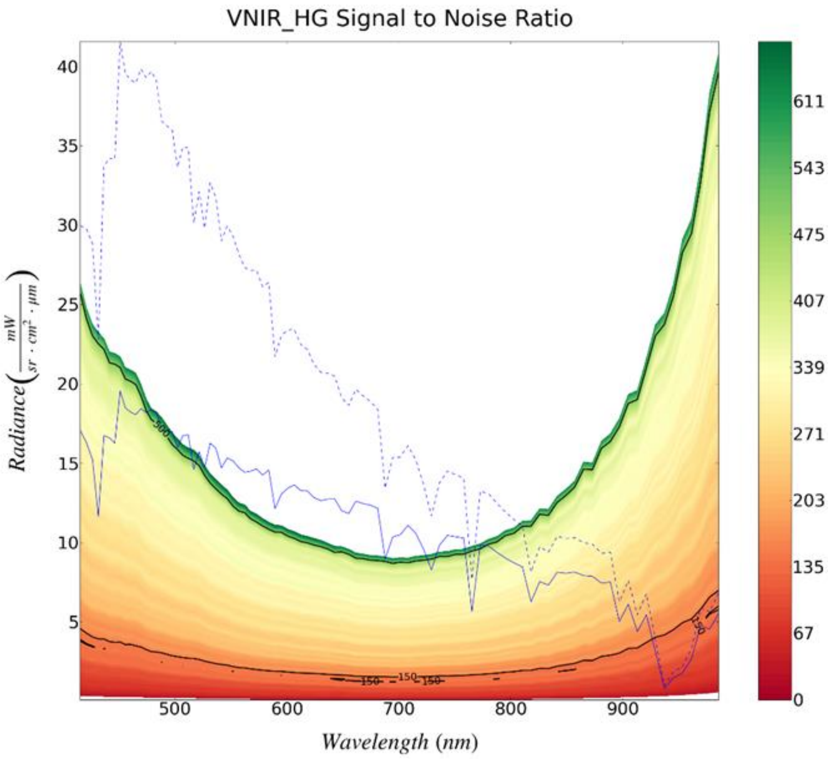

Figure 7-14 SNR contour map for VNIR high gain from the LED linearity observations observed on 23.06.2025. The reference radiance is shown with a blue line and after bandwidth normalization to a 10 nm pixel (dotted). Contour lines with SNR values of 150 and 500 are also shown in black.

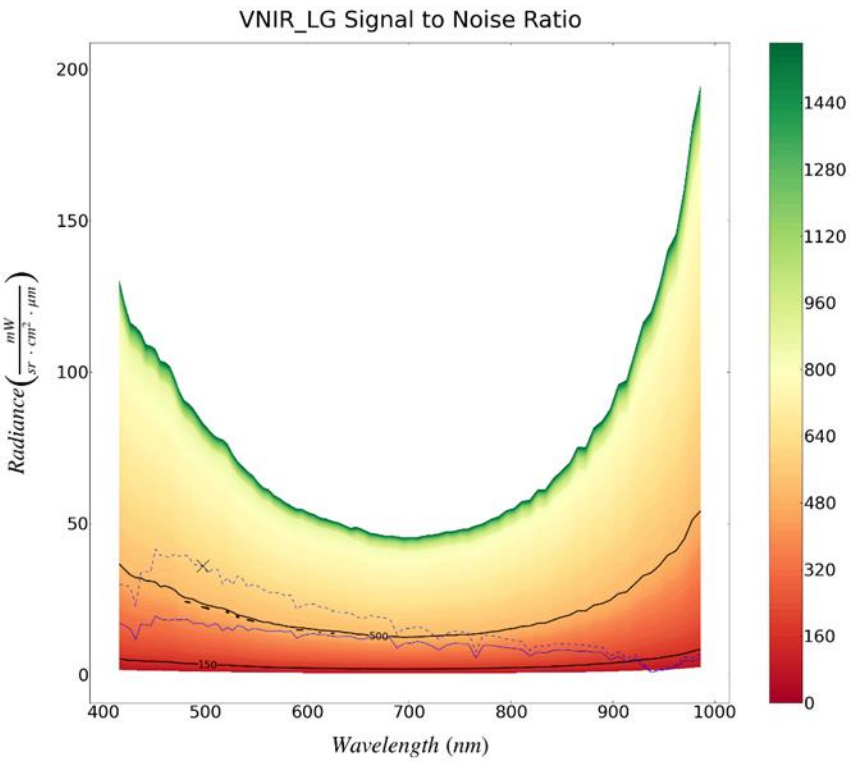

Figure 7-15 SNR contour map for VNIR low gain from the LED linearity observations observed on 23.06.2025. The reference radiance is shown with a blue line and after bandwidth normalization to a 10 nm pixel (dotted). Contour lines with SNR values of 150 and 500 are also shown in black. The mission requirement is evaluated at 495 nm for a radiance value of 36 mW/cm^2/μm/sr (marked with a black cross) and is expected to be greater than 500.

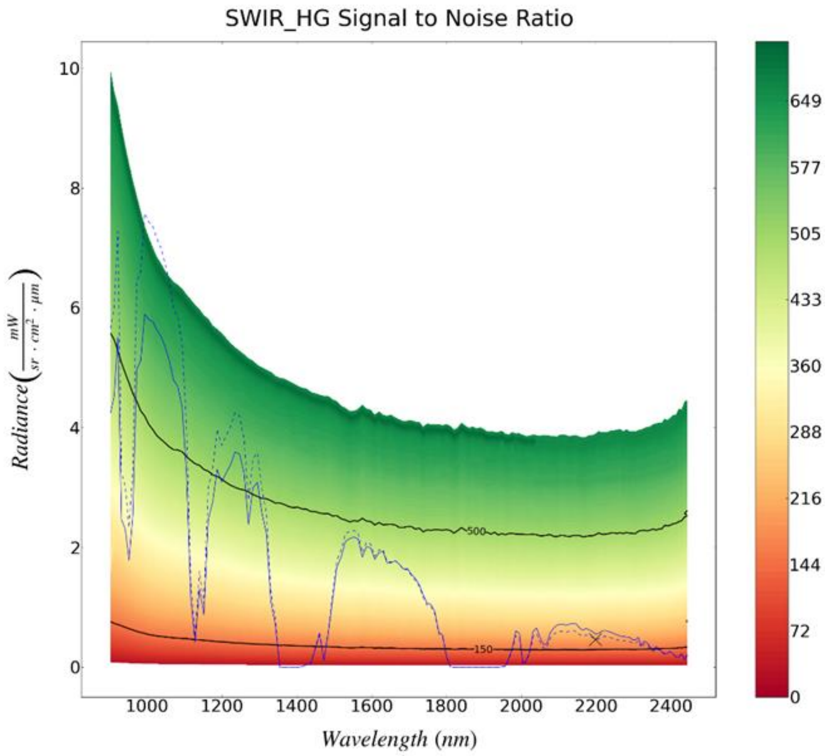

Figure 7-16 SNR contour map for SWIR high gain from the LED linearity observations observed on 23.06.2025. The reference radiance is shown with a blue line and after bandwidth normalization to a 10 nm pixel (dotted). Contour lines with SNR values of 150 and 500 are also shown in black. The mission requirement is evaluated at 2200 nm for a radiance value of 0.5 mW/cm^2/μm/sr (marked with a black cross) and is expected to be greater than 150.

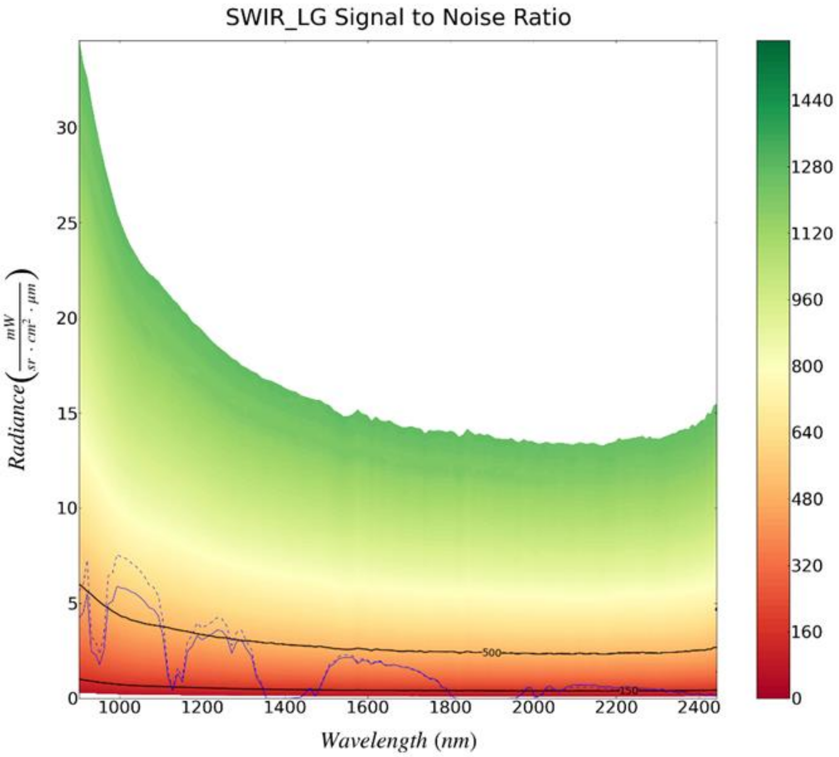

Figure 7-17 SNR contour map for SWIR low gain from the LED linearity observations observed on 23.06.2025. The reference radiance is shown with a blue line and after bandwidth normalization to a 10 nm pixel (dotted). Contour lines with SNR values of 150 and 500 are also shown in black.

The SNR values at the reference radiance spectrum are given in the table below (Table 7-9). The SNR is not determined in absorption regions and when the reference is too low or too high relative to the measured values in the linearity calibration.

Sensor	Wavelength (nm)	Reference Radiance (mW/sr/cm2/µm)	SNR Low gain	SNR High gain
VNIR	415.15	16.70	306.30	318.93
VNIR	420.73	16.30	305.56	316.6
VNIR	426.10	15.23	304.44	311.45
VNIR	431.29	11.66	258.21	276.07
VNIR	436.32	16.76	323.55	338.77
VNIR	441.23	16.62	326.58	335.65
VNIR	446.03	16.28	325.11	339.74
VNIR	450.76	19.57	378.06	373.44
VNIR	455.45	18.50	371.73	375.98
VNIR	460.11	18.24	371.18	378.8
VNIR	464.75	18.08	372.79	378.08
VNIR	469.38	18.46	385.40	391.85
VNIR	474.01	18.20	384.49	479.93
VNIR	478.64	18.40	392.44	
VNIR	483.28	18.18	393.75	
VNIR	487.94	17.08	384.45	
VNIR	492.62	17.03	390.36	
VNIR	497.33	17.01	399.09	
VNIR	502.07	16.01	387.75	
VNIR	506.84	16.75	408.91	
VNIR	511.64	16.82	415.98	
VNIR	516.48	14.64	379.31	
VNIR	521.36	15.74	399.91	
VNIR	526.28	14.73	390.48	
VNIR	531.24	16.29	447.84	
VNIR	536.24	15.97	450.59	
VNIR	541.29	14.72	424.57	
VNIR	546.39	15.34	454.56	
VNIR	551.53	15.17	459.65	
VNIR	556.73	14.75	457.28	
VNIR	561.98	14.44	457.37	
VNIR	567.29	14.51	465.69	
VNIR	572.66	14.67	460.73	
VNIR	578.09	14.27	461.66	
VNIR	583.58	14.59	488.42	
VNIR	589.14	12.15	426.10	
VNIR	594.76	13.06	460.08	
VNIR	600.47	13.44	463.26	
VNIR	606.24	13.65	478.88	
VNIR	612.10	13.29	471.31	
VNIR	618.06	13.28	476.44	
VNIR	624.07	12.84	464.10	
VNIR	630.15	12.66	461.44	
VNIR	636.29	12.75	477.84	
VNIR	642.48	12.76	490.48	
VNIR	648.73	12.02	469.22	
VNIR	655.05	11.85	466.20	
VNIR	661.43	12.62	482.14	
VNIR	667.87	12.47	482.62	
VNIR	674.38	12.37	483.92	
VNIR	680.96	12.17	476.93	
VNIR	687.60	8.98	388.14	
VNIR	694.31	10.37	447.40	
VNIR	701.10	10.51	448.86	
VNIR	707.95	11.11	465.19	
VNIR	714.87	10.60	447.81	
VNIR	721.86	9.60	404.92	
VNIR	728.92	8.29	369.27	
VNIR	736.03	9.84	405.29	
VNIR	743.21	10.47	425.98	
VNIR	750.45	10.38	414.32	
VNIR	757.74	10.30	414.46	
VNIR	765.09	5.67	286.05	

VNIR	772.49	9.85	386.52	
VNIR	779.94	9.80	376.53	478.55
VNIR	787.44	9.40	369.67	363.14
VNIR	794.99	9.05	348.89	365.64
VNIR	802.59	8.74	329.61	343.32
VNIR	810.23	8.48	321.17	338.94
VNIR	817.92	6.28	274.54	310.94
VNIR	825.65	7.56	291.62	311.34
VNIR	833.42	7.33	288.23	307.91
VNIR	841.23	8.15	293.55	313.88
VNIR	849.08	8.08	287.92	307.84
VNIR	856.96	8.16	285.82	308.24
VNIR	864.88	7.94	267.94	296.48
VNIR	872.82	7.89	261.81	295.34
VNIR	880.80	7.46	245.79	270.24
VNIR	888.79	7.53	243.79	263.54
VNIR	896.81	5.04	182.74	224.48
VNIR	904.85	6.14	196.14	243.52
VNIR	912.90	4.40	151.53	176.76
VNIR	920.96	5.47	169.87	223.06
VNIR	929.02	3.16	111.84	142.52
VNIR	937.10	0.82		62.47
VNIR	945.17	1.51		77.35
VNIR	953.25	1.79		83.93
VNIR	961.33	2.71	86.35	100.76
VNIR	969.41	4.78	120.61	148.36
VNIR	977.49	4.57	106.30	134.78
VNIR	985.58	5.30	114.24	136.71
SWIR	901.08	5.24	524.21	
SWIR	910.68	4.53	433.98	
SWIR	920.42	5.51	492.46	
SWIR	930.29	2.47	308.66	
SWIR	940.30	2.31	304.03	
SWIR	950.43	1.79	263.41	
SWIR	960.69	2.55	338.12	
SWIR	971.07	4.98	512.66	
SWIR	981.56	5.12	531.27	
SWIR	992.17	5.90	585.02	
SWIR	1002.90	5.81	589.64	
SWIR	1013.73	5.78	593.06	
SWIR	1024.66	5.64	594.97	
SWIR	1035.69	5.53	593.64	
SWIR	1046.82	5.35	590.20	
SWIR	1058.04	5.13	579.78	
SWIR	1069.34	4.80	561.61	
SWIR	1080.73	4.69	557.98	
SWIR	1092.19	4.35	540.16	
SWIR	1103.73	3.27	459.00	
SWIR	1115.34	1.17	242.06	
SWIR	1127.00	0.42	106.99	
SWIR	1138.73	1.32	270.72	
SWIR	1150.50	0.88	203.56	
SWIR	1162.31	2.47	407.07	
SWIR	1174.16	2.77	439.19	
SWIR	1186.04	3.31	491.19	
SWIR	1197.94	3.10	474.37	
SWIR	1209.87	3.25	492.14	
SWIR	1221.81	3.39	507.98	
SWIR	1233.76	3.60	531.71	
SWIR	1245.73	3.57	530.61	
SWIR	1257.70	3.25	505.06	
SWIR	1269.68	2.39	428.30	
SWIR	1281.67	3.00	489.22	
SWIR	1293.65	3.09	504.73	
SWIR	1305.62	2.58	454.57	
SWIR	1317.60	2.24	419.90	
SWIR	1329.56	1.10	272.69	
SWIR	1341.51	0.71	202.28	
SWIR	1353.44	0.01		

SWIR	1365.36	0.01		
SWIR	1377.25	0.01		
SWIR	1389.12	0.01		
SWIR	1400.97	0.01		
SWIR	1412.78	0.01		
SWIR	1424.56	0.04		
SWIR	1436.31	0.07		
SWIR	1448.02	0.30	102.33	
SWIR	1459.68	0.55	171.06	
SWIR	1471.31	0.11		
SWIR	1482.89	0.57	179.18	
SWIR	1494.43	1.13	294.38	
SWIR	1505.93	1.67	376.38	
SWIR	1517.39	1.84	404.73	
SWIR	1528.80	2.10	439.39	
SWIR	1540.17	2.15	449.23	
SWIR	1551.50	2.18	450.11	
SWIR	1562.78	2.15	445.59	
SWIR	1574.02	1.84	400.75	
SWIR	1585.21	2.02	431.29	
SWIR	1596.36	2.00	428.28	
SWIR	1607.46	1.81	407.64	
SWIR	1618.51	1.92	418.45	
SWIR	1629.52	1.94	425.74	
SWIR	1640.48	1.74	398.49	
SWIR	1651.39	1.75	399.70	
SWIR	1662.25	1.78	405.76	
SWIR	1673.07	1.73	400.35	
SWIR	1683.83	1.64	390.97	
SWIR	1694.55	1.65	392.45	
SWIR	1705.21	1.56	375.96	
SWIR	1715.83	1.49	367.98	
SWIR	1726.39	1.38	350.51	
SWIR	1736.91	1.21	326.44	
SWIR	1747.38	1.07	299.72	
SWIR	1757.80	1.05	298.80	
SWIR	1768.17	0.93	273.64	
SWIR	1778.49	0.59	199.98	
SWIR	1788.76	0.54	186.84	
SWIR	1798.98	0.19	76.82	
SWIR	1809.16	0.02		
SWIR	1819.29	0.00		
SWIR	1829.37	0.00		
SWIR	1839.41	0.00		
SWIR	1849.40	0.00		
SWIR	1859.34	0.00		
SWIR	1869.24	0.00		
SWIR	1879.09	0.00		
SWIR	1888.90	0.00		
SWIR	1898.66	0.00		
SWIR	1908.37	0.00		
SWIR	1918.05	0.00		
SWIR	1927.67	0.00		
SWIR	1937.26	0.00		
SWIR	1946.80	0.01		
SWIR	1956.29	0.02		12.11
SWIR	1965.74	0.16		91.33
SWIR	1975.15	0.33		159.82
SWIR	1984.52	0.61		234.74
SWIR	1993.85	0.57		228.75
SWIR	2003.13	0.06		41.37
SWIR	2012.37	0.12		68.69
SWIR	2021.57	0.27		140.25
SWIR	2030.73	0.60		236.77
SWIR	2039.84	0.66		249.50
SWIR	2048.92	0.50		212.34
SWIR	2057.96	0.39		177.08
SWIR	2066.95	0.39		176.40
SWIR	2075.91	0.58		228.76

SWIR	2084.83	0.65		249.66
SWIR	2093.70	0.71		261.05
SWIR	2102.54	0.72		264.97
SWIR	2111.34	0.72		261.08
SWIR	2120.11	0.71		259.43
SWIR	2128.83	0.73		266.21
SWIR	2137.52	0.73		267.35
SWIR	2146.17	0.73		264.52
SWIR	2154.78	0.66		251.01
SWIR	2163.36	0.62		243.02
SWIR	2171.90	0.65		250.40
SWIR	2180.41	0.63		242.37
SWIR	2188.88	0.60		237.33
SWIR	2197.32	0.56		224.44
SWIR	2205.72	0.57		224.82
SWIR	2214.08	0.61		235.37
SWIR	2222.42	0.62		237.27
SWIR	2230.72	0.60		234.36
SWIR	2238.98	0.59		229.53
SWIR	2247.22	0.56		224.30
SWIR	2255.42	0.54		218.60
SWIR	2263.58	0.52		212.61
SWIR	2271.72	0.52		212.43
SWIR	2279.82	0.51		208.90
SWIR	2287.90	0.51		209.49
SWIR	2295.94	0.47		198.89
SWIR	2303.95	0.46		197.46
SWIR	2311.92	0.51		208.99
SWIR	2319.87	0.37		168.58
SWIR	2327.79	0.44		189.13
SWIR	2335.67	0.41		182.53
SWIR	2343.52	0.34		160.62
SWIR	2351.35	0.29		139.64
SWIR	2359.14	0.35		163.20
SWIR	2366.90	0.31		145.91
SWIR	2374.64	0.26		131.39
SWIR	2382.34	0.23		119.01
SWIR	2390.02	0.24		122.84
SWIR	2397.66	0.27		130.17
SWIR	2405.28	0.22		113.67
SWIR	2412.86	0.17		95.00
SWIR	2420.42	0.17		87.64
SWIR	2427.95	0.23		115.90
SWIR	2435.45	0.13		65.86
SWIR	2442.92	0.20		101.65

Table 7-9 SNR values per wavelength for VNIR and SWIR low and high gains

Radiometric calibration updates

The following calibration products were generated and delivered:

Product	Type	Date of Generation	Date of Validity Start	Date of Validity End	Delivered to
ENMAP01-CTB_RAD-20250510T000000Z_V040100_20250414T063519Z	CTB_RAD	14.04.2025	10.05.2025	04.07.2025	DIMS
ENMAP01-REF_SUN-20250510T000000Z_V040100_20250414T063519Z	REF_SUN	14.04.2025	10.05.2025	04.07.2025	DIMS

Table 7-10 Generated radiometric calibration tables

7.5.4 Geometric Calibration

There have been no new geometric calibration tables generated in the reporting period.

Type of Calibration Table	ID of Calibration Table	Date of Generation	Date of Validity Start	Date of Validity End
None				

Table 7-11 Generated new geometric calibration tables

The performance of the geometric calibration table is assessed in chapter 7.6.3.

7.6 Internal Quality Control

7.6.1 Archive

Within the given time period (01.04.2025 to 30.06.2025), 2056 datatakes with a total of 20631 tiles were acquired and archived (remark: additional datatakes acquired during this period but for which the archiving is pending might be missing in the statistics).

The overall quality rating statistics are listed in Table 7-12, and in relation to the Solar Zenith Angle (SZA) in Table 7-13. Also these ratings are further detailed for the VNIR and SWIR detector in Table 7-14, showing a nominal performance rating for the given quality thresholds.

In addition, the rating for the atmospheric conditions for the scenes are depicted in Table 7-15. When setting the atmospheric quality rating in relation to the illumination conditions (i.e., large SZA) during data acquisition (Table 7-16), ~3% of the “reduced quality” ratings and ~2% of the “low quality” ratings can be related to low Sun angles / night time acquisitions. In addition, the “low qualityAtmosphere” rating can be further related to high cloud cover (58% of the low qualityAtmosphere tiles) and the unavailability of enough DDV pixels (71%) (see Table 7-17). Consequently, the rating is absolutely reasonable and can be explained.

Parameter	Value	Percentage	Number of tiles
overallQuality	Nominal	99,68%	20582
	Reduced	<0.1%	20
	Low	0.1%	29

Table 7-12 Overall quality rating statistics

Parameter	Number of tiles	Sub-Parameter	Number of tiles
overallQuality = Low	29		
		Thereof with SZA > 70°	29

Table 7-13 Overall quality rating in relation to Sun Zenith Angle (SZA)

Parameter	Number of tiles	Sub-Parameter	Number of tiles
overallQuality = Reduced	20		
		Thereof with qualityVNIR nominal	0
		Thereof with qualitySWIR nominal	20
overallQuality = Low	29		
		Thereof with qualityVNIR nominal or reduced	3
		Thereof with qualitySWIR nominal or reduced	19

Table 7-14 Reduced and low quality rating statistics

Parameter	Value	Percentage
QualityAtmosphere	Nominal	43%
	Reduced	13%
	Low	44%

Table 7-15 QualityAtmosphere rating statistics

Parameter	Number of tiles	Sub-Parameter	Number of tiles
overallAtmosphere = Reduced	2684		
		Thereof with SZA > 60°	59
		Thereof with SZA > 70°	16
		Thereof with SZA > 80°	0
overallAtmosphere = Low	9105		
		Thereof with SZA > 60°	244
		Thereof with SZA > 70°	45
		Thereof with SZA > 80°	29

Table 7-16 QualityAtmosphere rating in realtion to Sun Zenith Angle (SZA)

Parameter	Number of tiles	Sub-Parameter	Number of tiles
overallAtmosphere = Low	8152		
		Thereof with Cloud Cover > 66%	5249
		Thereof with DDV warnings	6450

Table 7-17 QualityAtmosphere rating in relation to Cloud Cover and DDV availability

Remark about definition of EnMAP low quality collection

The quality rating of EnMAP products is based on image parameters, such as illumination conditions (i.e., sun elevation angle) and image defects, and on possible anomalies in the image data or instrument telemetry. These parameters are retrieved during the pre-processing and are added to the metadata and quality layers for every archived L0 product. In EOWEB GeoPortal two collections of EnMAP L0 products are available: "EnMAP-HSI (L0)" and "EnMAP-HSI (L0), Low Quality". An L0 product is assigned to the low-quality collection if the corresponding metadata item qualityFlags.overallQuality is equal to 2 (low quality). This happens for products with a significant number of striping, saturation, artefact or dead pixels, when the screening of data and instrument indicates non-nominal behavior or, in the majority of cases, when the sun elevation angle is less than or equal to 0 (e.g., night scenes). A detailed definition of qualityFlags. overallQuality is given in Sec. 4.4.9 in the L1B ATBD (EN-PCV-TN-4006).

7.6.2 Level 1B

7.6.2.1 Radiometric Performance

Defective / de-calibrated detector elements

Using the Detector Map components, an offline check of possibly defective or de-calibrated detector elements is conducted. In particular, a detector element is identified as "possibly defective" if it is suspicious in at least 75% of the useful tiles. Note that this analysis is based on L1B_RAD data, so no dead / defective pixel interpolation was carried out. Within the given reporting period, the following indications for defective pixels are found for the VNIR and the SWIR camera:

VNIR (total of 16021 tiles, with 15891 suitable for analysis):

Newly found suspicious pixels in green, previously detected in **black**, no longer present ones in ~~red~~.

Band	Cross-track element
19	187
85	14
89	395

Note that the band index starts at 1.

SWIR (total of 16021 tiles, with 15782 suitable for analysis):

Newly found suspicious pixels in green, previously detected in **black**, no longer present ones in ~~red~~.

NOTE: due to the change in SWIR band configuration within the period Q3 2023, the band index from band 45 till 75 did change by +1 (with bands 45, 74 & 75 newly added) w.r.t. the reports before Q3 2023.

Band	Cross-track element	Band	Cross-track element	Band	Cross-track element
1	817	33	560	85	525
2	235, 286, 593, 673	38	241	91	973
4	362, 363, 418	~~39~~	~~486~~	92	677, 973
5	687	48	511	96	341, 819
7	472, 910	50	311, 344, 395	100	513
8	801	53	97	101	318
9	124	54	941	102	925

11	715	56	221, 965	106	107
14	29, 684	58	632, 922	107	265, 764
16	535	59	89, 90	108	886
20	84	61	312	111	315
28	104	63	123	118	837
29	~~855~~, 928	66	93		
30	360, 855	69	864		
31	360	72	801, ~~844,~~ 845		

Dead detector elements

Within the given reporting period, the statistics for dead pixels are provided in Table 7-18 and Table 7-19. When comparing these numbers to the estimates in Ch. 7.5.1, one must bear in mind that the latter is based on the full detector readout configuration, while the numbers provided in the following are related to the standard readout configuration as provided in the user product. Because of the smaller readout area, these following dead pixel numbers are lower in comparison.

Parameter	Number of dead pixels	Percentage of tiles in reporting period
DeadPixelsVNIR	137	100%

Table 7-18 Dead pixel statistics, VNIR

Parameter	Number of dead pixels	Percentage of tiles in reporting period
DeadPixelsSWIR	1509	100%

Table 7-19 Dead pixel statistics, SWIR

Saturation and radiance levels

Within the given reporting period, no indications for increased saturation defects are found for the VNIR and the SWIR camera (see Table 7-20 and Table 7-21).

Parameter	Value (per mille of scene)	Percentage of tiles
SaturationCrosstalkVNIR	0	90%
	> 0 per mille	9.6%
	> 10 per mille	1.9%

Table 7-20 Saturation statistics, VNIR

Parameter	Value (per mille of scene)	Percentage of tiles
SaturationCrosstalkSWIR	0	91%
	> 0 per mille	8.6%

	> 10 per mille	0.6%

Table 7-21 Saturation statistics, SWIR

Other radiometric artifacts

Within the given reporting period, the striping performance is similar to the one encountered during the Commissioning Phase. Within PCV, different de-striping approaches were tested, and the selected one by M. Brell (GFZ) is implemented in processor version V01.02.00 (07.03.2023).

Apart from this, no indications for an increase in general radiometric artifacts are found for the VNIR and the SWIR camera (see following tables).

Parameter	Value (number of pix)	Percentage of tiles
generalArtifactsVNIR	0	0%
	> 0	100%
	> 10	4.3%
	> 100	0.4%
	> 1000	0%

Table 7-22 Artifacts statistics (without striping), VNIR

Parameter	Value (number of pix)	Percentage of tiles
generalArtifactsSWIR	0	0%
	> 0	100%
	> 10	100%
	> 25	1.6%
	> 100	0.2%
	> 1000	0%

Table 7-23 Artifact statistics (without striping), SWIR

7.6.2.2 **Spectral Performance**

For the analysis of the spectral stability, the Detector Maps of all Earth datatakes acquired in the reporting period were used. Note that no smile correction was applied, so the analysis shows only on the instrument characteristics. At the wavelengths of stable atmospheric features (760 nm Oxygen absorption and CO2 absorption at ~2050 nm), simulations of spectral shifts were carried out by resampling the absorption in the interval of +/- 3.0 nm with steps of 0.05 nm. Then the signal of the Detector Maps and the simulated shifted absorptions were normalized, and a least-square fit was used where the sensed absorption matches the simulations. Also an additional polynomial fitting was applied, as especially the CO2 absorption band region has low signal an is thus significantly influenced by noise.

For the VNIR, when aggregating the shifts (Figure 7-18) the mean derivation is almost constant in across-track direction and -as before- around 0.6 nm towards shorter wavelengths, underpinning the consistency with the in-orbit spectral calibration and especially regarding the shape of the spectral smile. Note that of course these results are consistent within the limitations of this vicarious approach. Additionally, the variability of the vicariously estimated spectral calibration can be expressed as the standard deviation at 1 sigma is below 0.3 nm, which includes the spectral stability of EnMAP and as well the variations of the used Earth datatakes and the limitations of the method.

In summary, for the VNIR the estimated differences to the CTB_SPC consistent with the results of previous reporting periods, confirming the validity of the spectral calibration and the spectral stability of the instrument taking into accounts the limitations of the vicarious approach.

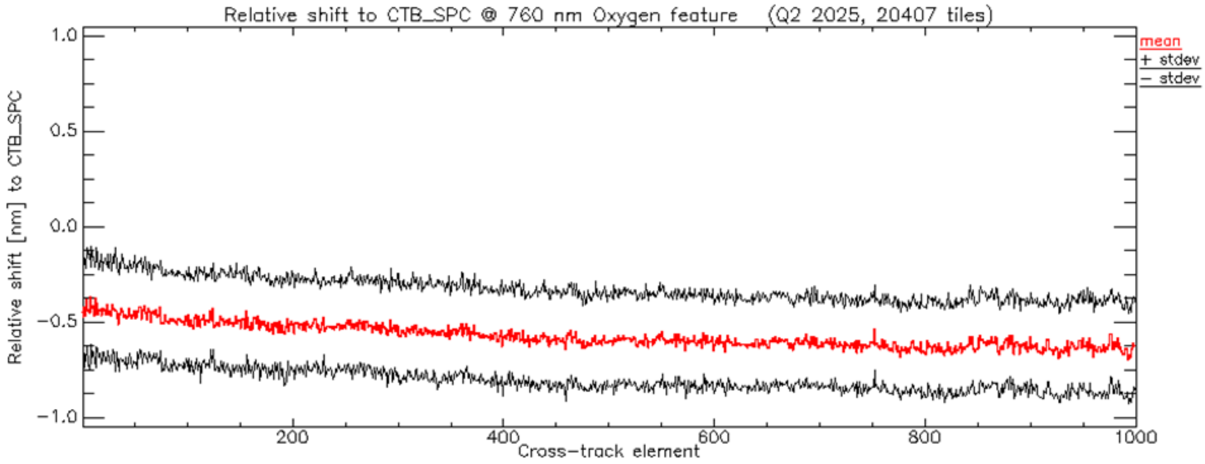

Figure 7-18 VNIR estimated spectral shift at 760 nm w.r.t the valid spectral calibration table (CTB_SPC), and relative spectral stability expressed at 1 sigma (Q2 2025, 15920 tiles)

For this analysis, the reference is thus not the nominal center wavelengths (i.e., a single number per band), but the CW per cross-track pixel, thus explicitly including the spectral smile (see Figure 7-19).

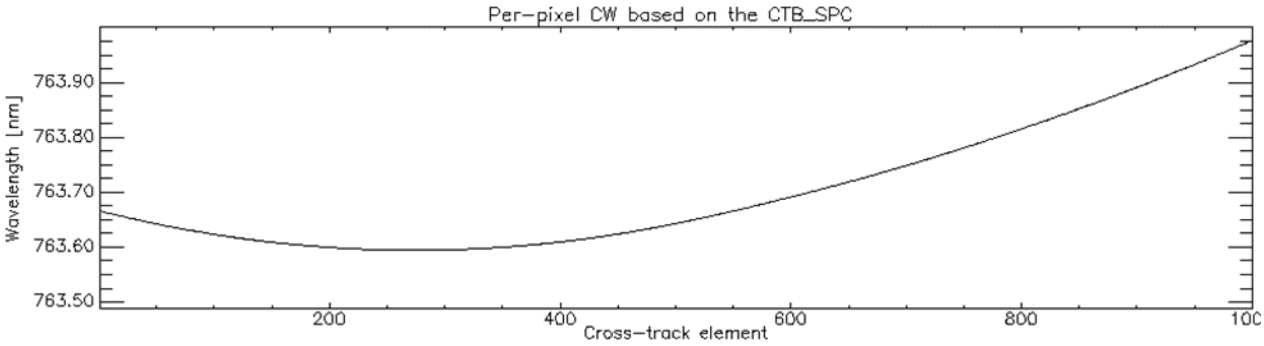

Figure 7-19 Center wavelengths per cross-track pixel based on the spectral calibration table (VNIR band 62) in the calibration table (CTB_SPC).

For the SWIR having less pronounced atmospheric absorption features, more influence of the background and a much lower signal level, the fitting also results in more clutter, as shown in Figure 7-20.

In order to demonstrate that the mean derivation to the CTB_SPC is within the spread of the data, the mean and standard deviation are calculated using the relative values, as shown in Figure 7-20. For Q2 2025, a small shift of ~0.4 nm towards longer wavelengths is visible when comparing to CTB_SPC (Figure 7-21). This shift is equal for all cross-track elements, so the shape of the spectral smile did not change and is well represented in the CTB_SPC. When comparing this small spectral shift to the results in the past quarter, the tendency towards longer wavelengths by ~0.5 nm was also present, but then with a larger magnitude and within a larger clutter in the fitted data. In addition, the spread around the estimated mean with a standard deviation of ~0.4 nm (1 sigma) indicates no significant change of the good overall stability of the instrument.

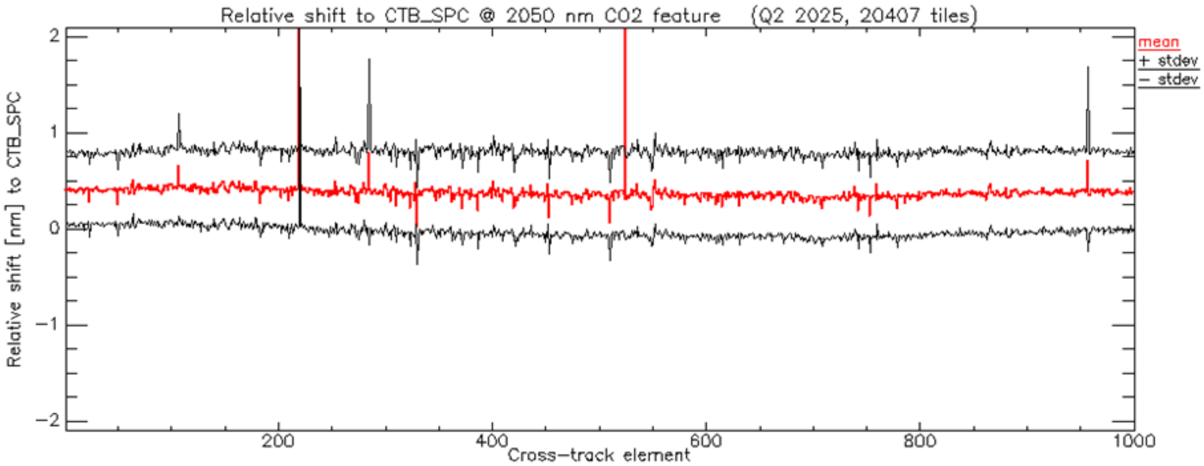

Figure 7-20 SWIR estimated spectral shift at 2050 nm w.r.t the valid spectral calibration table (CTB_SPC, shown below), and relative spectral stability expressed at 1 sigma (Q2 2025, 17894 tiles)

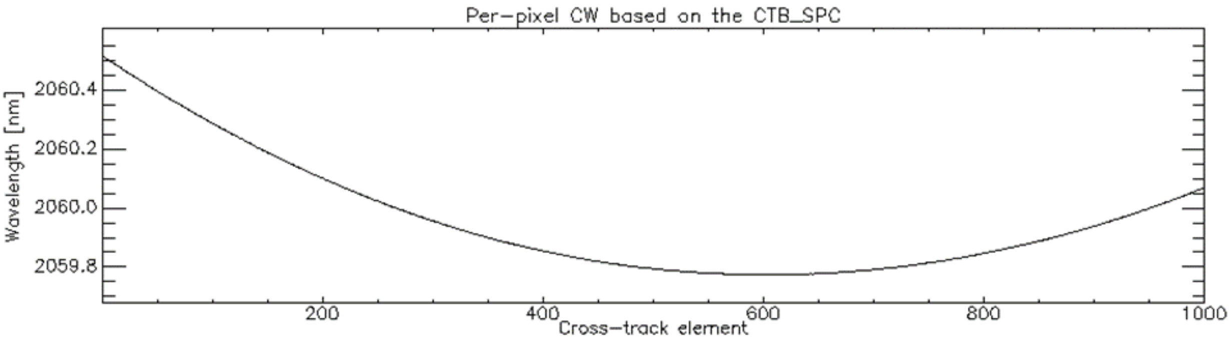

Figure 7-21 Center wavelengths per cross-track pixel based on the spectral calibration table (SWIR band 86).

7.6.2.3 Routine check of scenes in context of updates in CTB_RAD, CTB_SPC calibration tables

7.6.2.3.1 CTB_RAD

In the context of routine checks after radiometric calibration update, Table 7-24 shows the summary.

Table 7-24 Validated CTB_RAD (from 19.04.2025)

Validated CTB	ENMAP01-CTB_RAD-20250419T000000Z_V040100_20250414T122853Z
Datatake used	 ENMAP01-____L0-DT0000125690_20250423T015038Z_008 Figure 7-22 Datatake used (Nullarbor coastline, Australia)

Summary of result	New CTB_RAD was confirmed by QC.
	• VNIR, for the given scene:
	  ○
	  ○ relative changes to P34 are slight larger as between periods before (still below 0.25%), with first 5 bands show slightly higher changes

	◦ for given scene, the absolute change is between -0.025 and +0.01 ◦ The changes are quite stable across the detector ◦ Fringing is again visbile in higher bands • SWIR, for the given scene: ◦ ◦ relative and absolute change to P34 are very small (below 0.07% for most bands), smaller than for P33-P34 ◦ only band 7 shows slightly higher changes (0.15%) but this is still very small and of no concern

7.6.2.3.2 CTB_SPC

In the context of routine checks after spectral calibration update, Table 7-25 shows the summary.

Table 7-25 Validated CTB_SPC

Validated CTB	None
Datatake used	
Summary of result	

7.6.3 Level 1C

This report covers the timeframe from 01.04.2025 to 30.06.2025. No geometric calibration was performed during this period.

In the timeframe of this report, 2056 datatakes have been acquired. In 1531 of those datatakes (~74 %), enough ground control points (GCP) and independent check points (ICP) were found to perform a geometric accuracy assessment. The datatakes without enough GCPs were not assessed quantitatively, but a random subset of them was inspected visually. The vast majority of those datatakes was either almost fully covered with clouds or showing only water, desert or rain forest. The behavior is thus as expected..

The assessment of the RMSE values in the metadata is shown below in Figure 7-23.

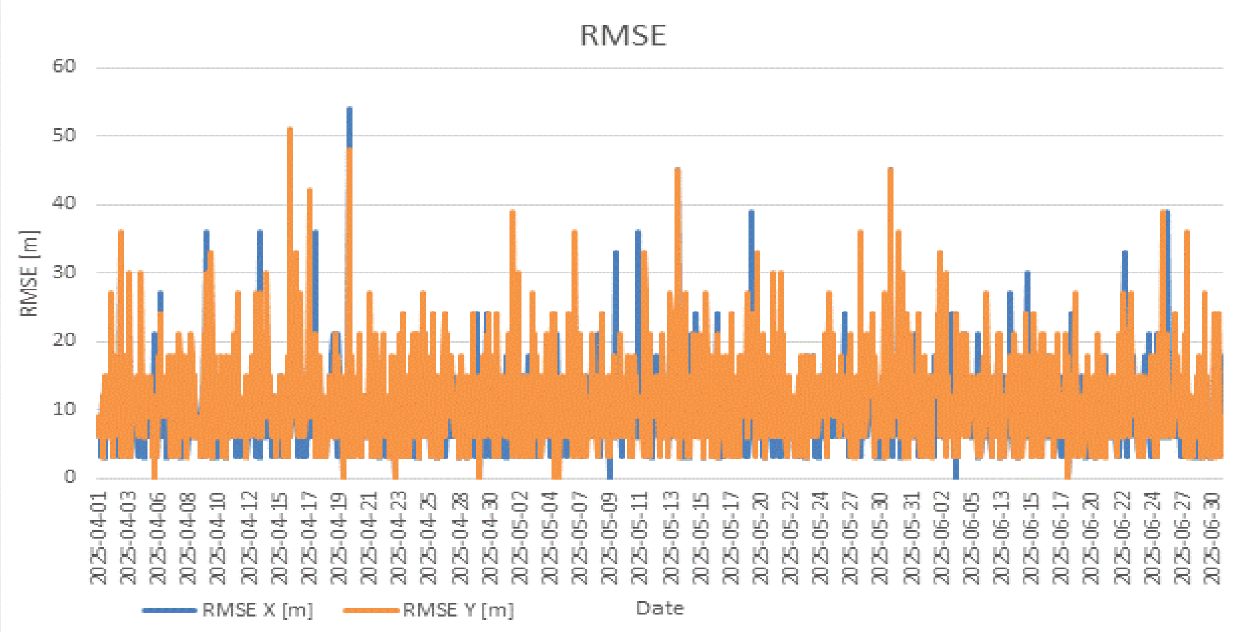

Figure 7-23 Assessment of RMSE values, calculated based on found ICPs, for all datatakes where ICP could be found

In x-direction, 12 datatakes (~0.8%) had an RMSE value above 30 m (1 GSD), whereas in y-direction, 17 datatakes (~1.1%) are above this threshold. For most of those datatakes, only very few GCP and ICP could be found during processing, making the results less reliable. The mean values are 8.99 m in x-direction and 11.16 m in y direction. This shows a very high geolocation accuracy for the datatakes where matching was possible. The requirement GRD-PCV-0155 (1 GSD) is thus fulfilled.

The average boresight angles, which can be interpreted as the correction and thus the error of the scene if no GCPs could have been found, correspond to approximately -2 m in x direction with a standard deviation of approximately 22 m and -44 m in y direction with a standard deviation of approximately 42 m on ground. It is reasonable to assume that the scenes where no GCPs could be found are in the same accuracy range and thus well within the requirement of 100 m (GRD-PCV-0150). Note that the x and y direction mentioned in this report are not in the image coordinate system but in UTM, as the evaluation is done on L1C products..

7.6.3.1 **Geometric accuracy**

EnMAP L1C products are matched against a reference image (Sentinel-2 data, if not stated otherwise) by using image matching techniques to assess the geometric accuracy. At the obtained checkpoints (CP), statistics are calculated to provide mean and RMSE values (Figure 7-24) for each scene. Note that the obtained accuracy in the analysis is always w.r.t. the reference image. This report covers EnMAP data from 01.04.2025 to 30.06.2025. A random sample of 561 L1C tiles was selected based on visual inspection of the catalogue quicklooks (e.g. to avoid cloudy images).

The requirement GRD-PCV-0155 shall be fulfilled:

The geolocation accuracy at nadir look direction of level 1C and 2A products shall be better than 1 GSD (1 sigma) in each direction with respect to reference images provided that reference images are available and sufficient similarity.

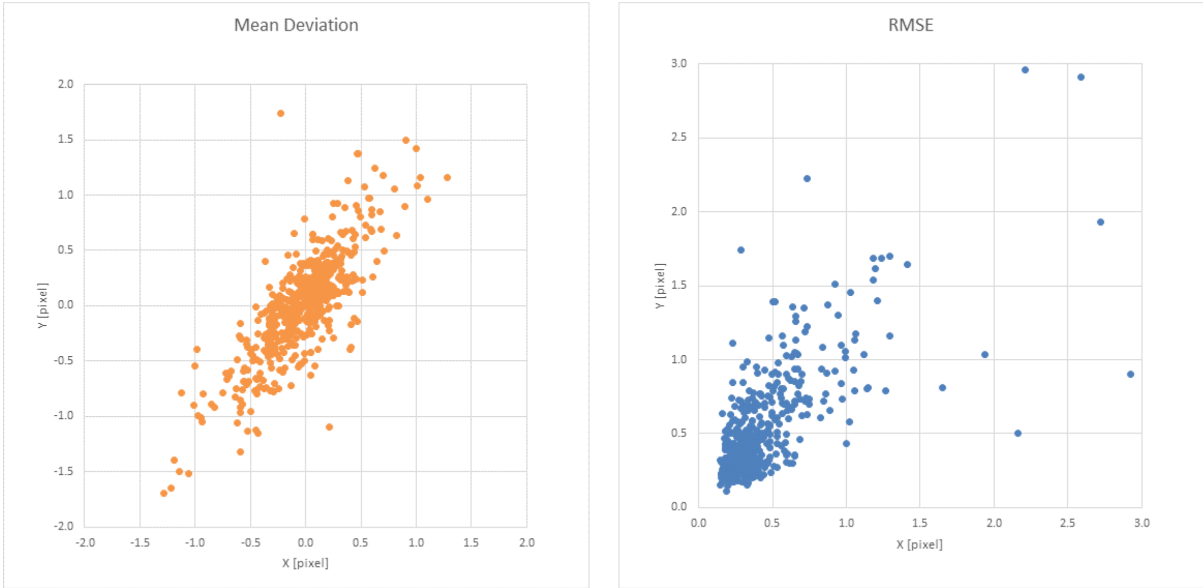

Figure 7-24 Mean deviation of EnMAP L1C products in pixel (left). RMSE value for EnMAP L1C products in pixel (right)

Note, that during processing the boresight angles and the geometric accuracy related quality flags are calculated on datatake level while in the figures and tables above, the accuracy is assessed per tile. The mean values over all 561 L1C tiles are -0.03 and 0.00 pixel in mean deviation with a standard deviation of 0.40 and 0.48 pixel while the mean RMSE values are 0.35 and 0.46 pixel, all in x and y direction respectively. The data show that for the vast majority of scenes the accuracy wrt. reference image is better than one pixel and thus the requirements are fulfilled. Compared to the last geometric QC report, the values are very stable (see Figure 7-26).

7.6.3.2 Co-registration accuracy

In this section, the co-registration accuracy is checked against the Space Segment requirement SRDS-PIM-0050 (EN-KT-RFW-003 is also to be considered here):

*The HS-Imager shall be designed such, that the geometric co-registration is ≤ 20 % of the nominal Ground Sampling Distance (0.2 * GSD linear displacement in both directions).*

For the assessment of co-registration accuracy, the SWIR data of EnMAP L1C products are matched against the corresponding VNIR data and the mean deviation values shown in this section (Figure 7-25).

This report covers EnMAP data from 01.04.2025 to 30.06.2025. A random sample of 561 L1C tiles was selected based on visual inspection of the catalogue quicklooks (e.g. to avoid cloudy images).

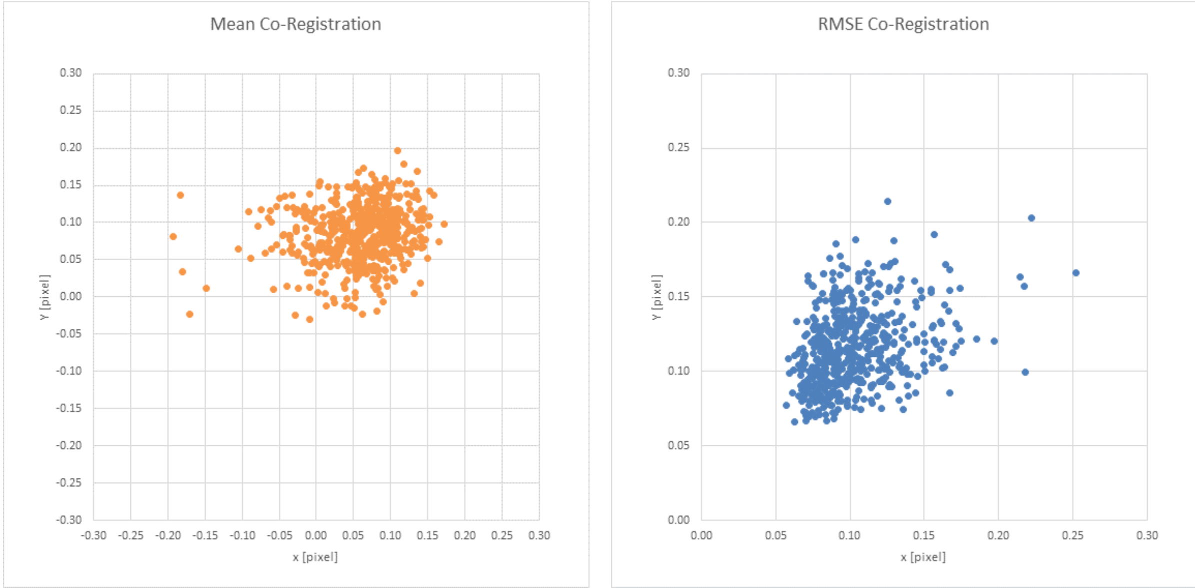

Figure 7-25 Mean deviation in pixel between VNIR and SWIR data of EnMAP L1C products (left). RMSE in pixel between VNIR and SWIR data of EnMAP L1C Products (right)

The data show, that the mean co-registration is well within the requirement. Note that the theoretical accuracy of the used matching algorithm is 0.1 pixel, and as can be seen in the RMSE values, still some mismatches were not removed by the blunder detection techniques that were applied. The mean deviation over all analyzed tiles are 0.06 pixel in x-direction with a standard deviation of 0.05 pixel and 0.09 pixel in y direction with a standard deviation of 0.04 pixel. Compared to the results in the previous geometric QC report, the values are very stable as can be seen in Figure 7-26.

7.6.3.3 Development of geometric performance

Since the launch of EnMAP on April 1st 2022, the geometric performance has been improved significantly. This was achieved by different geometric calibrations and processor updates. Table 7-26 shows the measures performed, their date and their effect.

Date	Measure	Effect
01.08.2022	Fix of attitude processing	Improvement of absolute geolocation (w/o matching)
20.09.2022	Boresight Calibration	Improvement of absolute geolocation (w/o matching)
03.11.2022	1st Geometric Calibration	Improvement of absolute geolocation (w/o matching) Improvement of VNIR/SWIR co-registration (~0.8 pix -> ~0.4 pix)
11.02.2023	2nd Geometric Calibration	Improvement of VNIR/SWIR co-registration (~0.4 pix -> ~0.15 pix)
29.03.2023	Processor update (v01.02.00)	Improvement of VNIR/SWIR co-registration (~0.15 pix -> ~0.06 pix)
05.05.2023	Processor update (v01.03.01)	Improvement of geolocation accuracy

Table 7-26 Improvement of geometric performance

Figure 7-26 shows the development of the co-registration accuracy, measured as described in previous section. Again, after a significant improvement since commissioning phase, over the last report periods the accuracy has been very stable.

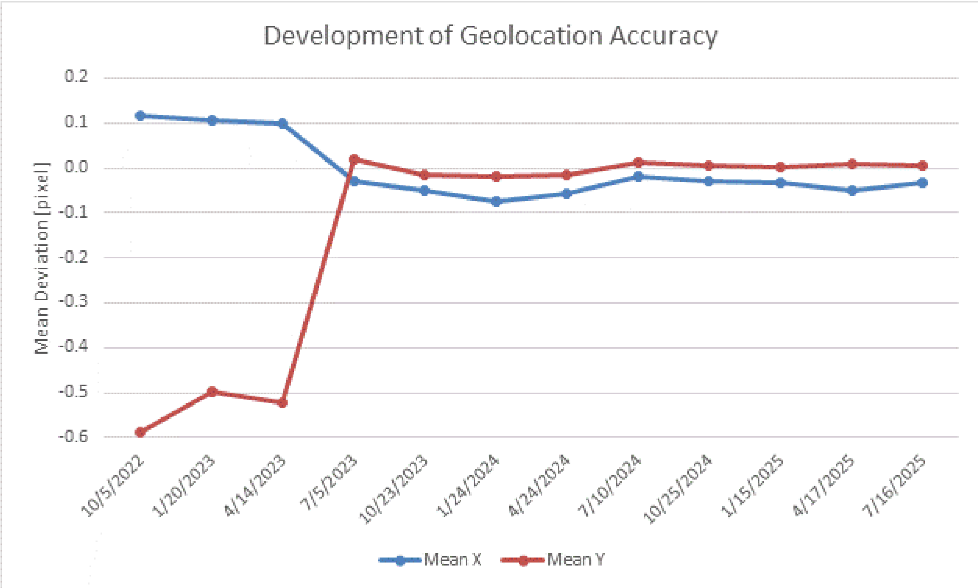

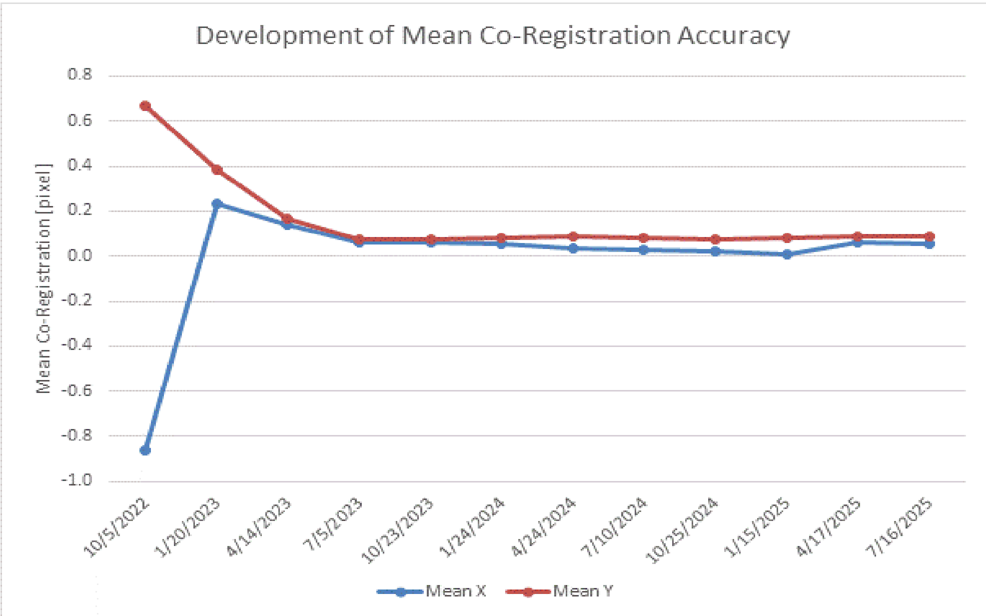

Figure 7-26 Development of co-registration accuracy based on the previous geometric QC reports

As most of the geometric processing – especially the matching against a reference image – is done on datatake level during L0 processing, the geometric accuracy and co-registration of data acquired earlier during the mission is not automatically improved when higher level products (L1B, L1C, L2A) are processed with the current processor version. However, during the currently ongoing L0 reprocessing of the whole archive, the geometric processing is executed with the latest processor version and geometric calibration table to make sure that the best geometric quality and co-registration is reached also for the reprocessed data. Users can recognize reprocessed data by checking the metadata tag **archivedVersion**: if the version is 01.03.00 or higher, then the geometric performance should be as analyzed in this report.

7.6.4 Level 2A

7.6.4.1 **Validity of generated L2A “water” data**

7.6.4.1.1 Analyzed scenes

The following scenes were taken into consideration:

DataTake - ID	Tile - ID	Location	L2A Option	Cirrus / Haze Removal	Overall Quality
130631	04	AUS, Rita Island	Water mode, water type “clear”	Cirrus	Nominal
132980	09	AUS, Windy Harbour	Water mode, water type “clear”	Cirrus	Nominal
132237	02	ITA, Lake Garda	Water mode, water type “clear”	Cirrus	Nominal

Table 7-27 Datatake IDs of analyzed water products

The below listed parameters were checked for above mentioned scenes by EOMAP:

Parameter	Check
Masking (Land, Water, Clouds, etc.)	No issues found.
Adjacency correction	No issues found.
Retrieval of atmospheric properties	No issues found.
Cirrus – correction	No issues found.
Retrieval of water leaving reflectance	No issues found.
Quality Mask	Under investigation.

7.6.4.1.2 Data Checks

- Masking

First, the geo mask is checked. The different parts of the scene shown masked (see Figure 7-27 and Figure 7-28) are classified as expected. The found cirrus clouds over water and the corresponding correction procedure are investigated more in the following.

Figure 7-27 Scene-ID 132237; RGB-Quicklook with Bands 611.02nm – 550.69nm – 463.73nm

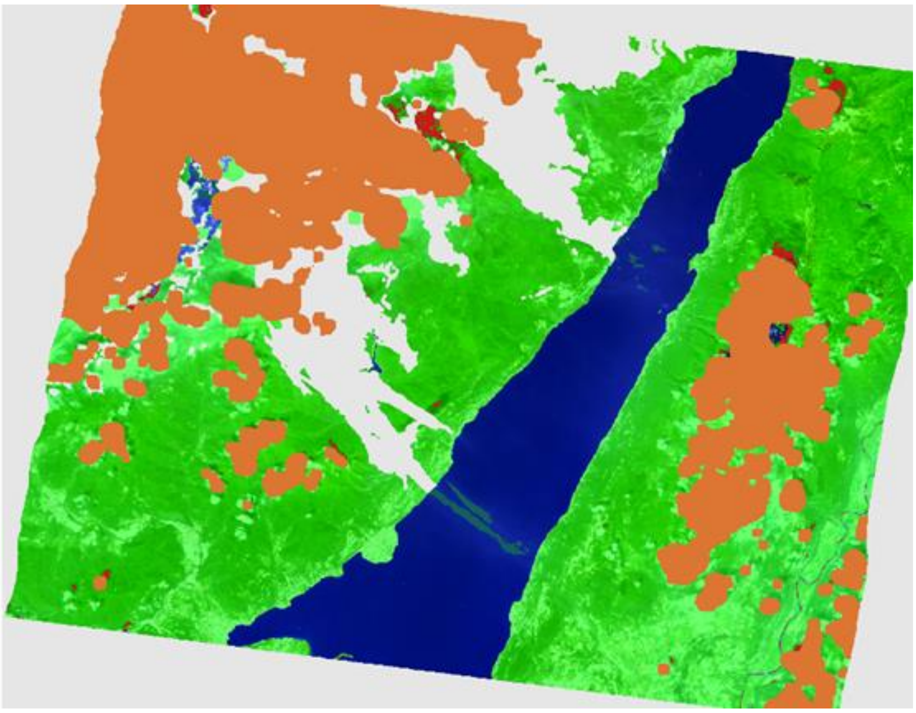

Figure 7-28 Scene-ID 132237; Geo Mask with Blue – Water, Green – Land, Orange – Clouds, Red – Cloud Shadow, Dark Green – Cirrus, White – NA

- Cirrus and Adjacency Correction

Next, we check for the cirrus and adjacency correction using the two sites 'AC1' and 'AC2' shown in Figure 7-27.

The coordinates of the sample locations are as follows:

AC 1: LAT 45.62931030 | LON 10.60868398

AC 2: LAT 45.65696964 | LON 10.67522001

For sampling, we choose two locations, one located over shallow water, the other over deep water (see Figure 7-27 for the sample locations).

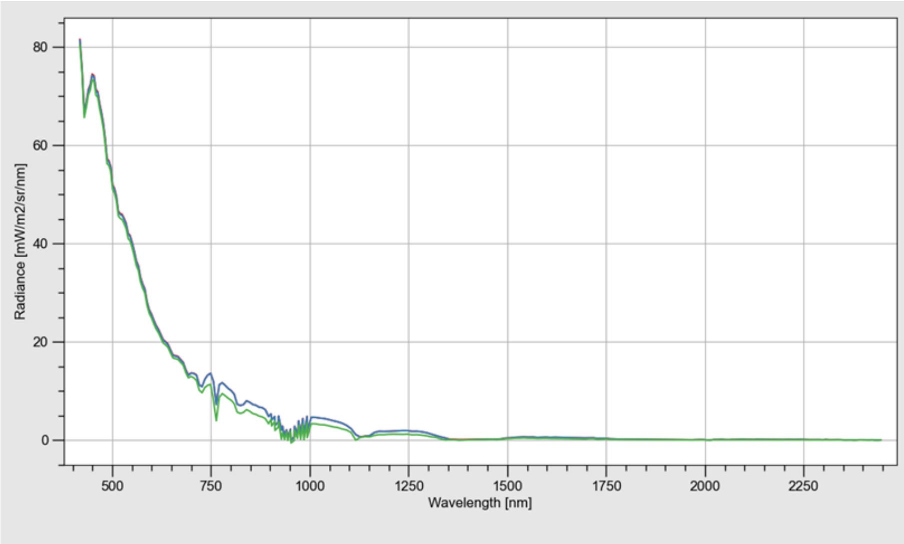

Figure 7-29 Scene-ID 132237; At-sensor-radiance sampled at location AC 1; red: measure, blue: cirrus corrected, green: adjacency corrected

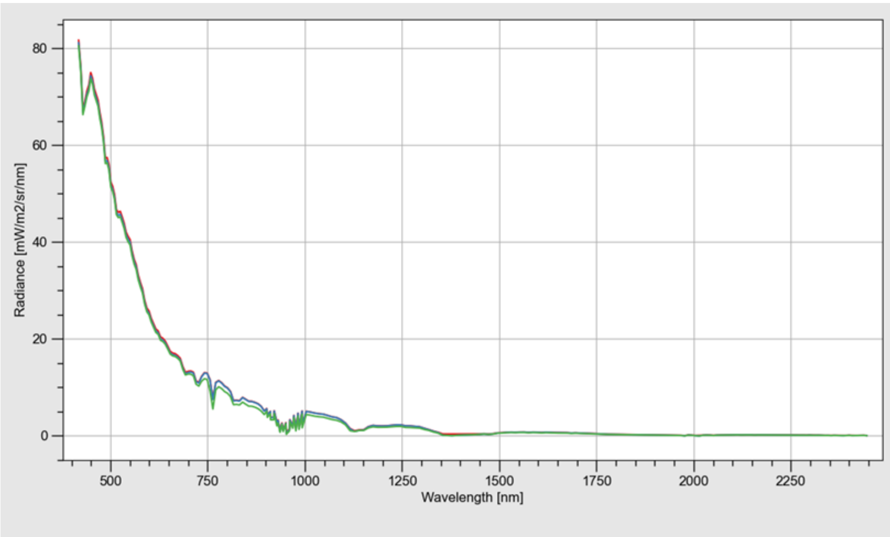

Figure 7-30 Scene-ID 132237; At-sensor-radiance sampled at location AC 2; red: measure, blue: cirrus corrected, green: adjacency corrected

Figure 7-29 and Figure 7-30 depict the sampled radiance-signal for location AC 1 AC 2, respectively. As can be already seen using the full spectral range, the adjacency correction sampled at AC 1 has a slightly stronger influence compared to the one sampled at AC 2. This is what we would expect, since AC 1 is located directly next to some very bright land part, thus the signal sampled over water is supposed to be much more affected.

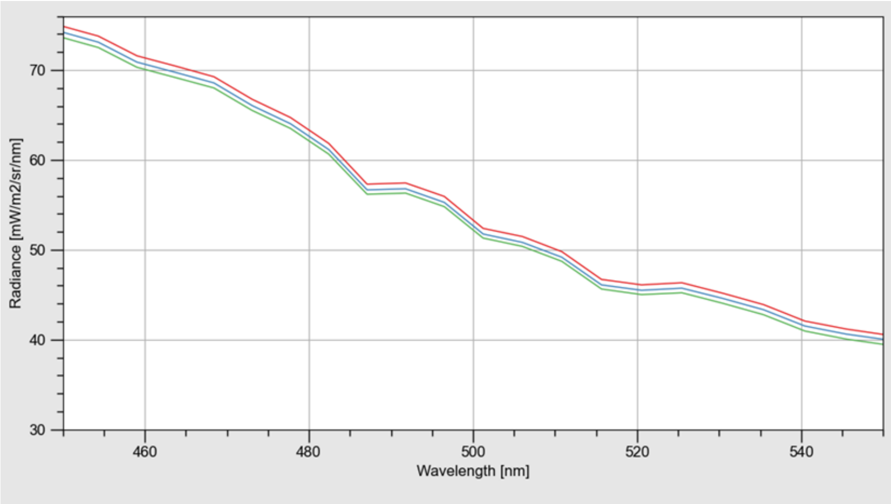

Figure 7-31 Scene-ID 132237; At-sensor-radiance sampled at location AC 2; red: measure, blue: cirrus corrected, green: adjacency corrected

To get a better impression of the correction procedures, Figure 7-31 crops the spectrum sampled at AC 2 for the wavelength range between 450nm and 550nm. First, the signal is attenuated by the cirrus correction since more than 100 cirrus-pixels were found within the scene. After the cirrus-correction is applied, the correction for adjacency further reduces the signal in order to diminish the effect bright land pixels do have.

- Reflectance Product

To get a better impression of the product normalized water leaving reflectance as the final one, Figure 7-33 shows the reflectance using the RGB channels 611.02nm, 550.69nm and 463.73nm.

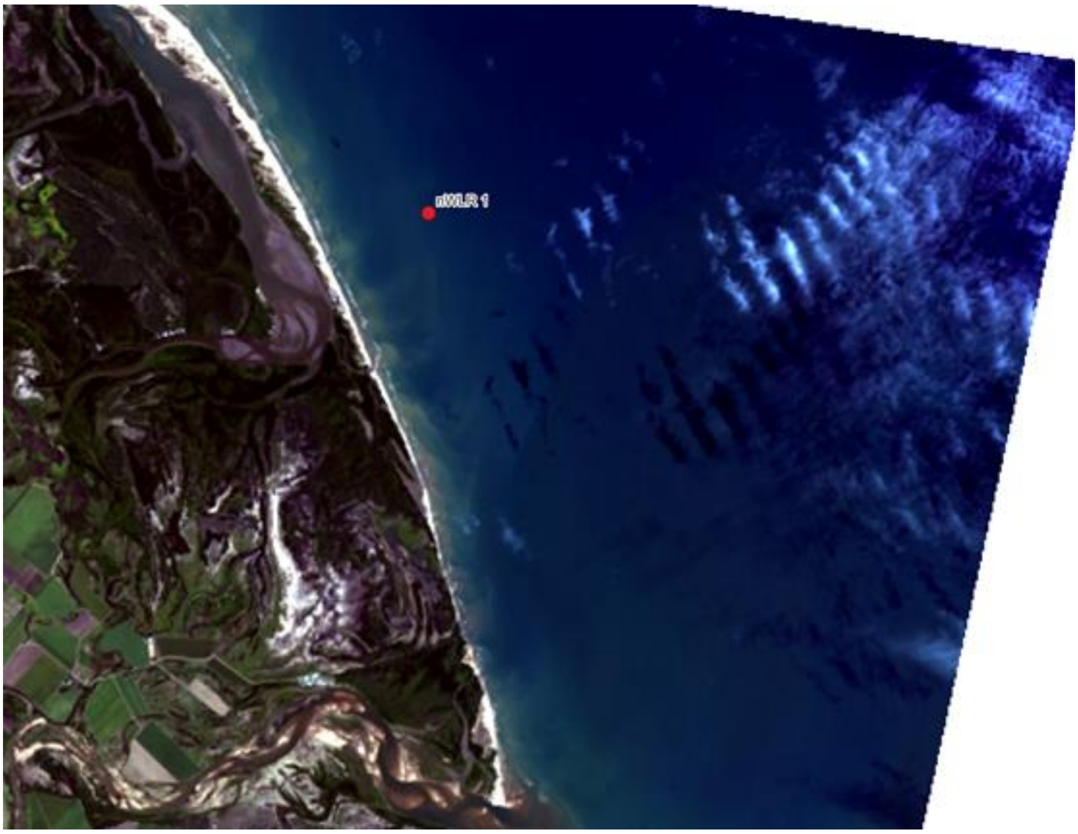

Figure 7-32 RGB-Quicklook of scene-ID 130631; Wavelengths for RGB: 611.02nm – 550.69nm – 463.73nm

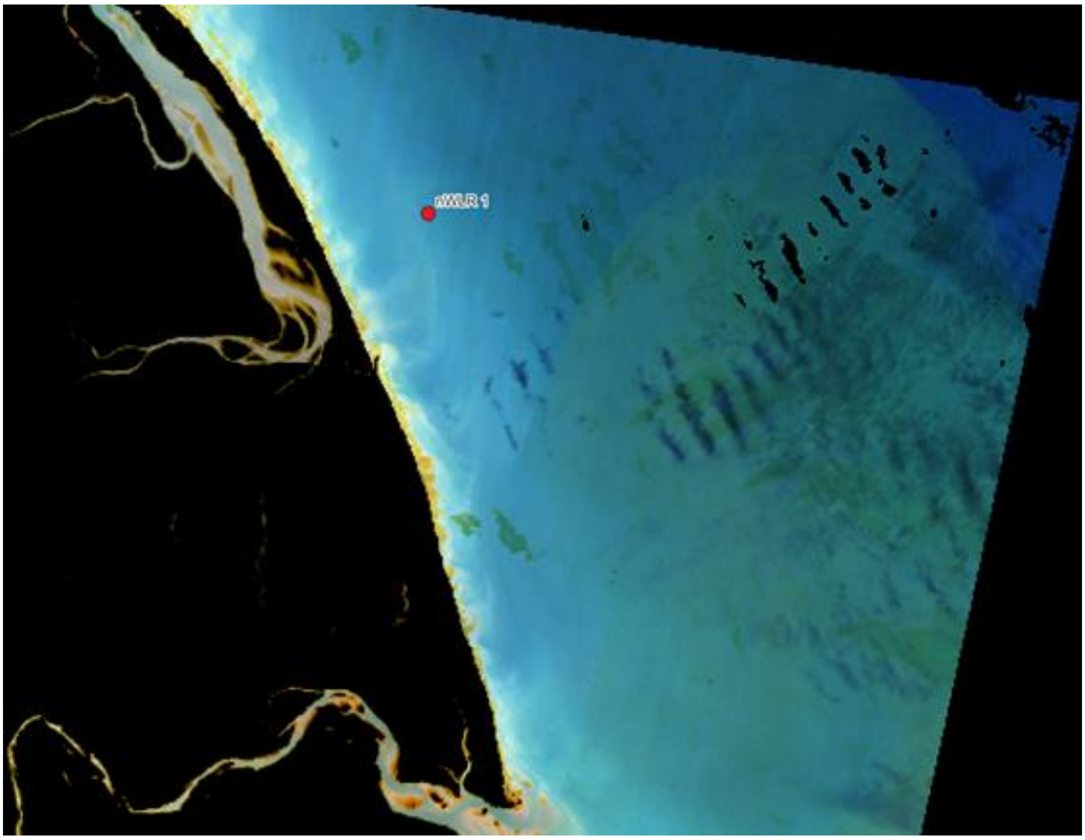

Figure 7-33 Normalized Water Leaving Reflectance of scene-ID 130631; Wavelengths for RGB: 611.02nm – 550.69nm – 463.73nm

For the two labeled locations in Figure 7-32, the sampling coordinates are as follows:

nWLR 1: LAT -19.52660743 | LON 147.56320312

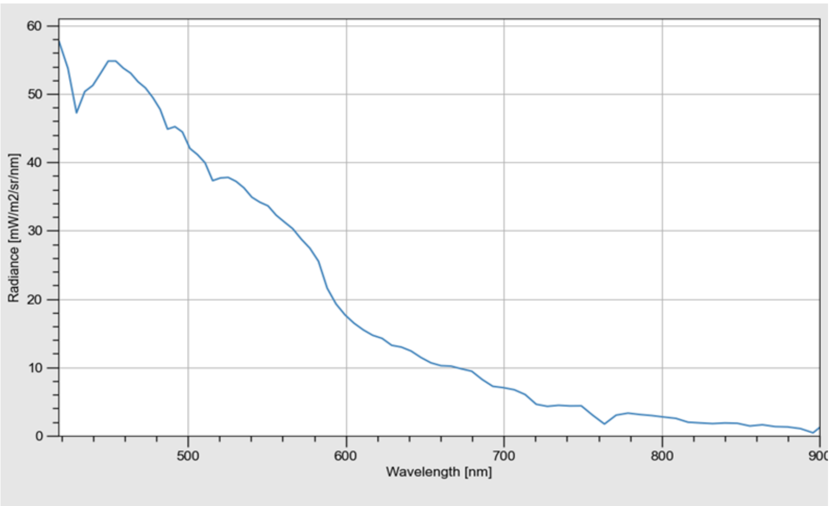

Figure 7-34 Scene-ID 130631; At-sensor-radiance sampled at location nWLR 1

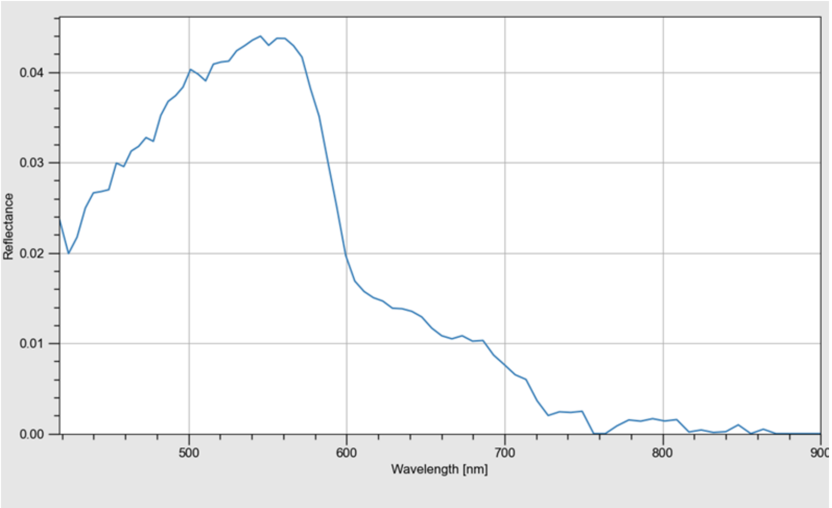

Figure 7-35 Scene-ID 130631; nWLR sampled at location nWLR 1

Figure 7-34 depict the at-sensor-radiance sampled at location nWLR1. Figure 7-35 shows the corresponding normalized water leaving reflectance (nWLR). As can be seen in Figure 7-32, the location suffers from serious amounts of sedimentary input, thus exacerbating the atmospheric correction. By using the SWIR channels for this task, we are capable to deal with the sediment load in order to derive a typical maritime spectrum of nWLR, as can be seen in Figure 7-35.

Summing up, the atmospheric correction workflow works as intended.

7.6.4.2 **Validity of generated L2A "land" data**

7.6.4.2.1 Analyzed scenes

Within the time interval between 01.04.2025 to 30.06.2025, an interactive in-depth analysis has been conducted for the following scenes:

Datatake-ID	Tile-ID	date	location	L2A option	cirrus and haze removal	Archived Version	processor version	Overall Quality	Quality Atm
132776	30	28.05.25	Spain, Cartagena	land	yes	01.05.02	V010502	Nominal	Nominal
131190	17	21.05.25	Khazakstan, close to lake Balkash	land	no	01.05.02	V010502	Nominal	Nominal
131190	18	21.05.2025	Khazakstan, close to lake Balkash	land	no	01.05.02	V010502	Nominal	Nominal
137176	5	20250621	Nahr al Khabur River, Syria	land	no	01.05.02	V010502	Nominal	Reduced

Table 7-28 Datatake IDs of analyzed land products

For the selection of L2A data, several data takes acquired within the reporting period and covering different landscapes at different conditions were analyzed.

7.6.4.2.2 Data Checks

In the following, the different tiles were checked for the shape and magnitude of the BOA_ref spectra. Also, the quality of the generated masks is evaluated as well as possible differences in the overlapping areas of neighboring tiles. Additionally, the land-water masking was investigated, as this is critical when using the L2A “land” and the L2A “water” processing.

For all tiles the visual image impression is fine. For the masking, there are known issues of mis-classifications which are currently being investigated. The BOA_ref spectra all show the typical shape and magnitude, indicating the correct L2A correction. The overlapping regions between two neighboring tiles match very well (geometrically and spectrally).

- **Spain, Cartagena, 28.05.2025 (DT 132776, tile 30)**

As shown in Figure 7-36, the Land-Water separation for this scene affected by strong sun glint is accurate, correctly representing even the small structures within the saline works in the center of the image subset. Also when comparing the L2A “land” product to the L2A “water” product, the correct separation of land and water areas can be seen in Figure 7-37.

Regarding the masking of clouds, many bright greenhouse areas close to settlements are incorrectly masked as clouds due to the high signal level (see Figure 7-36).

When checking the spectra of single pixels of the L2A “land” product (Figure 7-38), the spectral signatures for the various materials are as expected, showing a general smooth spectral behaviour and the expected reflectance range. Also when comparing the “land product” and “water product” spectra for shallow water, despite having different units the spectra all are plausible and as expected (see Figure 7-39). Note that the water spectra are affected by strong sun glint, limiting the usability for subsequent analysis.

To conclude, the L2A processing is accurate for the land-water masking also in shallow waters, while the separation of clouds with bright and sometimes saturated pixels of greenhouses is challenging, resulting in some misclassifications. The shape and magnitude of the BOA_ref spectra are as expected, also when comparing the land and water processing.

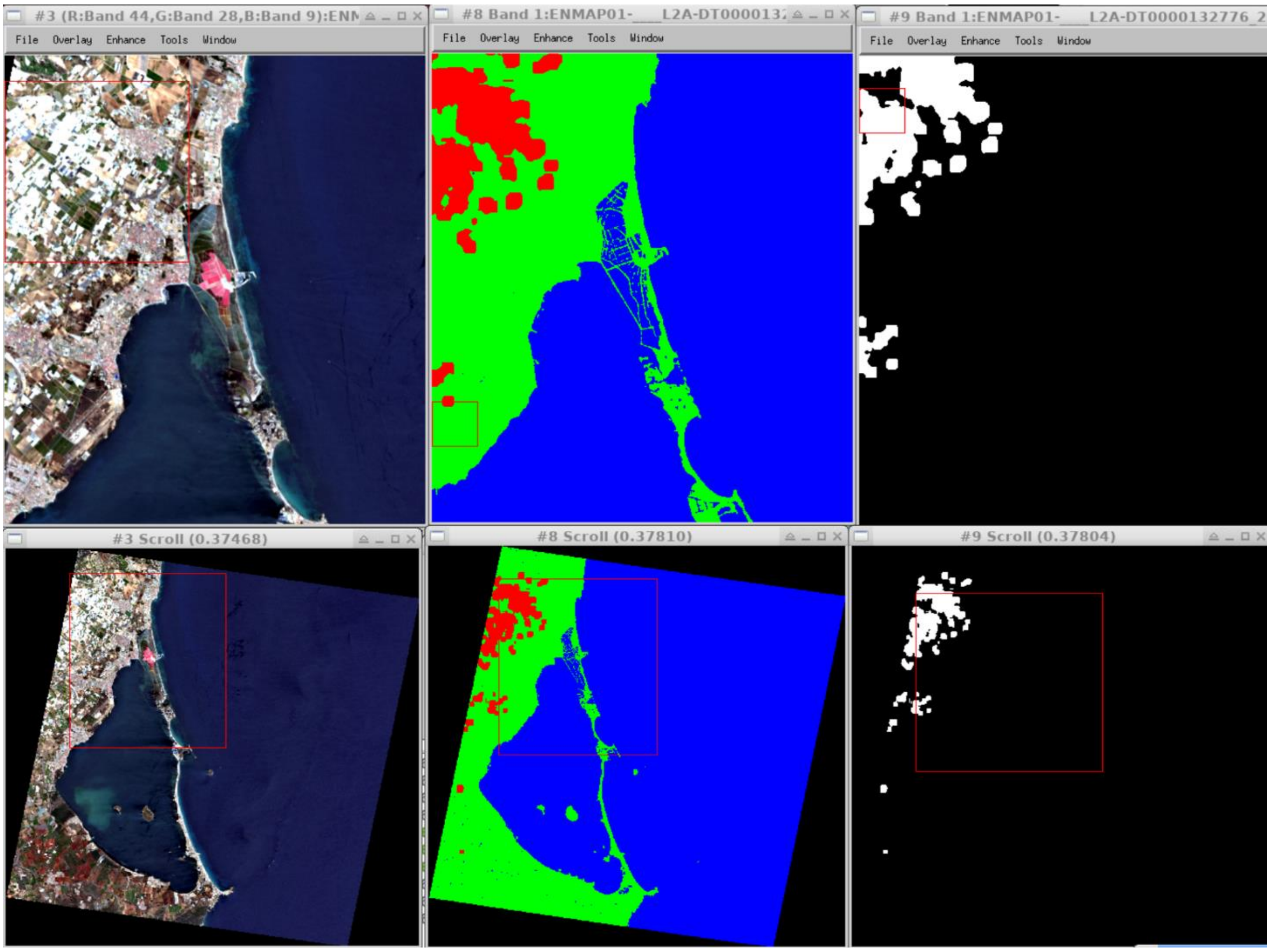

Figure 7-36 EnMAP L2A CIR composite (bands 75-45-28) of scene DT132776, tile 30 and its corresponding masks (QL quality classes) with blue = water and red = clouds and green = land and the cloud mask

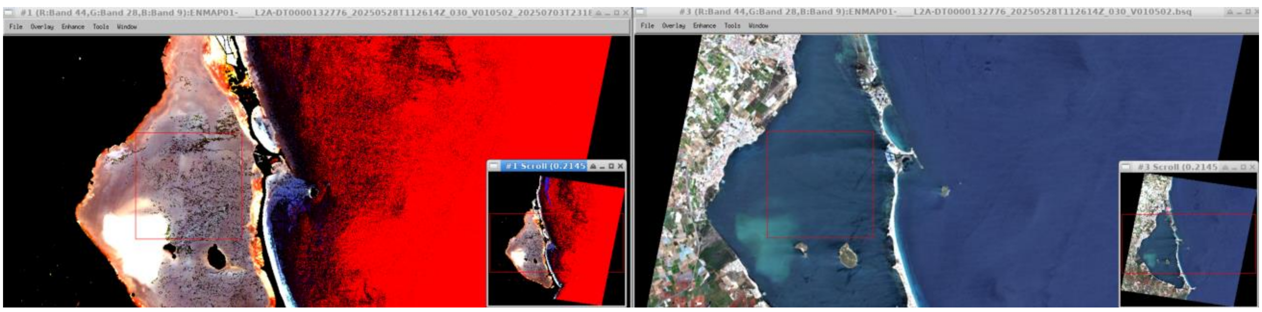

Figure 7-37 RGB composites of the L2A “water” product (left) and the RGB composite of the L2A “land” product for scene DT132776, tile 30, which is affected by sun glint. Note that for water, the default image stretch when opened in ENVI causes an incorrect color impressions, which is not due to the EnMAP data.

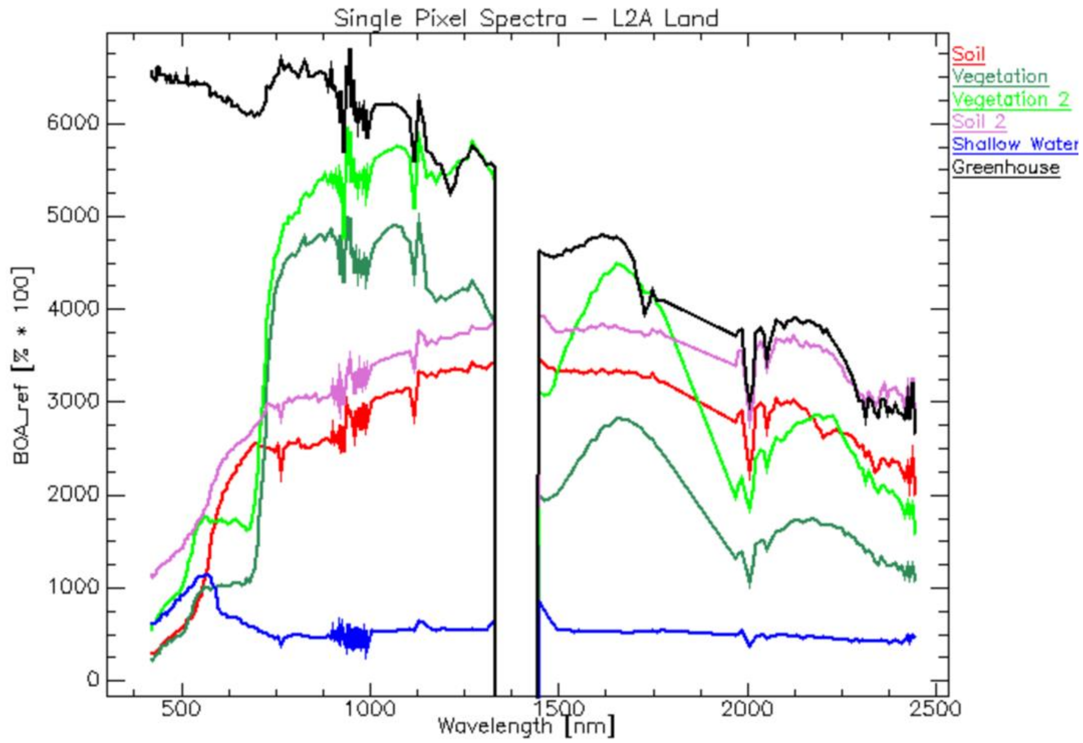

Figure 7-38 Single pixel spectra of the L2A "land" product.

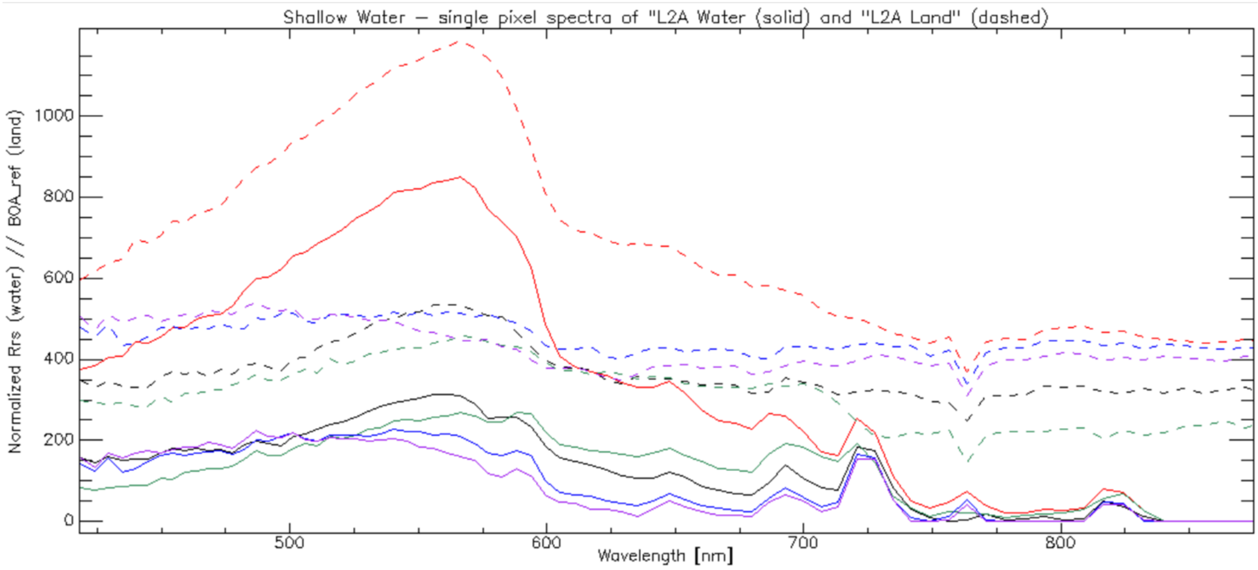

Figure 7-39 Single pixel spectra of the L2A "water" product (solid lines) and the L2A "land" product (dashed) for shallow water pixels affected by sun glint. Note the difference in units (normalized water leaving reflectance for "water", and bottom-of-atmosphere reflectance for "land").

- **Nahr al Khabur River, Syria, 21.06.2025 (DT 137176, tile 5)**

The EnMAP scene DT 137176, tile 5, acquired over Syria (Figure 7-40) includes a mixture of arid soil / sand surfaces, as well as irrigated agriculture areas and inland river surrounded by wetlands. The L2A image impression is fine, showing no artefacts. The masking of land and water areas is accurate, representing the various river arms and sidearms, wetlands as well as ponds in the irrigated agriculture areas.

The corresponding spectral signatures (Figure 7-41) of various surfaces show the expected spectral behavior of arid soils, irrigated vegetation and wetlands.

In summary, the L2A processing of the scene is as expected.

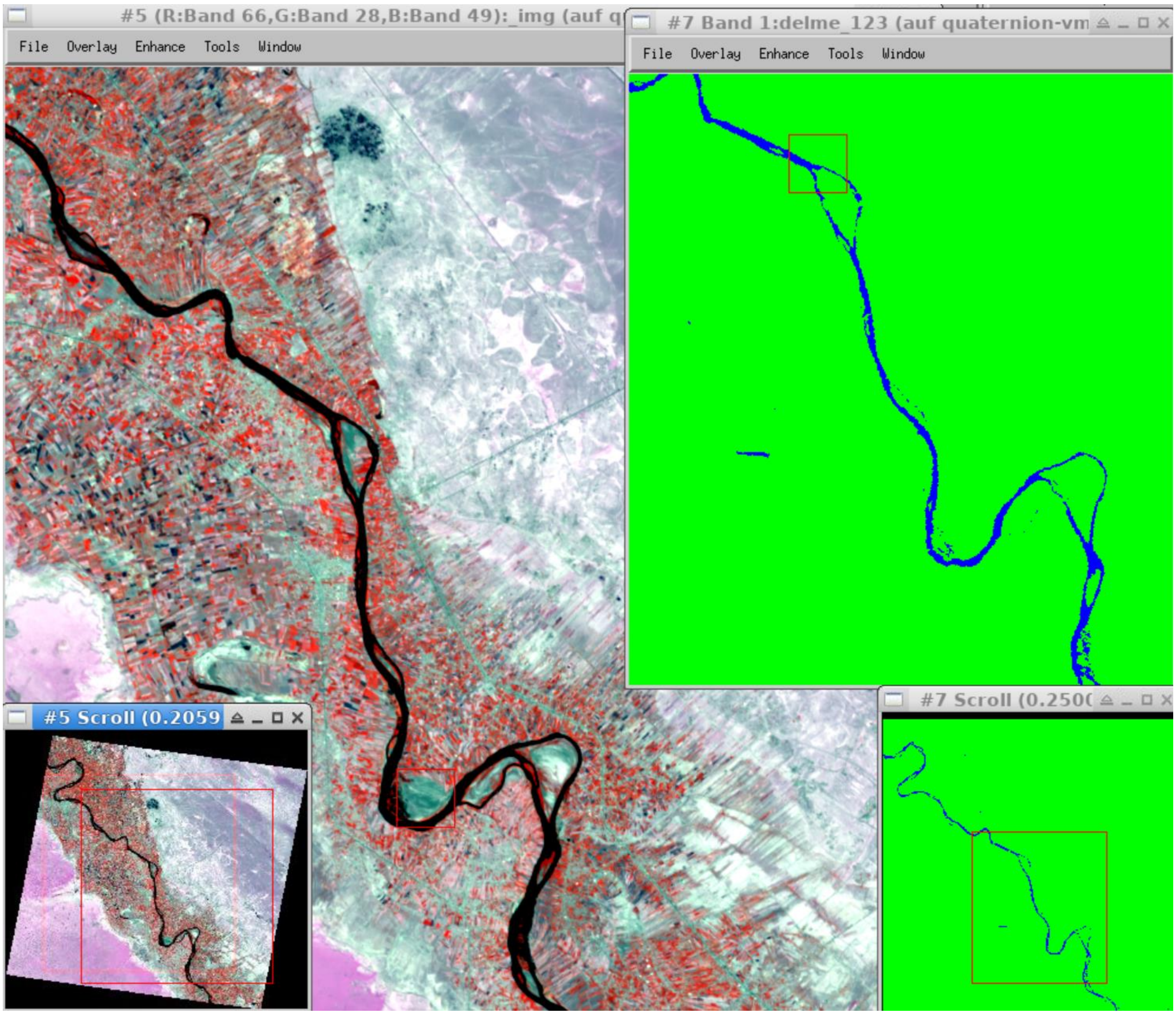

Figure 7-40 DT137176 Tile 5, Check of masks: Corresponding quality layers (from left to right) EnMAP CIR composite, QL quality classes

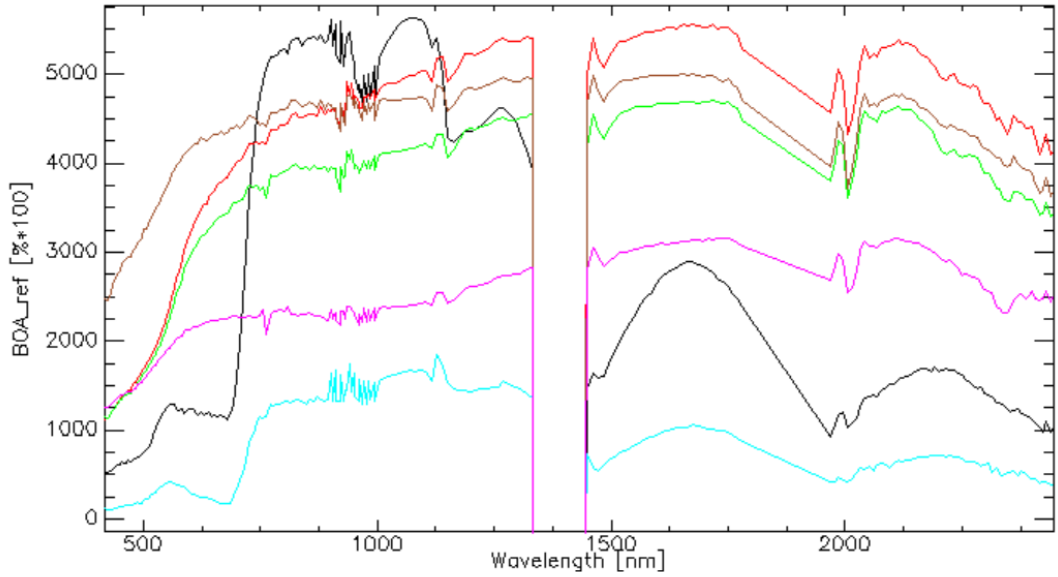

Figure 7-41 DT137176 Tile 5, spectra of various surfaces

- **Khazakstan, close to lake Balkash lake, (DT 131190, tile 17)**

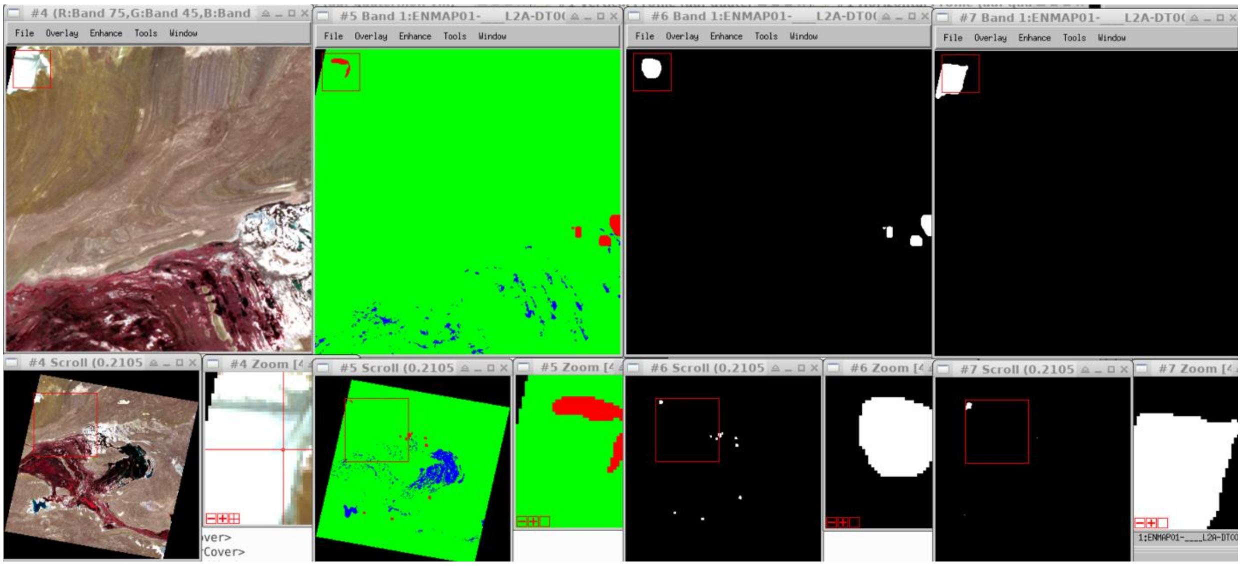

Figure 7-42 DT131190 Tile 17, Check of cloud mask: Corresponding quality layers (from left to right) EnMAP CIR composite, QL quality classes, QL cloud mask, QL snow mask

Within this scene in Khazakstan (Figure 7-42), the masking of land and water is correct and represents well the differences between shallow waters and dried out areas. The deposits of salt/gypsum crusts on soils (white areas in the CIR image) leads in some parts of the scene to some confusion with clouds, which is explainable by the similarly bright and smooth spectra of both objects.
Similarly, the area masked as “snow” in the northwestern part is likely incorrect, as the spectral signature in the VNIR and SWIR (see Figure 7-43) for snow and thick salt crusts are similar. Note that there is a clear separation between this thick salt crust and the also bright pixels of the soils with salt/gypsum crusts.
Checking the spectral signatures of other surfaces in the scenes, all signatures are as expected, see Figure 7-44, indicating a correctly working atm. correction.

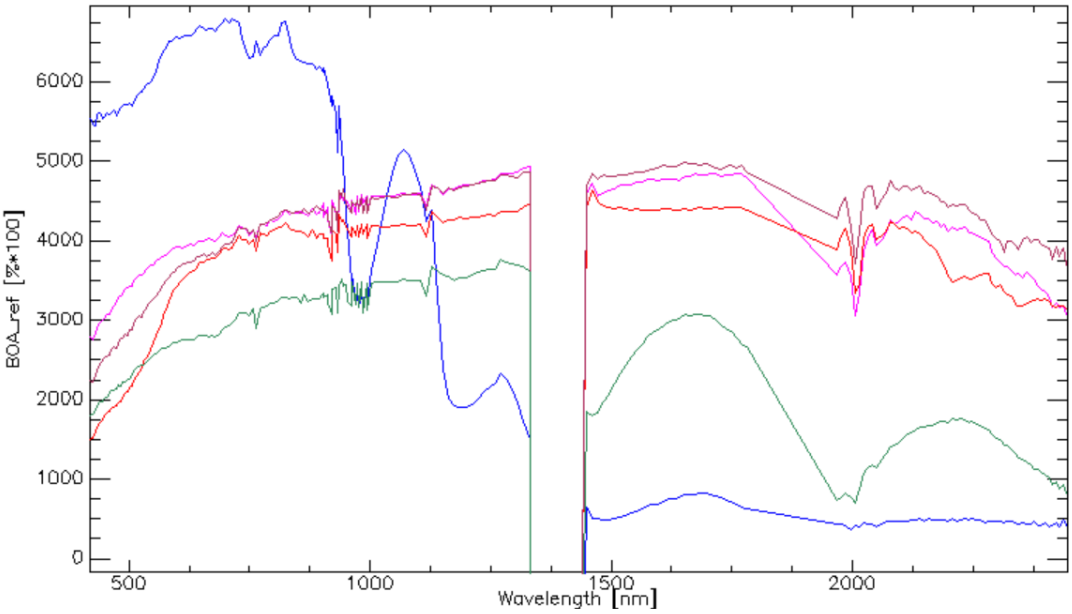

Figure 7-43 DT131190 Tile 17, spectra of various bright salt/gypsum surfaces. Blue: spectral signature of thick salt/gypsum crust masked as “snow”; other colors: spectral signatures of soils affected by salt/gypsum.

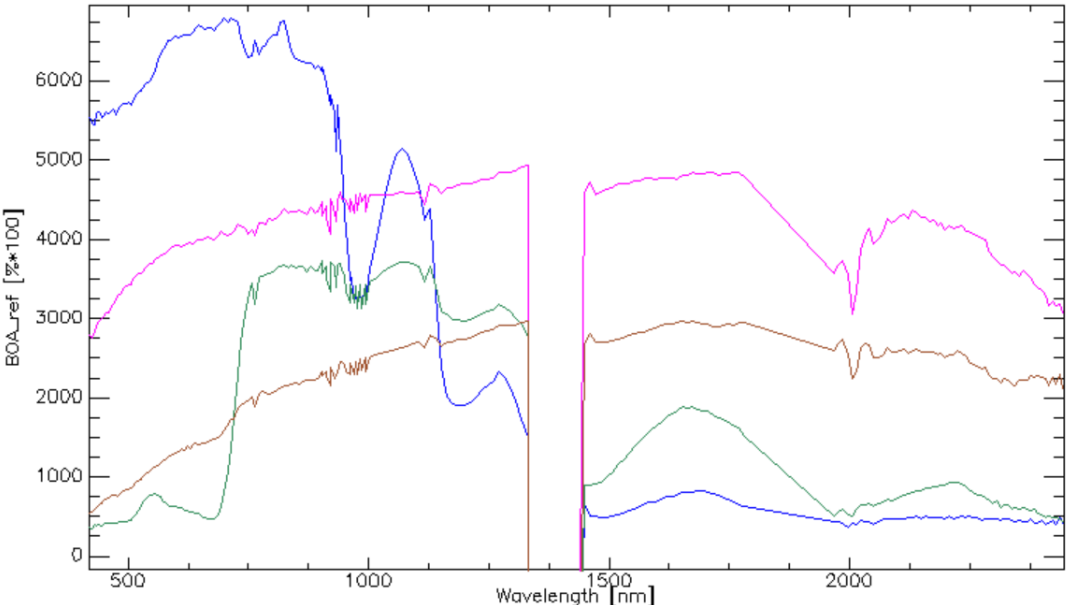

Figure 7-44 DT131190 Tile 17, spectra of various surfaces: blue: thick salt/gypsum crust; pink: soils affected by salt/gypsum; green: healthy vegetation; brown: mixture of soil and dry vegetation.

- **Khazakstan, close to lake Balkash lake, (DT 131190, tile 18)**

For the neighboring scene (Figure 7-45) being homogeneous grass- and dryland, the masking is correct, as are the spectral signatures (Figure 7-46) showing the expected smooth behavior. As no salt/gypsum crusts occur, the whole tile is correctly masked as “land” without any “clouds” or “snow” masks assigned.

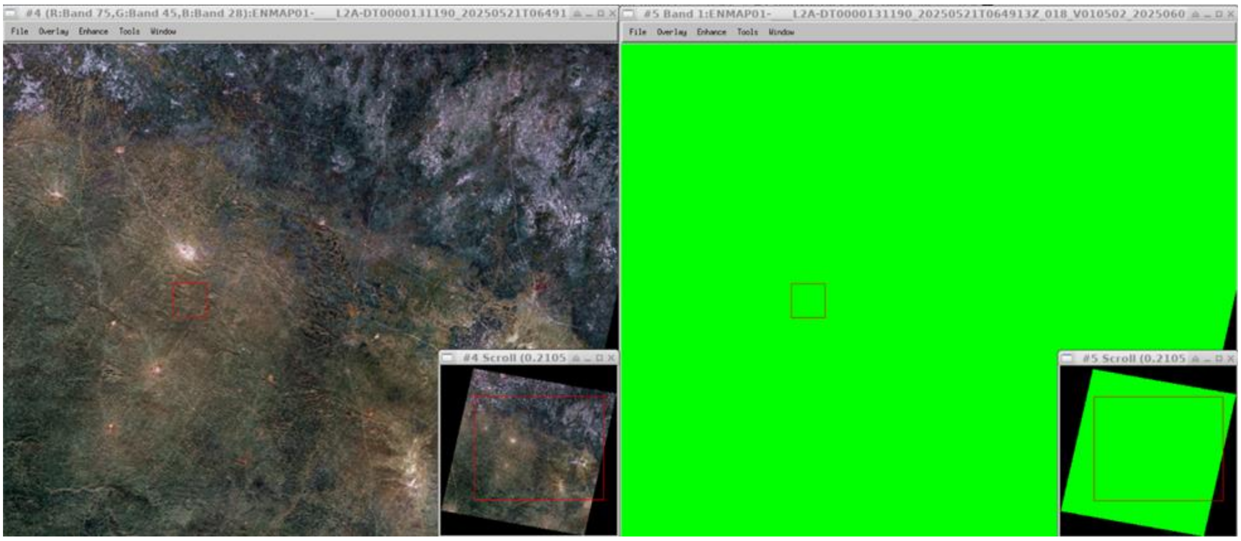

Figure 7-45 DT131190 Tile 18, Check of cloud mask: Corresponding quality layers (from left to right) EnMAP CIR composite, QL quality classes

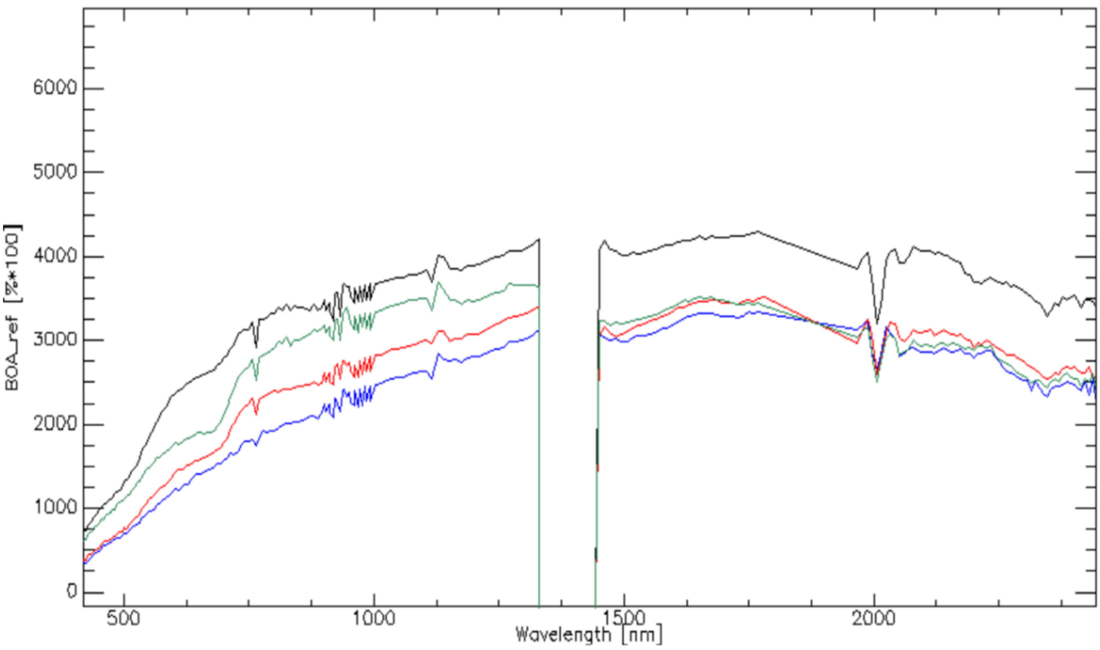

Figure 7-46 DT131190 Tile 17, spectra of various surfaces

- **Overlapping area – consistency check for Khazakstan, close to lake Balkash lake, (DT 131190, tiles 17 & 18)**

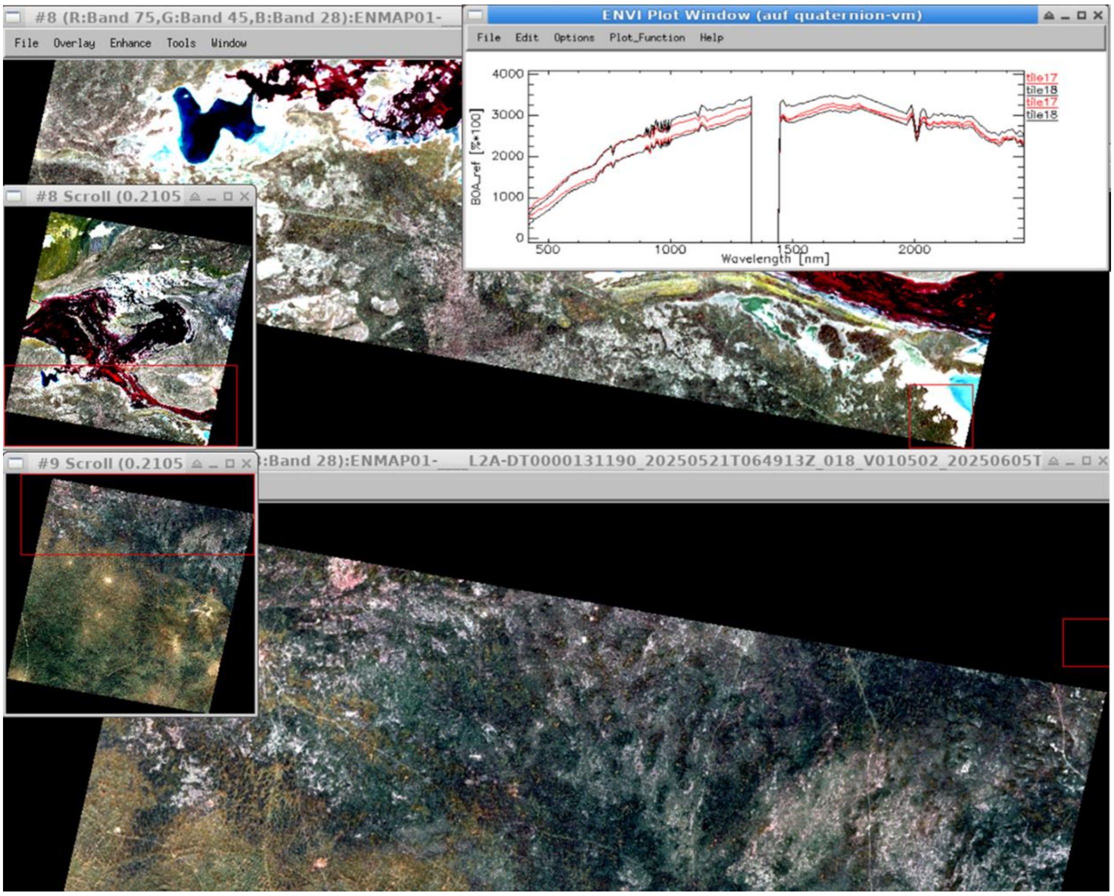

Figure 7-47 Overlapping area of the two neighboring tiles (EnMAP CIR composites, image stretch optimized to match overlapping region)

When analyzing the overlapping region between these two tiles (Figure 7-47), the spectra in this region are highly similar, indicating a good atmospheric correction across tiles where both AOT and WV estimates are similar for the adjacent regions in both tiles.

8 External Product Validation

The standard quality parameters were validated in the external product validation process for the reporting period. The validation included 106 Level 1B, 187 Level 1C and 62 Level 2A products. Some new matchups with reference measurements could be implemented in the reporting period.

8.1 Level 1B

The following validation scenarios were performed to validate Level 1B products:

- TOA Radiance
- Spatially coherent radiometric miscalibration (striping artifacts; along- and across-track)
- Signal-to-Noise Ratio (SNR)
- Spectral validation

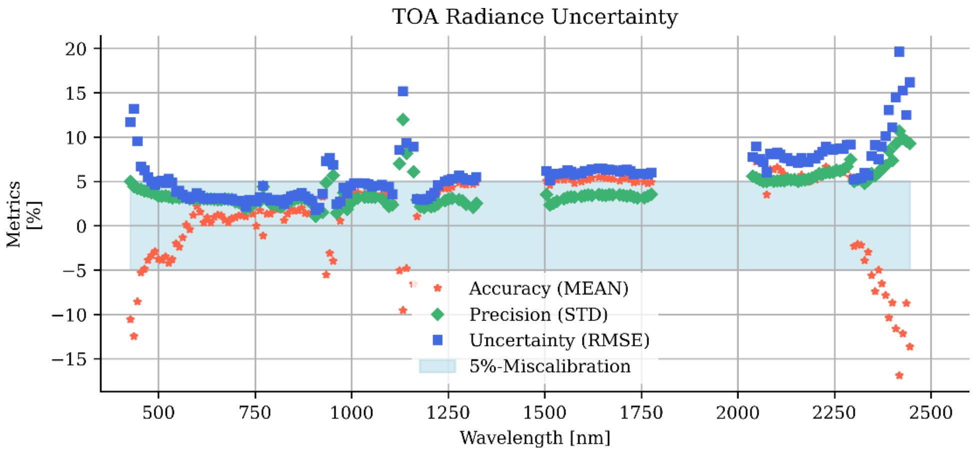

Figure 8-1 Errors between EnMAP TOA radiance and propagated TOA radiance from in situ measurements against wavelength for all TOA validation sites based on 42 matchups.

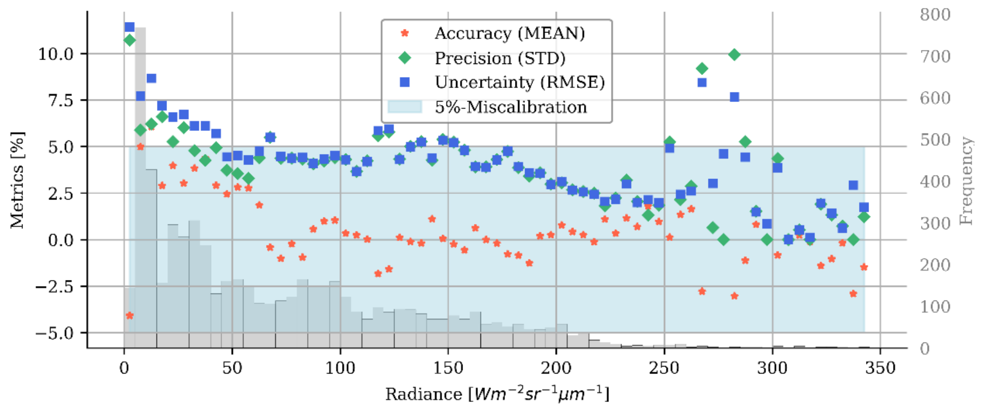

Figure 8-2 Errors between EnMAP TOA radiance and propagated TOA radiance from in situ measurements against radiance level for all TOA validation sites based on 42 matchups.

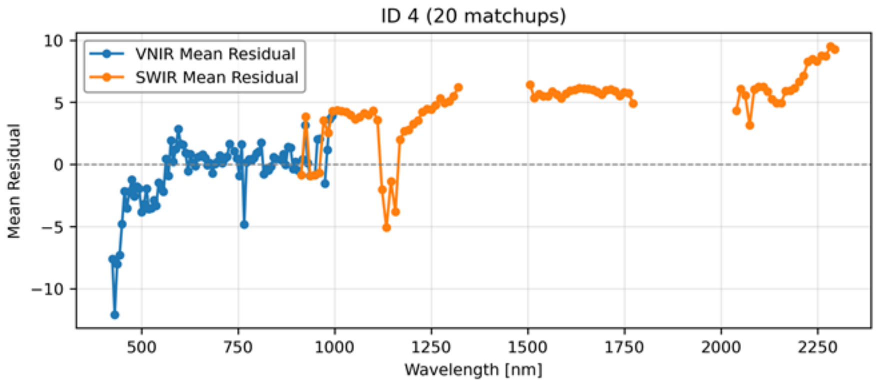

(a)

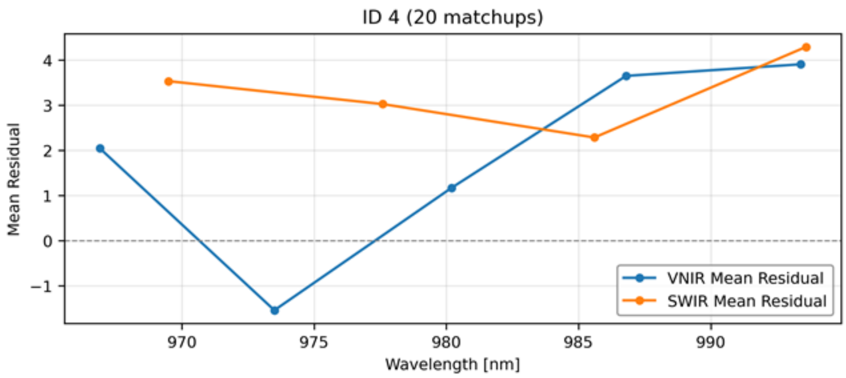

(b)

Figure 8-3 Mean difference between EnMAP TOA radiance and propagated TOA radiance from RadCalNet measurements against wavelength at Gobabeb. Figure a) shows the whole wavelength spectrum, Figure b) shows a zoom to 960 to 1000 nm.

For the VNIR spectrum, the TOA radiance comparison shows an RMSE < 5%. For the SWIR spectrum, the RMSE is slightly higher: 6% in the 1500–1750 nm range and 7.5% in the 2000–2250 nm range. As in previous reports, higher RMSE values occur near the detector wavelength edges and within the water-absorption bands. The overall increase in RMSE compared with earlier reports can be attributed to the updated RadCalNet reference at Gobabeb, which introduces a higher positive bias of the EnMAP data relative to the in-situ measurements (see report 2025 Q1). Because RMSE is computed relative to the radiance level, this bias inflates deviations in low-radiance regions, such as 2000–2250 nm, as also seen in Figure 8-2.

For the first time, radiometric validation of TOA radiance was performed separately for the VNIR and SWIR channels. Figure 8-3a shows the mean deviation for the VNIR and SWIR detectors at the RadCalNet site Gobabeb. Figure 8-3b shows the deviation in the detectors' overlap region (960–1000 nm). Across most wavelengths, the SWIR detector exhibits a clear positive bias of approximately 4–6 $Wm^{-2}sr^{-1}\mu m^{-1}$ relative to the in-situ radiance, whereas the VNIR detector shows only a small positive—or even slightly negative—bias. However, in the overlap region (985–1000 nm) the VNIR detector also shows a comparable positive bias. This contrasts with the BOA reflectance validation (Section 8.3), where the difference in bias between the VNIR and SWIR detectors is also evident within the overlap region. This anomaly is under investigation.

Regarding the spatially-coherent radiometric miscalibration, no significant anomalies were detected for the VNIR and SWIR across-track direction, indicating that the implemented correction algorithm works very well. SWIR along-track artifacts at wavelengths with a vital gradient/feature are still visible. However, there are currently no needs to implement a correction, as there are hardly user complaints and a perfect correction is apparently not feasible. The mentioned artifacts are well within the mission requirements of < 5 %.

The SNR assessment was updated based on 204 tiles with the product version 01.05.02 (VNIR 106 and SWIR 98) and was found to be very stable (VNIR: 402:1; SWIR: 260:1) compared to the previous evaluations and inside the mission requirements (VNIR > 343:1 @495 nm SSD 4.7 nm; SWIR > 137:1 @2200 nm & SSD 8.4 nm).

There have been no updates to the product versions of the EnMAP tiles regarding the spectral smile since the previous report. Consequently, the results are expected to remain consistent with those previously presented and are therefore assumed to continue meeting the mission requirements.

8.2 Level 1C

The following Level 1C validation scenarios have been performed:

- VNIR-to-SWIR spatial co-registration
- Absolute spatial accuracy

The spatial co-registration between VNIR and SWIR has been analyzed for 110 products with the product version 01.05.02. Compared to the previous report, the RMSEs in X and Y direction are slightly lower (6 and 6.4 m). Overall, the spatial co-registration performance is stable and well within the mission requirement of less than 30% of a pixel.

The quality of the absolute spatial accuracy is also stable. Once again, an RMSE of 10.4 m in X and 13.4 m in Y direction derived from 187 tiles with the product version 01.05.02 was achieved which is well inside the mission requirements (<30 m with GCPs in the image, <100 m without GCPs).

8.3 Level 2A

Land

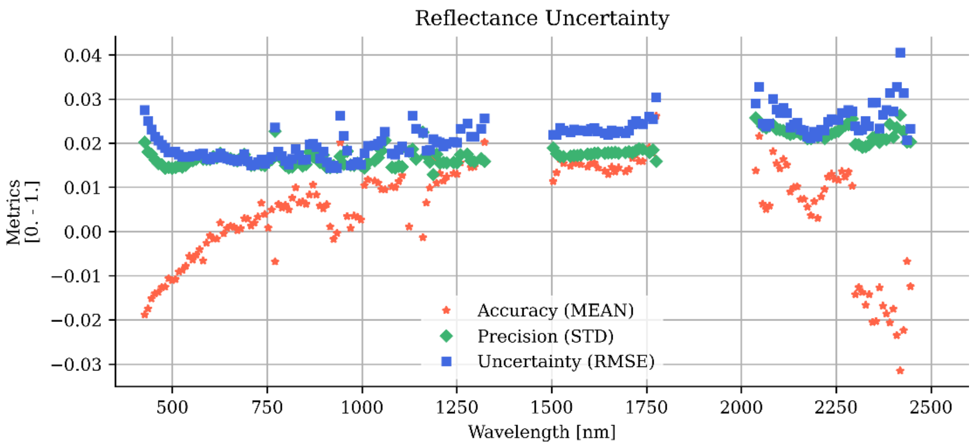

Figure 8-4 Errors between BOA reflectance from EnMAP and reference measurements against wavelength for all validation sites (62 matchups).

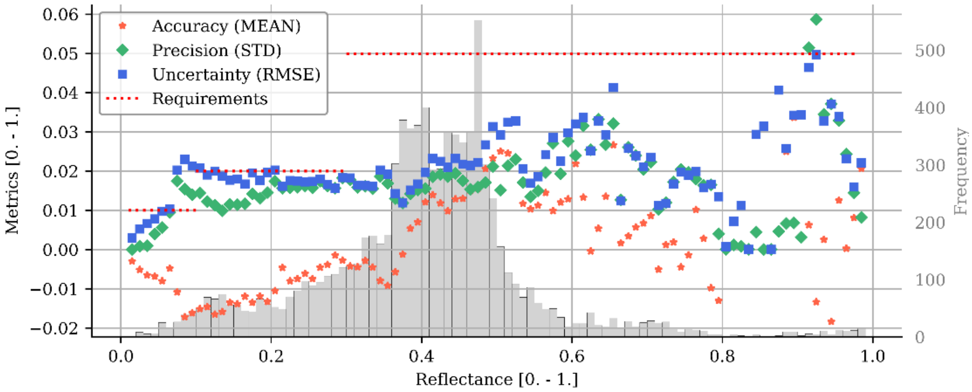

Figure 8-5 Errors between BOA reflectance from EnMAP and reference measurements against reflectance level for all validation sites (62 matchups).

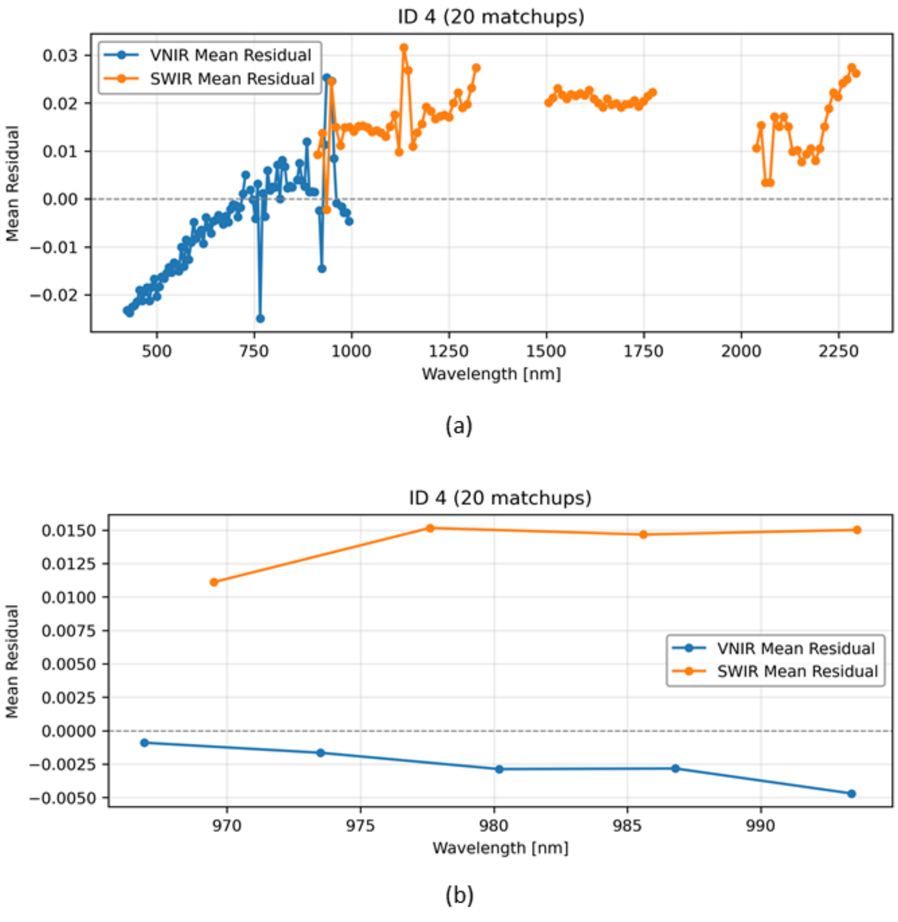

Figure 8-6 Mean difference between EnMAP BOA reference and BOA reference from RadCalNet measurements against wavelength based on 20 matchups at Gobabeb. Figure a) shows the whole wavelength spectrum, Figure b) shows a zoom to 960 to 1000 nm.

Eight new in-situ matchups were added to the L2A land quality assessment. The eight land matchups include measurements from the RadCalNet site Railroad Valley (RVUS), two from the newly integrated RadCalNet site Baotou Sand, and one from the July 2025 field campaign in Majadas, Spain. A total of 62 matchups were analysed. Across most of the VNIR range, RMSE values of approximately 1.75% reflectance were observed, while in the SWIR range the RMSE is around 2%. As in previous reports, higher residuals (up to 3% RMSE in terms of accuracy and precision) occur at the edges of the spectral domain, i.e., below

500 nm and above 2400 nm (Figure 8-4). Overall, the reflectance remains well within the mission requirements (Figure 8-5).

In addition, BOA reflectance was validated separately for the VNIR and SWIR detectors, as it was done for the TOA radiance validation. Analogously to the TOA radiance results, the SWIR shows a positive bias of 1.5–2% reflectance, whereas the VNIR exhibits a negative bias of about 2% at the lower end of the spectrum and no significant bias at the upper end (Figure 8-6a). In contrast to the TOA radiance validation, the SWIR also displays consistently higher values in the overlapping spectral region (960–1000 nm) by approximately 2% reflectance (Figure 8-6b). The causes of this are not yet clear and require further investigation.

Water

Five additional valid matchups of normalized water-leaving reflectance were included in the statistical analysis of this report—two from Lake Garda and three from Lake Trasimeno—bringing the total number of analyzed matchups to 63. The new matchups show uncertainties consistent with those of previous observations. Consequently, the water validation results still show a clear fulfilment of the mission requirements.

8.4 Summary of External Product Monitoring

In general, all validation and quality monitoring during the reporting period indicate that EnMAP product quality is stable and compliant with mission requirements. Local exceedances of the RMSE occur only in the TOA-radiance validation within specific spectral regions. These deviations are likely linked to the reference data and low-radiance conditions in the affected bands and will be monitored in subsequent validation.

9 Others

EnMAP Mission Operations and Status Publications:

- Lazzeri, G., Milewski, R., Foerster, S., Moretti, S., Chabrillat, S. (2025). Early Detection of Soil Salinization by Means of Spaceborne Hyperspectral Imagery, Remote Sens. 2025, 17, 2486. https://doi.org/10.3390/rs17142486

EnMAP Mission Operations and Status Presentations:

- **Space2Agriculture, Online Workshop "Carbon Farming"**
  - "ENMAP hyperspectral mission for mapping soil parameters". Presentation by S. Chabrillat et al.
- **EnMAP Workshop (Munich 02-04 April 2025)**
  - "The German hyperspectral Mission EnMAP – Mission status overview and observing strategy". Presentation by L. La Porta et al.
  - "Overview and Status of the Spacecraft from the Perspective of the Manufacturer". Presentation by R. Feckl et al.
  - "EnMAP imaging spectroscopy mission Science exploitation program: Science results 3 years after launch". Presentation by Sabine Chabrillat et al
  - "Three years of EnMAP Ground Segment Operations & Lessons Learned from the Foreground Mission 2024". Presentation by E. Carmona et al.
  - "Overview of EnMAP processor and calibration activities". Presentation by M. Pato et al.
  - "The Tasks of the EnMAP Ground Segment between Acquisition Request and Data Delivery". Poster by M. Habermeyer
  - "EnMAP data from a user's view" & "EnMAP's Payload Ground System from order tasking to downloading acquisitions". Poster by S. Baumann
  - "EnMAP Calibration". Poster by D. Marshall (EOC visit only)
  - "EnMAP Data Access". Tutorial by N. Pinnel
  - "Introduction to EnMAP Data Processing with EnPT: A Hands-On Tutorial". Tutorial by D. Scheffler
- **Living Planet Symposium LPS25 (Vienna 23-27 June 2025)**
  - "EnMAP Mission Status Overview". Presentation by L. La Porta et al.
  - "EnMAP Science Activities 3 Years After Launch: Highlights". Presentation by S. Chabrillat et al.
  - "EnMAP synergies with hyperspectral missions and international campaigns". Presentation by V. Krieger et al.
  - "International Cooperation in Space: Example of applications using time-series from EnMAP/PRISMA spaceborne imaging spectrometers". Presentation by S. Chabrillat
  - "Optimizing EnMAP Satellite Operations: Acquisition Strategies and Data Access". Poster by E. Carmona et al.

- “The EnMAP Foreground Mission – High priority acquisitions for enhanced science and synergies”. Poster by N. Pinnel et al.
- “Three Years in Orbit: Statistics from the Ground Segment of the EnMAP Mission”. Poster by M. Habermeyer et al
- “EnMAP data from a user‘s view”. Poster by S. Baumann et al.
- “Verifying the Spectral Performance of the EnMAP Imaging Spectrometer using Earth Datatakes – Data Quality Control Results from 3 Years in Orbit”. Poster by M. Bachmann et al.
- “EnPT: An Open-Source Tool for Custom Processing of EnMAP Hyperspectral Data”. Poster by D. Scheffler et al.